DISSERTATION

DETECTION OF DISEASE BIOMARKERS USING A NOVEL MULTI-ANALYTE IMMUNOASSAY

Submitted by

Meghan M. Caulum

Department of Chemistry

In Partial fulfillment of the requirements

For the Degree of Doctor of Philosophy

Colorado State University

Fort Collins, Colorado

Spring 2007

COLORADO STATE UNIVERSITY

January 31, 2007

WE HERBY RECOMMEND THAT THE DISSERTATION PREPARED UNDER OUR SUPERVISION BY MEGHAN M. CAULUM ENTITLED "DETECTION OF DISEASE BIOMARKERS USING A NOVEL MULTI-ANALYTE IMMUNOASSAY" BE ACCEPTED AS FULFILLING IN PART REQUIREMENTS FOR THE DEGREE OF DOCTOR OF PHILOSOPHY.

Committee on Graduate Work

C. Michael Elliott

Bruce A. Parkinson

Alan J. Kennan

Nicole Ehrhart

Advisor: Charles S. Henry

Department Head: Anthony K. Rappé

ABSTRACT OF DISSERTATION

DETECTION OF DISEASE BIOMARKERS USING A NOVEL MULTI-ANALYTE IMMUNOASSAY

Biomarkers provide clinicians with an important tool for disease assessment. Many different biomarkers have been discovered making it readily apparent that no single biomarker can be relied upon for accurate disease detection which has led towards the push for new multi-analyte screening methods. There are, however, currently few inexpensive multi-analyte methods that can use these biomarkers for disease detection in a point-of-care setting. This dissertation details the development of a novel immunoassay which bridges the gap between traditional immunoassays and high density microarrays by utilizing microfluidics, immunoassays and micellar electrokinetic chromatography (MEKC). This chemistry, the Cleavable Tag Immunoassay (CTI), is a low- to medium-density heterogeneous immunoassay designed to detect up to 20 analytes simultaneously. The multi-analyte CTI is shown to be a useful tool for the detection and quantification of cardiac biomarkers in serum samples. Limit of detection and linear range are reported for all of the biomarkers with LODs on the order of low ng/mL to low pg/mL. The linear range for each of the biomarkers spans the boundary between normal and elevated levels. In addition, the use of a combination of two surfactants in the run buffer which form mixed micelles is shown to improve resolution of CTI tags. Preliminary studies of cleavage kinetics using single particles for an integrated CTI analyzer are also presented

including demonstration of the ability to trap and release magnetic particles in a microchip device. Two methods for improving separation efficiency of poly(dimethylsiloxane) including the use of polyelectrolyte multilayers and a simple and effective way to generate a stable hydrophilic glass-like surface for use with microchip CE-EC and CE-fluorescence are also presented. The outcome of this dissertation demonstrates the marriage of immunoassays and microchip MEKC in the CTI shows promise as a new medium-density chemistry for rapid biomarker detection. This work is the first step towards the development of an integrated assay for rapid point-of-care analysis of AMI.

Meghan M. Caulum

Chemistry Department

Colorado State University

Fort Collins CO 80523

Spring 2007

ACKNOWLEDGEMENTS

I would like to thank my colleagues in the Henry group, especially Jon Vickers and Brian Dressen, with whom I was always able to brainstorm ideas about research. You have all been great to work with in my tenure here at Colorado State University. I would like to extend a special thank you to Lauren Ramsay and Brian Murphy for helping to get this project off the ground and running. You always understood the trials and tribulations associated with this project.

I would like to thank Jaimie VanBuren for being a great friend and a shoulder to lean on. I pass the torch to you. The "Lab Mom" job is in your hands now...good luck!

Many thanks go to my committee members for guidance and advice along the way.

Funding for this project came from the American Heart Association.

I can't say thank you enough to my family, especially my parents. You have been there with words of encouragement to keep me going on the long, sometimes bumpy, road to my PhD.

I would also like to say thank you to Neil Mensack for always being there through everything. Here's to what we have together and to many more wonderful years.

A thank you goes to Tach Costello…because without you nothing would get done around here.

Finally, I owe a great deal of thanks to Dr. Charles Henry, my advisor. Your invaluable advice and instruction will be with me in all my future endeavors. Thank you for everything.

TABLE OF CONTENTS

LIST OF FIGURES

LIST OF TABLES

LIST OF EQUATIONS

LIST OF ACRONYMS

2-DE	2-dimensional gel electrophoresis
AMI	Acute myocardial infarction
BCA	Bicinchroninic acid
BNP	B-type natriuretic protein
BSOCOES	*Bis*[2-succinimidyloxycarbonyloxy)ethyl]sulfone
CE	Capillary electrophoresis
CEC	Capillary electrochromatography
CEIA	Capillary electrophoretic immunoassay
CGE	Capillary gel electrophoresis
CIEF	Capillary isoelectric focusing
CK-MB	Creatinine kinase-MB isoform
CRP	C-reactive protein
CTI	Cleavable tag immunoassay
cTnI	Cardiac troponin I
cTnT	Cardiac troponin T
CVD	Cardiovascular disease
CZE	Capillary zone electrophoresis
DCC	N,N'-dicyclohexyl carbodiimide
DDAPS	N-dodecyl-N,N-dimethyl-3-ammonio-1-propane sulfonate

DIC	N,N'-diisoporpyl carbodiimide
DS	Dextran sulfate
DTT	Dithiothreitol
EC	Electrochemical detection
EDC	1-ethyl-3-(3-dimethylamionpropyl) carbodiimide
ELISA	Enzyme linked immunosorbent assay
EOF	Electroosmotic flow
FAM	Fluorescein isothiocyanate-cystamine
FAMB	Fluorescein isothiocyanate-cystamine-biotin
FEB	Fluorescein thyocarbamyl ethylenediamine-SS-biotin
FEGGB	Fluorescein thiocarbamyl ethylenediamine-Gly_2-biotin
FEGGGB	Fluorescein thiocarbamyl ethylenediamine-Gly_3-biotin
FHB	Fluorescein thyocarbamyl hexamethylenediamine-SS-biotin
FITC	Fluorescein isothiocyanate
FTED	Fluorescein thiocarbamyl ethylenediamine
FTHD	Fluorescein thiocarbamyl tetramethylenediamine
FTPD	Fluorescein thiocarbamyl hexamethylenediamine
HABA	2-(4-hydrozyazobenzene) benzoic acid
HMDS	Hexadimethyldisilazane
IACE	Immunoaffinity capillary electrophoresis
IHP	Inner Helmholtz plane
iPAD	Integrated pulsed amperometric detection
ITP	Isotachophoresis

LBL	Layer-by-layer
LC/MS	Liquid chromatography/mass spectrometry
LIF	Laser-induced fluorescence
LOD	Limit of detection
MALDI-TOF/MS	Matrix assisted laser desorption/ionization-time-of-flight/mass spectrometry
MCE	Microchip capillary electrophoresis
MEKC	Micellar electrokinetic chromatography
Myo	Myoglobin
OHP	Outer Helmholtz plane
PA	Poly(arginine)
PAA	Poly(acrylic acid)
PAD	Pulsed amperometric detection
PAH	Poly(allylamine) hydrochloride
PB	Poly(brene)
PBS	Phosphate buffered saline
PC	Poly(carbonate)
PDADMA	Poly(diallyl dimethylammonium)
PDMS	Poly(dimethylsiloxane)
PEI	Poly(ethyleneimine)
PEM	Polyelectrolyte multilayer
PETG	Poly(ethylene terephthalate) glycol
PMMA	Poly(methyl methacrylate)

PMT	Photo multiplier tube
PS	Poly(styrene)
PSS	Poly(styrene sulfonate)
SDS	Sodium dodecyl sulfate
SEC	Size exclusion chromatography
SELDI	Surface enhanced laser desorption ionization
SPR	Surface Plasmon resonance
TBS	Tris buffered saline
TCEP	Tris(2-carboxyethyl) phosphine
TEA	Triethylamine
TES	N-[tris(hydroxymethyl)methyl]-2-aminoethanesulfonic acid
THF	Tetrahydrofuran
TPE	Thermoset polyester
β-ME	2-mercaptoethanol
μ-TAS	Microscale total analysis system

CHAPTER 1

INTRODUCTION

1.1 Cardiovascular disease

Early detection is essential for diagnosis, treatment, and prevention of many diseases. One example where early detection is particularly important is cardiovascular disease (CVD).[1] In patients with CVD showing non-specific symptoms, cardiac biomarkers provide clinicians with an important additional tool for disease assessment.[2] In light of this fact, much research has focused on new tools to search for disease biomarkers.[3, 4] As more biomarkers are discovered, it has become readily apparent that no single biomarker can be relied upon for accurate disease detection,[5] leading towards the push for new multi-analyte point-of-care screening chemistry.[6, 7]

The World Health Organization (WHO) has set up criteria for the diagnosis of acute myocardial infarction (AMI), a major form of CVD, which state that in order to confirm the diagnosis the physician must confirm two of the following: history of chest pain, evolutionary changes on the electrocardiogram (ECG) and elevation of serial cardiac enzymes. The ECG, however, lacks diagnostic sensitivity (as low as 40-50%).[5] In patients who have definitive symptoms as well as a diagnostic ECG, biochemical markers play a minor roll in AMI diagnosis. The use of biochemical markers for diagnosis is critical, however, for those patients with nonspecific symptoms and a non-diagnostic

ECG.[5] A list of biomarkers including proteins and small molecules useful in screening for CVD and AMI is shown in Table 1.1.

Studies have shown that the availability of a rapid, real-time analysis methods of cardiac markers results in the reduction in length of hospital stay and overall laboratory costs producing shorter turnaround times.[8] In 4-8% of AMI patients, the diagnosis is missed which leads to higher mortality rates and the highest malpractice costs among Emergency Medicine physicians.[9] The signs and symptoms of AMI may be non-specific and accurate diagnosis may require up to 24-48 hours. The delay in diagnosis results in increased morbidity or death.[9] Early AMI diagnosis also allows for quick intervention and administration of anti-thrombotic therapy, fibrionolysis, and primary angioplasty.[1, 10]

The original methods for cardiac biomarker screening were enzyme activity assays for lactate dehydrogenase (LD), total creatinine kinase (CK) and its isoform CK-MB.[11] These screening methods have evolved into mass measurement methods that provide increased sensitivity and specificity.[11] Furthermore, monitoring the rise and fall of CK-MB serum levels has long been considered the benchmark for cardiac biomarkers because of the high sensitivity and selectivity.[12] In addition to CK-MB levels, emergency departments now measure levels of cardiac troponin T (cTnT), cardiac troponin I (cTnI), and myoglobin (Myo) in patients presenting with AMI symptoms.[2, 13] The advantage of screening for myoglobin is that it is released into the bloodstream earlier than CK-MB which in turn leads to an earlier diagnosis of AMI. A rise in Myo can be seen as early as one hr after AMI onset. Troponin levels rise above the upper reference limit at 4-8 hrs

Biomarker	Upper reference value (URF)	Time (hr) until increase above URF
CK-MB[14]	**0-9 µg/L**	**3 to 8**
Myoglobin[15]	**Male: 19-92 µg/L** **Female: 12-76 µg/L**	**1 to 3**
Troponin I (TnI)[14]	**< 10 µg/L**	**4 to 8**
Troponin T (TnT)[14]	**0-0.1 µg/L**	**4 to 8**
C-reactive protein (CRP)[16, 17]	**<10 mg/L**	
BNP (b-type natriuretic peptide)[18]	**>100 pg/mL**	
Homocysteine[19]	**10 µmol/L**	

Table 1.1. Biomarkers of acute myocardial infarction (AMI).

post-AMI and can remain elevated for up to 10 days. This can prove beneficial for diagnosis of late-presenting AMI patients and replaces the use of LD for this purpose.

There have been improvements in the methods for biomarker detection including the use of monoclonal antibodies for Enzyme Linked Immuosorbent Assays (ELISA). In addition, immunochromatography and solid-phase assays are also used to screen for biomarkers. Finally, point-of-care testing has been implemented using rapid analyzers capable of screening for one to several markers simultaneously.[20] There are also two commercially available qualitative colorimetric ELISA assays or "bedside" methods for AMI detection: CARDIAC STATus and TropT rapid assay. No single method exists, however, in which the *quantitative analysis* of whole blood for several markers is performed at the patient's bedside in an inexpensive, disposable device. The chemistry developed in this dissertation couples aspects of immunoassays and microchip micellar electrochromatograpy (MEKC) to provide a fast, efficient method to quantitatively screen for multiple biomarkers in serum samples in a format that can be miniaturized.

1.2 Methods for protein analysis

Currently there are several different methods available for performing analysis of proteins including Liquid Chromatography/Mass Spectrometry (LC/MS), Matrix Assisted Laser Desorption/Ionization–Time of Flight(MALDI-TOF)/MS, protein arrays, immunoassays including Enzyme linked immunosorbent assay (ELISA), and capillary electrophoresis (CE). Each of these will be briefly addressed in the sections that follow.

1.2.1 Mass spectrometry methods

Mass spectrometry (MS) methods provide excellent molecular specificity as well as detection sensitivity. MS has played a large role in structural identification of fatty acids, glycolipids and lipopolysaccarides.[21] LC/MS has become popular because of its high-throughput capabilities when compared to gel methods for protein identification. The LC/MS shot-gun approach has proved useful in screening for membrane proteins as well as post-translational protein modifications.[22] Matrix-assisted laser desorption/ionization (MALDI) was first reported by Tanaka and coworkers[23] and Karas and Hillenkamp[24] in 1988 as a useful ionization technique for MS to study large biopolymers with masses in excess of 200kDa. It is considered a soft ionization technique in which the function of the matrix is to absorb photon energy from the laser beam and transfer it to the sample and reduce intermolecular forces and aggregation of the biopolymer.[25] Both positive- and negative-ion analysis can be performed using MALDI. LC/MS and MALDI-TOF/MS instrumentation, however, is expensive and the process is time consuming. These methods are therefore used primarily for marker discovery.

1.2.2 2-Dimensional gel electrophoresis

2-Dimensional gel electrophoresis (2-DE) is the classical tool for multi-dimensional protein separations in complex mixtures providing the highest resolution in protein separations.[26, 27] 2-DE separates proteins by their isoelectric points (pIs) in the first dimension and by their mass in the second dimension. The resulting gel is stained in order to visualize the purified proteins for excision and concentration comparison. 2-DE,

however, is labor and time intensive and possesses a limited dynamic range for quantification and can not be used to detect membrane proteins.[28, 29]

1.2.3 Protein arrays

High throughput techniques such as protein microarrays have the ability to detect 100-1000s of proteins simultaneously with reduced sample consumption.[30] Protein array technology builds on DNA array technology using protein capture agents printed on glass slides, membranes, or plates instead of spotting DNA on a glass slide.[31] The theory and principles of protein microarray technology were first described by Roger Ekins in the ambient analyte theory.[32] The ambient analyte theory demonstrates the ability of miniaturized immunoassay systems to achieve superior sensitivity.[33] Ekins and colleagues demonstrated that a system that uses a small amount of sample as well as a small amount of immobilized capture reagents can possess better sensitivity over conventional immunoassay systems.[33, 34] Despite the increase in sensitivity with the use of microarrays, current protein array technology faces many challenges including selecting the correct surface chemistry to allow for selective immobilization of proteins, selection of appropriate binding and detection agents for the proteins of interest, and nonspecific adsorption.[35] Another issue with protein arrays is the actual arraying process. Arrayers are expensive, yet required, in order to achieve the desired spot size as well as the desired array density. Assembling arrays manually (without an arrayer) leads to several problems including a lack of ability to assemble a high density array, the possibility of a decrease in sensitivity, and an increase in sample and reagent consumption.[35, 36] There are several detection methods currently in use with protein

arrays including electrochemical detection (EC), surface plasmon resonance (SPR), surface enhanced laser desorption ionization (SELDI), rolling circle DNA amplification (RCA), and fluorescence coupled to a CCD camera or laser scanner with confocal optics.[36] However, all of these systems (except EC) require large and expensive instrumentation to achieve detection making their development as portable analyzers challenging.

1.2.4 Immunoassays

Immunoassays are one of the most effective means for the quantification of trace analytes in complex milieu such as serum or urine. They are among the most specific of analytical techniques, provide low detection limits (on the order of pg/mL), and can be used for a wide range of substances.[37] Immunoassays demonstrate both high selectivity due to the specificity of antigen/antibody interactions and high sensitivity due to fluorescent, chemiluminescent, or radioactive labels.[38] Traditional immunoassays, however, are labor intensive and time intensive due to multiple wash and incubation steps and can only detect a few proteins from one sample.

All immunoassays can be divided into two main categories, competitive and non-competitive. Competitive assays measure the number of antibody sites remaining unbound after a defined and limiting amount of antibody is incubated with an unknown sample. The signal obtained in a competitive assay is inversely proportional to the amount of analyte present.[39] Non-competitive immunoassays measure the amount of analyte bound to antibody sites and generates a signal proportional to the amount of analyte present. The sandwich immunoassay is a form of non-competitive immunoassay

that involves two antibodies, a capture antibody which is immobilized on a solid phase support and a detection antibody that is usually labeled with an enzyme.[40] The protein is "sandwiched" between the capture and detection antibodies in an antibody/antigen complex. In all forms of ELISA, the bound enzyme reacts with added substrate to generate a measurable product.

Capillary electrophoresis-based immunoassay (CEIA) is another type of immunoassay which addresses some of the problems associated with traditional immunoassay formats. CEIA is an analytical technique possessing several advantages over conventional immunoassays including faster analysis for single samples, reduced sample consumption (as low as 0.2 nL),[38] procedure simplicity, simultaneous determination of multiple analytes, and compatibility with automation.[41]

CEIA is considered a two dimensional technique with the first dimension being immunocapture which utilizes the specificity of antibody/antigen interactions and the second being a form of capillary electrophoresis, be it capillary zone electrophoresis (CZE), micellar electrokinetic chromatography (MEKC) or capillary gel electrophoresis (CGE) for separation and detection of the antigen, antibody, and the corresponding antibody/antigen complex.[42] It is the second dimension which makes CEIA so attractive when compared to other one dimensional techniques since the separation step virtually eliminates the possibility of a false positive because the desired complex can be resolved from the others in the sample.[43] Like traditional immunoassays, CEIA can be performed in either competitive or non-competitive forms with the non-competitive form providing greater sensitivity and larger linear dynamic range.[41] The two primary detection modes for CEIA are UV[44, 45] or LIF[46, 47] with detection limits of each technique reported to be 1

ng/mL and 1 pg/mL respectively.[43] There has also been a report of fg/mL detection limits.[48] In the last decade, the integration of CEIA in electrophoresis microchips has also been demonstrated.[49-51] Chip-based immunoassays have been used for the analysis of 10-12 cerebral spinal fluid (CSF) samples per hour for the simultaneous determination of multiple cytokines at pg/mL concentrations.[52] The disadvantages to CEIA when compared to ELISA include poor concentration sensitivity, lack of proven methods for parallel operation and high-throughput analysis (CEIA is a serial technique) as well as the need for monoclonal antibodies, more complicated expensive instrumentation, and the inability to change the molecular structure of the analytes to improve the separation.[53]

The move towards microscale analysis systems has given advantages such as reduced sample consumption; however, in some cases methods for preconcentration are needed for analytes present at low concentrations prior to analysis for required limits of detection in μL-nL volumes. A technique that is useful for analyte preconcentration is immunoaffinity capillary electrophoresis (IA-CE). In IA-CE a microchamber containing immobilized antibody designed to capture and concentrate the analytes of interest without sample pre-treatment is located near the capillary inlet.[54] IA-CE is also a useful way to purify compounds of interest from complex samples because the only analytes captured are those with corresponding antibodies immobilized on the surface of the microchamber. The purified, concentrated analytes are separated using capillary electrophoresis following desorption from the microchamber wall. IA-CE has been previously demonstrated for the determination of biological compounds such as neuropeptides.[55]

1.3 Capillary electrophoresis

The basic theory and practice of capillary electrophoresis (CE) was first described by Jorgenson in the early 1980s.[56, 57] It is a liquid phase analytical separation technique in which analytes are separated based on charge-to-hydrodynamic radius when an electric potential is applied to the solution.[58] One of the reasons CE has gained popularity as an analytical separation technique is the ability to effectively dissipate Joule heat. The surface-to-volume ratio of a typical capillary allows heat dissipation generated from large applied fields allowing for the application of electric fields upwards of 30,000V (~800 V/cm) when compared to a typical slab gel which is limited to 15-40 V/cm.[59] Other reasons CE is an attractive separation technique include improved resolution and the large increase in the number of theoretical plates (N) as compared to LC methods.

The velocity of an analyte in a capillary can be defined as the product of the apparent solute mobility (μ_{app}) and the applied field (E) as shown in Equation 1.1.

$$v = \mu_{app}E = (\mu_{ep} + \mu_{eo})E \qquad \textbf{(1.1)}$$

μ_{app} is further defined as the sum of the electrophoretic mobility (μ_{ep}) and the electroosmotic mobility (μ_{eo}). The electrophoretic mobility of a charged molecular species can be approximated from the Debye-Huckel-Henry theory which is represented by Equation 1.2. Based on Equation 1.2, a smaller, highly charged molecule will have a higher mobility when compared to a larger, minimally-charged species. The electroosmotic mobility is determined by the effect of the electroosmotic flow on the analyte.

$$\mu = q / 6\pi\eta r \quad \textbf{(1.2)}$$

Where:

q = charge on the particle

η = viscosity of the buffer

r = Stokes' radius of the particle

1.3.1. Electroosmotic Flow

Electroosmotic flow (EOF) was first identified in the late 1800s by Helmholtz.[58] EOF acts as a pumping mechanism to force the movement of all molecules (cations, neutral, and anions) toward the detector where the separation of analytes is ultimately determined by charge-to-hydrodynamic radius (electrophoretic mobility) of the molecules. Without electroosmotic flow, only the cations would be seen in normal polarity CE.

Electroosmotic flow is generated by the charge imbalance at a solid-liquid interface under the influence of an electric field.[60] An electric double layer, typically 10 nm thick for CE, is formed at the interface. In the case of CE, the fused silica surface of the capillary acts as the fixed anionic part of the double layer. Above pH 2 the silanol groups of capillary wall are ionized (SiO^-) and as a result there is a higher density of cationic species at the interface in order to balance the fixed negative charges forming a dense, static cationic layer known as the Stern layer or inner helmholtz plane (IHP). A more diffuse layer is formed farther away from the capillary wall known as the outer Helmholtz plane (OHP). Solvated cations in the OHP migrate in the direction of the

cathode under an applied field. Because of the hydrogen bonding of the waters of hydration to the bulk solution water molecules, the entire buffer solution is pulled toward the cathode. This phenomenon is known as "bulk flow" or EOF.

Electrokinetic behavior depends on the zeta potential (ζ) at the shear plane between the IHP and the OHP. Zeta potential can be defined by Equation 1.3.[58]

$$\zeta = \frac{\sigma_0}{\varepsilon K} \tag{1.3}$$

where:

σ_0 = charge density on the wall surface

ϵ = dielectric constant

$1/K$ = the thickness of the double layer, the Debye-Huckel parameter

An increase in ionic strength causes a decrease in 1/K or a compression of the double layer. The actual value of ζ determines the direction and velocity of EOF.

1.3.2. Modes of CE

Capillary electrophoresis can be operated in several different modes: capillary zone electrophoresis (CZE), micellar electrokinetic chromatography (MEKC), capillary gel electrophoresis (CGE), capillary electrochromatography (CEC), isotachophoresis (ITP) and capillary isoelectric focusing (CIEF). The two modes of capillary electrophoresis used for my dissertation work are CZE and MEKC and are therefore covered in the greatest amount of detail here. The simplest and most common mode is CZE. CZE is one of the most universal CE modes and is used for separating a wide range of analytes based on their electrophoretic mobility. Figure 1.1 shows the separation of

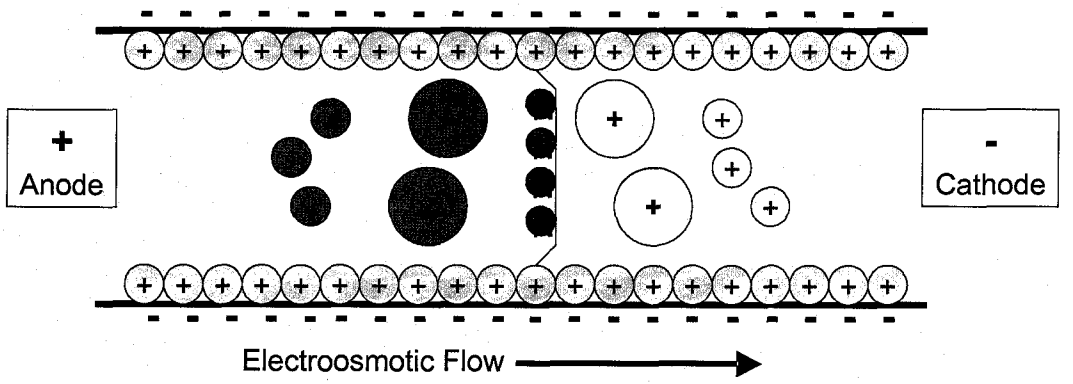

Figure 1.1 Separation of species in capillary zone electrophoresis. Separation occurs due to electrokinetic and electroosmotic flow. Also note the flat flow profile as compared to the parabolic profile seen in pressure driven separations.

charged species in CZE. One major drawback to CZE is its inability to separate neutral species.

MEKC was developed by Terabe to provide a mechanism for the separation of neutral species.[61] In MEKC, molecules spend time partitioning between the aqueous phase and the interior of the micelles which act as a pseudostationary phase with a migration velocity and/or direction that is different from the mobile phase.[62] Micelles are molecular aggregates of surfactant molecules into which analytes can partition based on hydrophobicity, ionic attraction, and/or hydrogen bonding.[38] The concentration at which individual surfactant molecules begin to form micelles is known as the critical micelle concentration (cmc). The amount of time the species spends within the micelle determines the migration time. A neutral analyte which spends no time in the micelle will migrate with the electroosmotic flow, t_0, whereas one which spends all of its time in the micelle will migrate at the micelle migration time, t_{mc}. Molecules which spend time in both phases will migrate at an intermediate time, t_r. A schematic of MEKC is shown in Figure 1.2.[63] The most commonly used surfactant for MEKC is sodium dodecyl sulfate (SDS) which has a cmc in water of approximately 8 mM.[62]

Capillary gel electrophoresis is primarily used for the separation of biopolymers such as DNA. CGE separates charged analytes based on their size [64] and is the choice for high-throughput genome sequencing[65] and the detection of gene mutations.[66] Capillary isoelectric focusing combines the resolving power of gel electrophoresis with CE. In CIEF proteins are separated based on pIs in a pH gradient created by carrier ampholytes. Ampholytes are mixtures of synthetic chemicals with differing pIs. Isotachophoresis is primarily used as an on-column pre-concentration technique.[58] ITP

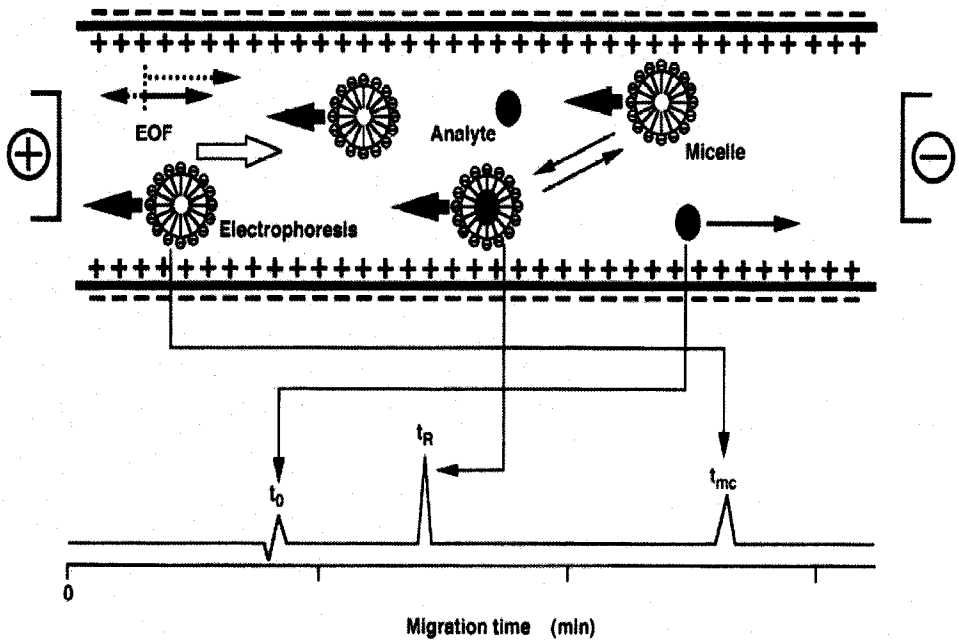

Figure 1.2. Micellar electrokinetic chromatography.[63]

methods were developed by Foret et al.[67] Large sample volumes can be injected when using ITP with at least a 2-fold increase in sensitivity.

1.4 Microchip capillary electrophoresis

Microchip capillary electrophoresis (CE) has, in recent years, had a major impact on the field of chemical separations. Since the first reports of microscale total analysis systems (μTAS),[68] there has been an increase in development of analytical systems in the microchip format because μTAS can be engineered to perform the same analyses as conventional scale systems including DNA sequencing and fragment analysis,[69-72] proteomic separations,[73, 74] and environmental analysis.[75, 76] The great interest in microchip CE and microfluidics in general is due to the potential to generate complex chemical synthesizers and analyzers that provide the power of an entire chemical laboratory on a single chip.[77] Furthermore, significant reductions in sample and reagent volumes, materials and instrumentation cost, and analysis times relative to traditional instrumentation can be achieved using microchip CE and microfluidics.[78]

Early work in microchip CE used glass substrates for fabrication of capillary channels.[79-81] Glass provided an attractive initial material because the fabrication techniques are well established, the surface chemistry is similar to the fused silica used with traditional CE, and the substrates have excellent optical clarity. Glass, however, is relatively difficult and expensive to micromachine, requiring expensive cleanroom time and corrosive etchants (HF). Thermal bonding which is typically used in the fabrication of glass microchips is also considered time consuming. The geometry (depth and width) of channels fabricated in glass is also limited by the etching technique used during

fabrication. Finally, optical quality glass is expensive relative to many other materials that can be used for microfluidics and microchip CE. In light of these problems, several groups have focused efforts on producing microchips from polymer substrates.[78, 82, 83] Numerous polymers have been used for microchip CE, including poly(methylmethacrylate) (PMMA), [82, 84-86] poly(carbonate) (PC),[87, 88] polyester,[83, 89] and poly(dimethylsiloxane) (PDMS).[80, 90] A benefit of most polymeric devices is that they can be fabricated outside a cleanroom environment. One polymer in particular, poly(dimethylsiloxane) (PDMS), has gained a great deal of attention due to the ease of fabrication outside a clean room, the ease of constructing complex geometries, and the relatively inexpensive cost of materials.[91] Furthermore, methods for integrating pumps and other functional elements can be easily integrated in PDMS devices.[92] Chip fabrication will be described in Chapter 2.

1.5 Dissertation Summary

The focus of the research contained within this dissertation was to develop a novel immunoassay to perform multi-analyte protein profiling by coupling cleavable tags with microchip separations. This chemistry, the cleavable tag immunoassay (CTI) is a medium-density heterogeneous immunoassay designed to detect 1-20 proteins simultaneously. This dissertation is divided into 7 chapters. The first chapter (this chapter) contains background information on cardiovascular disease, current protein detection methods, and capillary electrophoresis. The second chapter discusses microchip fabrication and operation and the construction of the laser induced fluorescence (LIF) system on which the majority of data was collected. Chapter 3 focuses on synthetic

methods used to produce the tag library for the immunoassay. In chapter 4, discussion is focused on characterization of the CTI utilizing the components developed in chapters 2 and 3. Chapter 5 focuses on improvements made to separation efficiency of PDMS microchips. Chapter 6 covers solid-phase bead-based kinetics studies on PDMS microchips as preliminary work for integration of the CTI as a micro-total analysis system (μTAS) and the final chapter, chapter 7, summarizes work on this project to date and outlines future directions.

1.6 References

(1) Christenson, R. H.; Azzazy, H. M. E. *Clinical Chemistry* **1998**, *44*, 1855-1864.
(2) Zaninotto, M.; Altinier, S.; Lachin, M.; Celegon, L.; Plebani, M. *Am J Clin Pathol* **1999**, *111*, 399-405.
(3) Lynch, J. R.; Blessing, R.; White, W. D.; Grocott, H. P.; Newman, M. F.; Laskowitz, D. T. *Stroke* **2004**, *35*, 57-63.
(4) Hanash, S. *Nature* **2003**, *422*, 226-232.
(5) Harrison, A.; Amundson, S. *Am J Emerg Med* **2005**, *23*, 371-378.
(6) Plebani, M.; Zaninotto, M. *Int J Clin Lab Res* **1999**, *29*, 56-63.
(7) Bogen, S. A.; Sompuram, S. R. *BioDrugs* **2004**, *18*, 387-398.
(8) Christenson, R. H.; Azzazy, H. M. *Clin Chem* **1998**, *44*, 1855-1864.
(9) Rusnak, R. A.; Stair, T. O.; Hansen, K.; Fastow, J. S. *Ann Emerg Med* **1989**, *18*, 1029-1034.
(10) Rosalki, S. B.; Roberts, R.; Katus, H. A.; Giannitsis, E.; Ladenson, J. H.; Apple, F. S. *Clin Chem* **2004**, *50*, 2205-2213.
(11) Apple, F. S., Henderson, A. Ralph In *Tietz Textbook of Clinical Chemistry* 3ed.; Burtis, C. A., Ashwood, Edward R., Ed.; W.B Saunders Company: Philadelphia, 1999, pp 1178-1203.
(12) Christenson, R. H.; Newby, L. K.; Ohman, E. M. *Md Med J* **1997**, *Suppl*, 18-24.
(13) Bhayana, V.; Henderson, A. R. *Lancet* **1993**, *342*, 1554.
(14) Lin, J. C.; Apple, F. S.; Murakami, M. M.; Luepker, R. V. *Clin Chem* **2004**, *50*, 333-338.
(15) In *Tietz Fundamentals of Clinical Chemistry* Burtis, C. A., Ed.; W.B. Saunders Company: Philadelphia, 2001, pp 682-697.
(16) Rao, M.; Jaber, B. L.; Balakrishnan, V. S. *Semin Dial* **2006**, *19*, 129-135.
(17) Martin, C. M.; Almond, J. *Consult Pharm* **2006**, *21*, 188-191, 195-186, 205-186.
(18) Jernberg, T.; James, S.; Lindahl, B.; Johnston, N.; Stridsberg, M.; Venge, P.; Wallentin, L. *Eur Heart J* **2004**, *25*, 1486-1493.
(19) Bodi, V.; Sanchis, J.; Llacer, A.; Facila, L.; Nunez, J.; Bertomeu, V.; Pellicer, M.; Chorro, F. J. *Int J Cardiol* **2005**, *98*, 277-283.

(20) Panteghini, M.; Cuccia, C.; Pagani, F.; Turla, C. *Clin Cardiol* **1998**, *21*, 394-398.
(21) Apffel, A.; Chakel, J.; Udiavar, S.; Hancock, W. S.; Souders, C.; Pungor, E., Jr. *J Chromatogr A* **1995**, *717*, 41-60.
(22) Wu, C. C.; Yates, J. R., 3rd *Nat Biotechnol* **2003**, *21*, 262-267.
(23) Biemann, K. *Annu. Rev. Biochem.* **1992**, *61*, 977-1010.
(24) Karas, M.; Hillenkamp, F. *Anal. Chem.* **1988**, *60*, 2299-2301.
(25) Zenobi, R.; Knochenmuss, R. *Mass Spectrom. Rev.* **1998**, *17*, 337-366.
(26) Vlahou, A.; Fountoulakis, M. *J Chromatogr B Analyt Technol Biomed Life Sci* **2005**, *814*, 11-19.
(27) O'Farrell, P. H. *J. Biol. Chem.* **1975**, *250*, 4007-4021.
(28) Fountoulakis, M.; Juranville, J. F.; Tsangaris, G.; Suter, L. *Amino Acids* **2004**, *26*, 27-36.
(29) Fountoulakis, M.; Juranville, J. F. *Anal Biochem* **2003**, *313*, 267-282.
(30) Wilson, D. S.; Nock, S. *Angew Chem Int Ed Engl* **2003**, *42*, 494-500.
(31) Zhu, H.; Snyder, M. *Curr Opin Chem Biol* **2001**, *5*, 40-45.
(32) Ekins, R. P. *J Pharm Biomed Anal* **1989**, *7*, 155-168.
(33) Templin, M. F.; Stoll, D.; Schrenk, M.; Traub, P. C.; Vohringer, C. F.; Joos, T. O. *Trends Biotechnol* **2002**, *20*, 160-166.
(34) Ekins, R.; Chu, F. *Ann Biol Clin (Paris)* **1992**, *50*, 337-353.
(35) Huang, R. P. *Front Biosci* **2003**, *8*, d559-576.
(36) Stoll, D.; Templin, M. F.; Schrenk, M.; Traub, P. C.; Vohringer, C. F.; Joos, T. O. *Front Biosci* **2002**, *7*, c13-32.
(37) Hage, D. S.; Nelson, M. A. *Anal. Chem.* **2001**, *73*, 199A-205A.
(38) Schultz, N. M.; Tao, L.; Rose, D. J.; Kennedy, R. T. In *Handbook of Capillary Electrophoresis,* 2nd ed.; Landers, J. P., Ed.; CRC Press: Boca Raton, 1997, pp 611-637.
(39) Hafner, F. T.; Kautz, R. A.; Iverson, B. L.; Tim, R. C.; Karger, B. L. *Anal. Chem.* **2000**, *72*, 5779-5786.
(40) Clark, B. R., Engvall, E. In *Enzyme-Immunoassay*; Maggio, E. T., Ed.; CRC Press, Inc.: Boca Raton, 1980, pp 167-179.
(41) Yeung, W. S.; Luo, G. A.; Wang, Q. G.; Ou, J. P. *J Chromatogr B* **2003**, *797*, 217-228.
(42) Bao, J. J. *J Chromatogr B* **1997**, *699*, 463-480.
(43) Guzman, N. A.; Phillips, T. M. *Anal. Chem.* **2005**, *77*, 61A-67A.
(44) Nielsen, R. G.; Rickard, E. C.; Santa, P. F.; Sharknas, D. A.; Sittampalam, G. S. *J. Chromatogr.* **1991**, *539*, 177-185.
(45) Liu, X.; Xu, Y.; Ip, M. P. *Anal. Chem.* **1995**, *67*, 3211-3218.
(46) Schultz, N. M.; Huang, L.; Kennedy, R. T. *Anal. Chem.* **1995**, *67*, 924-929.
(47) Evangelista, R. A.; Chen, F. T. *J Chromatogr A* **1994**, *680*, 587-591.
(48) Phillips, T. M.; Smith, P. *Biomed Chromatogr* **2003**, *17*, 182-187.
(49) Chiem, N.; Harrison, D. J. *Anal. Chem.* **1997**, *69*, 373-378.
(50) Koutny, L. B.; Schmalzing, D.; Taylor, T. A.; Fuchs, M. *Anal. Chem.* **1996**, *68*, 18-22.
(51) Chiem, N. H.; Harrison, D. J. *Clin Chem* **1998**, *44*, 591-598.
(52) Wang, Q.; Luo, G.; Ou, J.; Yeung, W. S. *J Chromatogr A* **1999**, *848*, 139-148.
(53) Heegaard, N. H.; Kennedy, R. T. *J Chromatogr B* **2002**, *768*, 93-103.

(54) Guzman, N. A. *J Chromatogr B* **2000**, *749*, 197-213.
(55) Phillips, T. M. *Anal. Chim. Acta* **1998**, *372*, 209-218.
(56) Jorgenson, J. W.; Lukacs, K. D. *Anal. Chem.* **1981**, *53*, 1298-1302.
(57) Jorgenson, J. W.; Lukacs, K. D. *Science* **1983**, *222*, 266-272.
(58) Oda, R. P.; Landers, J. P. In *Handbook of Capillary Elecrophoresis,* 2nd ed.; Landers, J. P., Ed.; CRC Press: Boca Raton, 1997, pp 1-47.
(59) Rocheleau, M. J. a. D., N. J. *J. Microcol. Sep.* **1992**, *4*, 449.
(60) Mammen, M.; Carbeck, J. D.; Simanek, E. E.; Whitesides, G. M. *Journal of the American Chemical Society* **1997**, *119*, 3469-3476.
(61) Terabe, S. T., Otsuka, K., and Ando, T. *Anal. Chem.* **1985**, *57*, 834.
(62) Mazzeo, J. R. In *Handbook of Capillary Electrophoresis*; Landers, J. P., Ed.; CRC Press: Boca Raton, 1997, pp 49-73.
(63) Watanabe, T.; Terabe, S. *J Chromatogr A* **2000**, *880*, 311-322.
(64) Garcia-Canas, V.; Gonzalez, R.; Cifuentes, A. *Journal of Separation Science* **2002**, *25*, 577-583.
(65) Dolnik, V. *Journal of Microcolumn Separations* **1994**, *6*, 315-330.
(66) Ren, J. C. *J. Chromatogr. B* **2000**, *741*, 115.
(67) Rashkovetsky, L. G.; Lyubarskaya, Y. V.; Foret, F.; Hughes, D. E.; Karger, B. L. *J. Chrom. A* **1997**, *781*, 197-204.
(68) Manz, A.; Graber, N.; Widmer, H. M. *Sensors and Actuators B-Chemical* **1990**, *1*, 244-248.
(69) Wang, H.; Zhang, Y.; Yan, B.; Liu, L.; Wang, S. P.; Shen, G. L.; Yu, R. Q. *Clinical Chemistry* **2006**, *52*, 2065-2071.
(70) Qi, D. M.; Bao, Y. Z.; Weng, Z. X.; Huang, Z. M. *Polymer* **2006**, *47*, 4622-4629.
(71) Hashimoto, M.; Barany, F.; Soper, S. A. *Biosens Bioelectron* **2006**, *21*, 1915-1923.
(72) Bienvenue, J. M.; Duncalf, N.; Marchiarullo, D.; Ferrance, J. P.; Landers, J. P. *J Forensic Sci* **2006**, *51*, 266-273.
(73) He, Z. H.; Gao, N.; Jin, W. R. *Journal of Chromatography B-Analytical Technologies in the Biomedical and Life Sciences* **2003**, *784*, 343-350.
(74) Ressine, A.; Ekstrom, S.; Marko-Varga, G.; Laurell, T. *Anal. Chem.* **2003**, *75*, 6968-6974.
(75) Hompesch, R. W.; Garcia, C. D.; Weiss, D. J.; Vivanco, J. M.; Henry, C. S. *Analyst* **2005**, *130*, 694-700.
(76) Sano, M.; Nishino, I.; Ueno, K.; Kamimori, H. *Journal of Chromatography B-Analytical Technologies in the Biomedical and Life Sciences* **2004**, *809*, 251-256.
(77) Jackson, D. J.; Naber, J. F.; Roussel, T. J., Jr.; Crain, M. M.; Walsh, K. M.; Keynton, R. S.; Baldwin, R. P. *Anal Chem* **2003**, *75*, 3643-3649.
(78) Duffy, D. C.; McDonald, J. C.; Schueller, O. J. A.; Whitesides, G. M. *Anal Chem* **1998**, *70*, 4974-4984.
(79) Manz, A.; Harrison, D. J.; Verpoorte, E. M. J.; Fettinger, J. C.; Paulus, A.; Ludi, H.; Widmer, H. M. *J. Chromatogr.* **1992**, *593*, 253-258.
(80) Harrison, D. J.; Fluri, K.; Seiler, K.; Fan, Z. H.; Effenhauser, C. S.; Manz, A. *Science* **1993**, *261*, 895-897.
(81) Harrison, D. J.; Manz, A.; Fan, Z. H.; Ludi, H.; Widmer, H. M. *Analytical Chemistry* **1992**, *64*, 1926-1932.

(82) Soper, S. A.; Ford, S. M.; Qi, S.; McCarley, R. L.; Kelly, K.; Murphy, M. C. *Analytical Chemistry* **2000**, *72*, 642A-651A.
(83) Fiorini, G. S.; Lorenz, R. M.; Kuo, J. S.; Chiu, D. T. *Analytical Chemistry* **2004**, *76*, 4697-4704.
(84) Martynova, L.; Locascio, L. E.; Gaitan, M.; Kramer, G. W.; Christensen, R. G.; MacCrehan, W. A. *Anal Chem* **1997**, *69*, 4783-4789.
(85) Soper, S. A.; Ford, S. M.; Xu, Y.; Qi, S.; McWhorter, S.; Lassiter, S.; Patterson, D.; Bruch, R. C. *J Chromatogr A* **1999**, *853*, 107-120.
(86) Jikun Liu, T. P.; Woolley, A. T.; Lee, M. L. *Anal Chem* **2004**, *76*, 6948-6955.
(87) Liu, Y.; Wipf, D. O.; Henry, C. S. *Analyst* **2001**, *126*, 1248-1251.
(88) Nakamura, J.; La, D. K.; Swenberg, J. A. *J. Biol. Chem.* **2000**, *275*, 5323-5328.
(89) Uchiyama, K.; Nakajima, H.; Hobo, T. *Analytical and Bioanalytical Chemistry* **2004**, *379*, 375-382.
(90) Fogarty, B. A.; Heppert, K. E.; Cory, T. J.; Hulbutta, K. R.; Martin, R. S.; Lunte, S. M. *Analyst* **2005**, *130*, 924-930.
(91) Hu, S.; Ren, X.; Bachman, M.; Sims, C. E.; Li, G. P.; Allbritton, N. *Anal Chem* **2002**, *74*, 4117-4123.
(92) Unger, M. A.; Chou, H. P.; Thorsen, T.; Scherer, A.; Quake, S. R. *Science* **2000**, *288*, 113-116.

CHAPTER 2

MICROCHIP CE-LIF

As stated in chapter 1, early work in microchip CE focused on the use of glass substrates for fabrication of capillary channels.[1-3] Even though glass has several advantages for microchip separations over polymer substrates, it also has several disadvantages including materials cost and fabrication cost and time. In light of this, several groups have focused efforts on producing microchips from various polymeric substrates including thermoset polyester (TPE), poly(methyl methyacrylate) (PMMA) and PDMS.[4-6] PDMS has several attractive features including ease and cost of fabrication. PDMS also has optical properties similar to glass.[7] Because of these benefits, PDMS has become widely used in microchip fabrication. In this chapter, the complete process for assembling a PDMS microchip is described. This process includes fabrication of a master mold, PDMS production and sealing the chip together. The fabrication of poly(dimethylsiloxane) (PDMS) microchips using SU-8 molding has been described previously[5, 8-11] and is detailed in the text that follows.

2.1 Mold master production

A 3 inch silicon wafer was first cleaned with piranha solution (7:3 H_2SO_4:H_2O_2) for approximately 5 min followed by a thorough rinse with DI water. It was placed in a 65 °C oven to dry for 15 min. The dry wafer was coated with SU-8 2035 negative

photoresist (1 mL/inch of wafer) using a spin coater. The coated wafer was put through a soft bake process by first placing it on a 65 °C hotplate for 3 min followed by a 95 °C hotplate for 5 min. At this point a mask was placed on the coated wafer and the assembly exposed to a near-UV light source for 7 sec. The exposed wafer was post-baked on the 65 °C hot plate for 2 min followed by the 95 °C hot plate for 6 min. The unexposed photoresist was removed by immersing the wafer in propylene glycol methyl ether acetate for at least 30 min and the wafer placed back on the 65 °C hot plate for at least 30 min to remove any solvent remaining in the cured photoresist and to increase the adhesion of the SU-8 to the wafer. This process leaves a positive relief pattern on the surface of the silicon wafer. Once dry, the wafer was rinsed with acetone, methanol and DI water and allowed to dry. To increase hydrophobicity and prevent the adhesion of PDMS to the new mold, it was placed in a covered glass crystallization dish with 1 mL hexadimethyldisilazane (HMDS) and placed in a 65 °C oven for a minimum of 6 hours prior to PDMS molding. Figure 2.1 shows the steps involved in mold master production.

2.2 PDMS chip fabrication

A degassed mixture of Sylgard 184 elastomer and curing agent (10:1) (Dow Corning, Midland, MI) was poured on the mold master as well as spincoated on a blank glass slide (55 x 75 cm) at 2000 rpm and allowed to cure in a 65°C oven for at least 2hr. The PDMS piece removed from the mold master contains three of the four channel walls with the blank piece being the fourth wall. The glass slide was used instead of the typical blank piece of PDMS because of the small working distance of the optical lens in the LIF

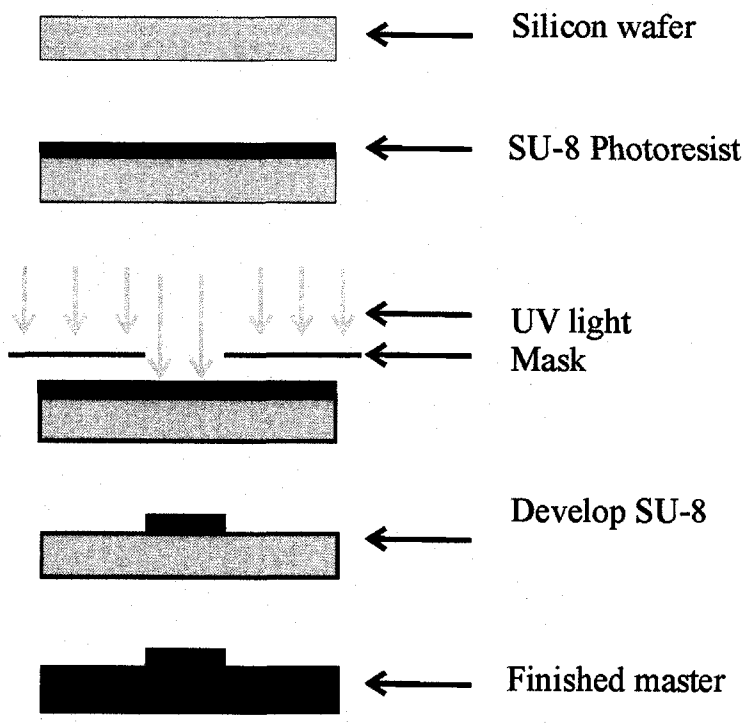

Figure 2.1. Fabrication of mold master.

setup. The cured PDMS was removed from the mold and the reservoirs punched using a standard 6mm hole punch. The surfaces of the two pieces of PDMS were cleaned using methanol and dried in a 65 °C oven for 15 min. Following this the two pieces were placed in an air plasma cleaner (Harrick Plasma Cleaner/Sterilizer PDS-32G) and oxidized at high power for 30 s. The two pieces of PDMS were then immediately brought into conformal contact to form an irreversible seal which is strong enough such that the two pieces could not be pulled apart without destroying the microchip. The process outlined above is illustrated in Figure 2.2.

2.3 Fluorescence detection methods for microchip CE

Unless otherwise noted, all data was collected using laser-induced fluorescence coupled to a photomultiplier tube (PMT) for detection. The detection point was 2.5 cm from the double T injector. The excitation source was a solid state laser (λ_{ex}= 475 nm) (B & W Tech, Inc.) and a PMT (Hamamatsu) was used for fluorescence detection. The setup was similar to the epi-fluorescence system in the inverted microscope and was based on similar designs reported by Johnson and Landers.[12] The laser light was first reflected at a 90° angle with respect to the laser housing using a dichroic mirror and then focused on the microchip channel using an objective lens (40x). The dichroic mirror has a wavelength cutoff between the excitation and emission wavelength of fluorescein in order to allow the emitted light to pass through the mirror to the PMT for detection via a second series of lenses and mirrors. Since the dichroic mirror does not block 100 % of the blue laser light from traveling to the PMT, a band-pass filter with a center wavelength of

A)

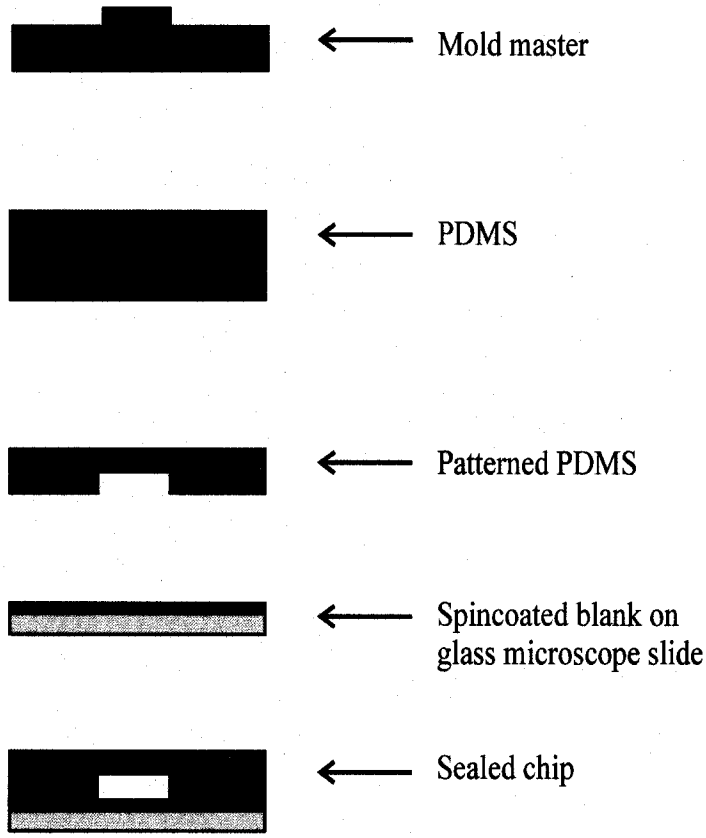

B)

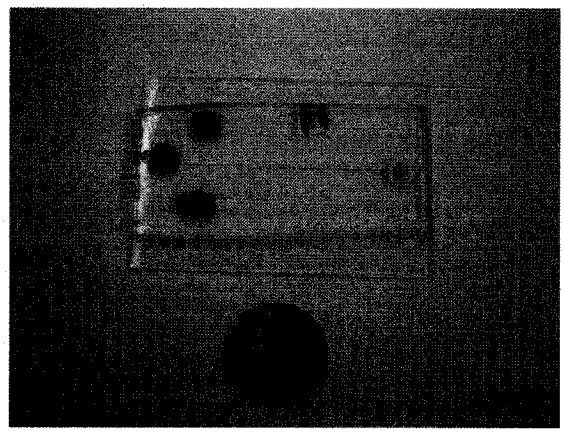

Figure 2.2. PDMS microchip assembly. A) Schematic of assembly process. B) Finished chip. A quarter is included in B for size comparison.

510 nm (± 10 nm) is placed directly in front of the PMT detection window. A diagram of the LIF system is shown in Figure 2.3.

Some data was collected using an inverted microscope (Nikon, TE-2000U) using epi-fluorescence with a Hg arc lamp as an excitation source and a CCD camera for detection. Data was analyzed using Metamorph Imaging System software (Molecular Devices). In these cases, the difference in detection methods will be stated.

2.4 Microchip operation

Sample introduction on a microchip is performed in three different ways, 1) hydrodynamic injection,[13] 2) hydrostatic pressure injection,[14] and 3) electrokinetic injection.[15] Electrokinetic injection can be further divided into gated and pinched injection.[16] A 250 μm double-T injector with pinched injection was employed for all experiments.[16-18] Pinched injection allows for more control over sample volume and reduces electrokinetic bias compared to gated injection. During pinched injection a high potential (+410 V) is applied to the sample reservoir and a negative bias (-160 V) is applied to the sample waste while the buffer reservoir and buffer waste reservoir are kept at +410 V to draw the sample across the separation channel to the sample waste which forms the sample plug in the channel. The buffer waste reservoir is normally kept at ground during injection which can lead to a minor amount of diffusion down the separation channel so in order to confine the sample plug to the double T intersection, a potential (+410 V) is applied to the buffer waste reservoir during injection to yield a true pinched injection. Both variations of pinched injection were imaged on an inverted microscope using fluorescein isothiocyanate (FITC) as the analyte and it was found that

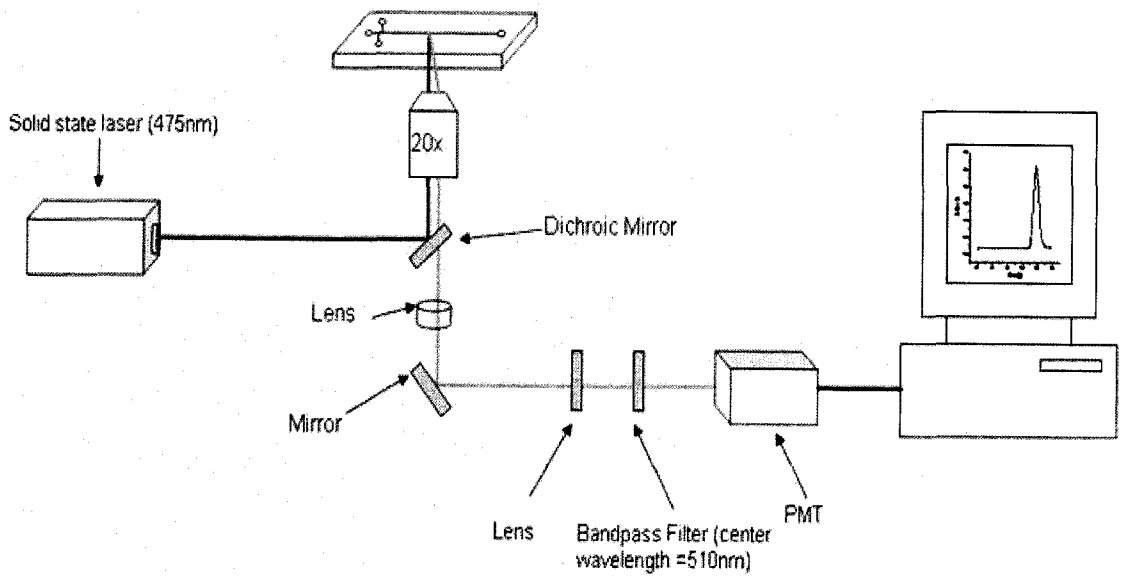

Figure 2.3. Schematic of CE-LIF instrumentation.

the sample plug is completely confined to the double T intersection with the true pinched injection whereas some degree of diffusion occurs when the buffer waste reservoir is kept at ground during injection. During separation, the buffer reservoir is switched to a higher potential (+1100 V) and buffer waste reservoir was set to ground in order to cause the sample plug to move down the channel towards the detector (Figure 2.4). A pull-back voltage of +410 V is applied during separation to the sample and sample waste reservoirs to prevent leakage into the separation channel. An injection volume of 625 pL was used for microchips coupled to fluorescence detection as determined experimentally with fluorescence video microscopy. All chips were preconditioned with a 30 min NaOH (0.1M) rinse followed by a 30 min conditioning step with buffer prior to use.

2.5 Characterization of the system

Since the use of microchip CE-LIF was new to the group and myself several studies had to be conducted to ensure the system was optimized. After the LIF system was completely assembled, FITC was run to test the functionality of the setup. FITC is also run as a standard to troubleshoot the LIF system. The first optimization study was performed to determine the ideal distance from the injector for detection. These studies were done using FTED, FTPD, and FTHD (synthesis described in Chapter 3) all at 1μM concentrations. Data was collected at 1, 2 and 3 cm from the injector. As shown in Figure 2.5, the signal is much larger at 1 cm when compared to 3 cm; however, there is little to no resolution between the three analytes. The products begin to separate at 2 cm and are completely resolved at 3 cm. The problem at 3 cm is the low signal. Based on these findings the detection point was set at 2.5 cm down the channel from the injector and as

A)

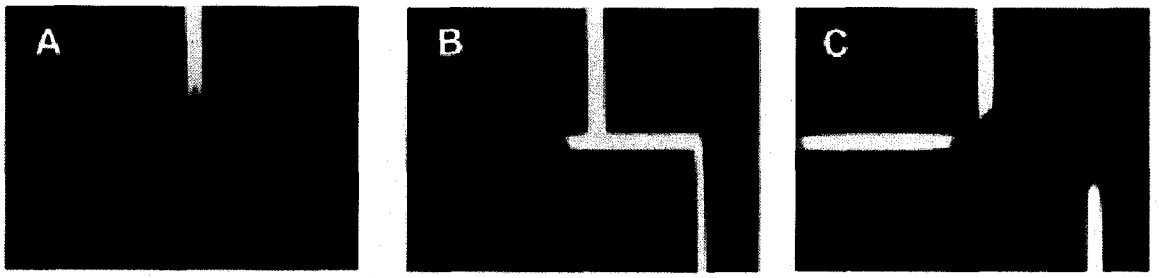

B)

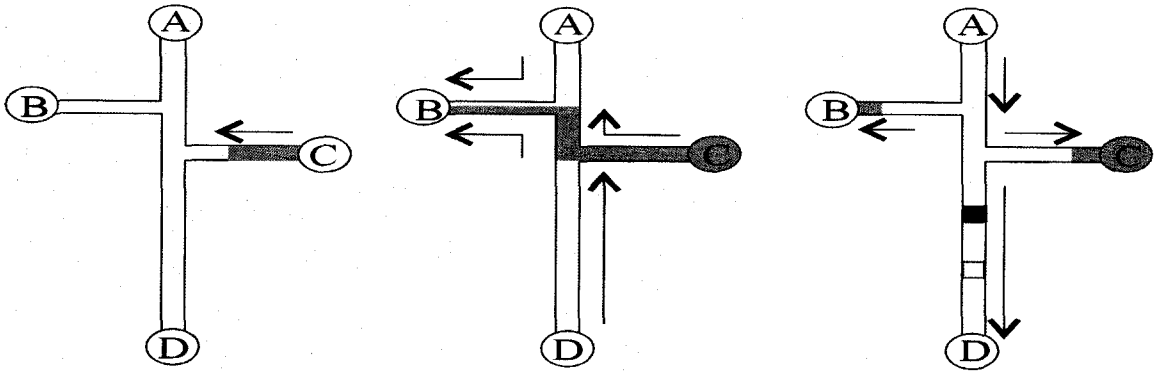

Figure 2.4. Pinched injection. A) Fluorescent images of pinched injection.[16] B) Schematic of flow during pinched injection corresponding to the images in A. The labels in B are as follows: A. Buffer reservoir, B. Sample waste, C. Sample, D. Buffer waste. The applied potentials during injection are A= +410V, B= -160V, C= +410V, and D= +410V. During separation A is switched to +1100V, B to +410V and D is switched to ground.

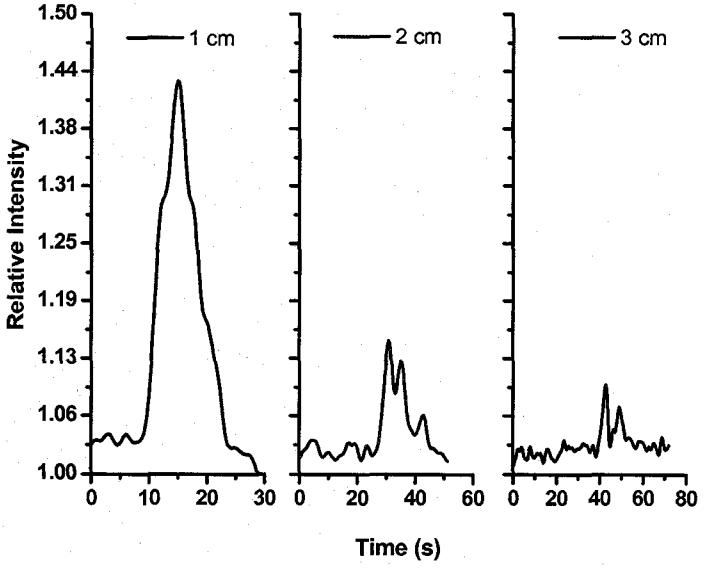

Figure 2.5. Comparison of detection distances. Analytes used were FTED, FTPD, and FTHD. Left) Electrpherogram collected at 1 cm from injection. Middle) Electropherogram collected at 2 cm from injection. Right) Electropherogram collected at 3 cm from injection. Experimental conditions: Field strength: 200 V/cm; Pinched injection time: 30 s; BGE: 10 mM tetraborate, 1.2 mM SDS. Detection performed using LIF system with a PMT for detection and a solid state laser for excitation (λ= 475 nm).

stated previously, was performed using a PMT. The data collection program used for the CE-LIF system was written by the PMT manufacturer (Hamamatsu) with a built-in signal integration function which also needed to be optimized so that analytes at low concentrations (low nM to high pM) could be detected and resolved from each other. If the integration was set too low, the analytes were not detected and in contrast if the integration time was set too high the analytes were detected but could show up as one peak instead of multiple analytes. Several concentrations of FITC and FTED in the low nM range were tested while varying the integration time and it was found that the ideal integration was between 100 and 250 ms.

2.6 Summary

This chapter outlined the processes involved in PDMS microchip production including the mold making process, as well as the start-to-finish assembly of a typical microchip used in the cleavable tag immunoassay. It also covered the assembly of the LIF system used for analysis and injection methods used in microchip CE. Optimization of the newly built microchip CE-LIF system was performed. Further optimization of separation efficiency is discussed in Chapter 5.

2.7 References

(1) Harrison, D. J.; Manz, A.; Fan, Z. H.; Ludi, H.; Widmer, H. M. *Anal. Chem.* **1992**, *64*, 1926-1932.

(2) Manz, A.; Harrison, D. J.; Verpoorte, E. M. J.; Fettinger, J. C.; Paulus, A.; Ludi, H.; Widmer, H. M. *J. Chromatogr.* **1992**, *593*, 253-258.

(3) Harrison, D. J.; Fluri, K.; Seiler, K.; Fan, Z. H.; Effenhauser, C. S.; Manz, A. *Science* **1993**, *261*, 895-897.

(4) Soper, S. A.; Ford, S. M.; Qi, S.; McCarley, R. L.; Kelly, K.; Murphy, M. C. *Anal. Chem.* **2000**, *72*, 642A-651A.

(5) McDonald, J. C.; Duffy, D. C.; Anderson, J. R.; Chiu, D. T.; Wu, H. K.; Schueller, O. J. A.; Whitesides, G. M. *Electrophoresis* **2000**, *21*, 27-40.
(6) Fiorini, G. S.; Lorenz, R. M.; Kuo, J. S.; Chiu, D. T. *Anal. Chem.* **2004**, *76*, 4697-4704.
(7) Hu, S.; Ren, X.; Bachman, M.; Sims, C. E.; Li, G. P.; Allbritton, N. *Anal Chem* **2002**, *74*, 4117-4123.
(8) Liu, Y.; Fanguy, J. C.; Bledsoe, J. M.; Henry, C. S. *Anal Chem* **2000**, *72*, 5939-5944.
(9) Liu, Y.; Vickers, J. A.; Henry, C. S. *Anal Chem* **2004**, *76*, 1513-1517.
(10) Liu, Y.; Wipf, D. O.; Henry, C. S. *Analyst* **2001**, *126*, 1248-1251.
(11) McDonald, J. C.; Whitesides, G. M. *Acc. Chem. Res.* **2002**, *35*, 491-499.
(12) Johnson, M. E.; Landers, J. P. *Electrophoresis* **2004**, *25*, 3513-3527.
(13) Backofen, U.; Matysik, F. M.; Lunte, C. E. *Anal. Chem.* **2002**, *74*, 4054-4059.
(14) Gai, H.; Yu, L.; Dai, Z.; Ma, Y.; Lin, B. *Electrophoresis* **2004**, *25*, 1888-1894.
(15) Tsai, C. H.; Yang, R. J.; Tai, C. H.; Fu, L. M. *Electrophoresis* **2005**, *26*, 674-686.
(16) Garcia, C. D.; Liu, Y.; Anderson, P.; Henry, C. S. *Lab Chip* **2003**, *3*, 324-328.
(17) Oleschuk, R. D.; Shultz-Lockyear, L. L.; Ning, Y. B.; Harrison, D. J. *Anal. Chem.* **2000**, *72*, 585-590.
(18) Jacobson, S. C.; Hergenroeder, R.; Koutny, L. B.; Ramsey, J. M. *Anal Chem* **1994**, *66*, 2369-2373.

CHAPTER 3

BUILDING A TAG LIBRARY

The CTI tag library has been generated by utilizing synthetic methods well-known to the bioconjugate community. Each synthesis pathway was chosen such that it would contain at most three steps and use commercially available starting materials for easy replication in other laboratories. The methods used for tag synthesis produce tags composed of four functional elements: 1) the detection group, 2) the spacer group, 3) a chemically cleavable group, and 4) the conjugation group. The detection group is a fluorophore that can be easily detected by microchip CE. Initially, fluorescein was used as the detection group because it can be easily detected by laser induced fluorescence. The spacer group provides controlled variability in the charge-to-hydrodynamic radius to provide resolution during separation. Varying the chemistry of the spacer group alone can quickly and easily generate a large tag library. Simple diamines were used as the spacer group for the first set of tags. Ten of the hydrophilic amino acids in lengths up to 4-mers instead of the diamines could also be used to easily produce an additional 40 different tags using the same two step synthesis. The cleavable group is a chemical bond that can be broken by some means (chemical reaction, light, heat, etc) to produce a fragment. In all tags used in the current CTI, the cleavable group is a disulfide which is easily reduced by several different mild reducing agents. The conjugation group is responsible for attaching the tag to the detection antibody and can vary from a covalent attachment to

biotin-avidin interactions. All four of these groups can be varied to provide added resolution in the separation. All tags in the current library are cross-linked cleavable fluorescent tags with an affinity for streptavidin. The CTI tags and the resulting cleaved fragments used in this work are shown in Figure 3.1

3.1 Experimental methods

3.1.1 FRB sysnthesis

The first library of tags was produced using a simple two step synthesis with diamines that differed in mass. Each tag in this set of tags is generically known as FRB where R represents an ethylenediamine (C2), tetramethylenediamine (C4), or hexamethylenediamine (C6) spacer. Originally, FTED (fluorescein thiocarbamyl ethylenediamine) synthesis was carried out in tetrahydrofuran (THF). The product was then purified using flash chromatography with 100% methanol as the mobile phase. Even though a pure product could be obtained through this process, the amount of drying time required was excessive (on the order of days). Instead, the chosen FTED synthesis was adapted from a paper by Bertram et al.[1] Fluorescein isothiocyanate (FITC) (100mg) was reacted with ethylenediamine (C2) (200mg) in 10mL methanol containing 10mL/L triethylamine overnight at room temperature (22±2°C) to produce FTED which was washed three times with methanol and allowed to dry under a constant air flow. The final synthesis step was the reaction of FTED with Sulfo-NHS-SS-biotin in a 1:1 molar ratio at 4°C over 4 hrs. The synthesis steps can be seen in Figure 3.2. In order to monitor synthesis progress, electropherograms and NMR spectra were collected for each step. The ethylenediamine used in this reaction was first distilled over KOH in order to remove any

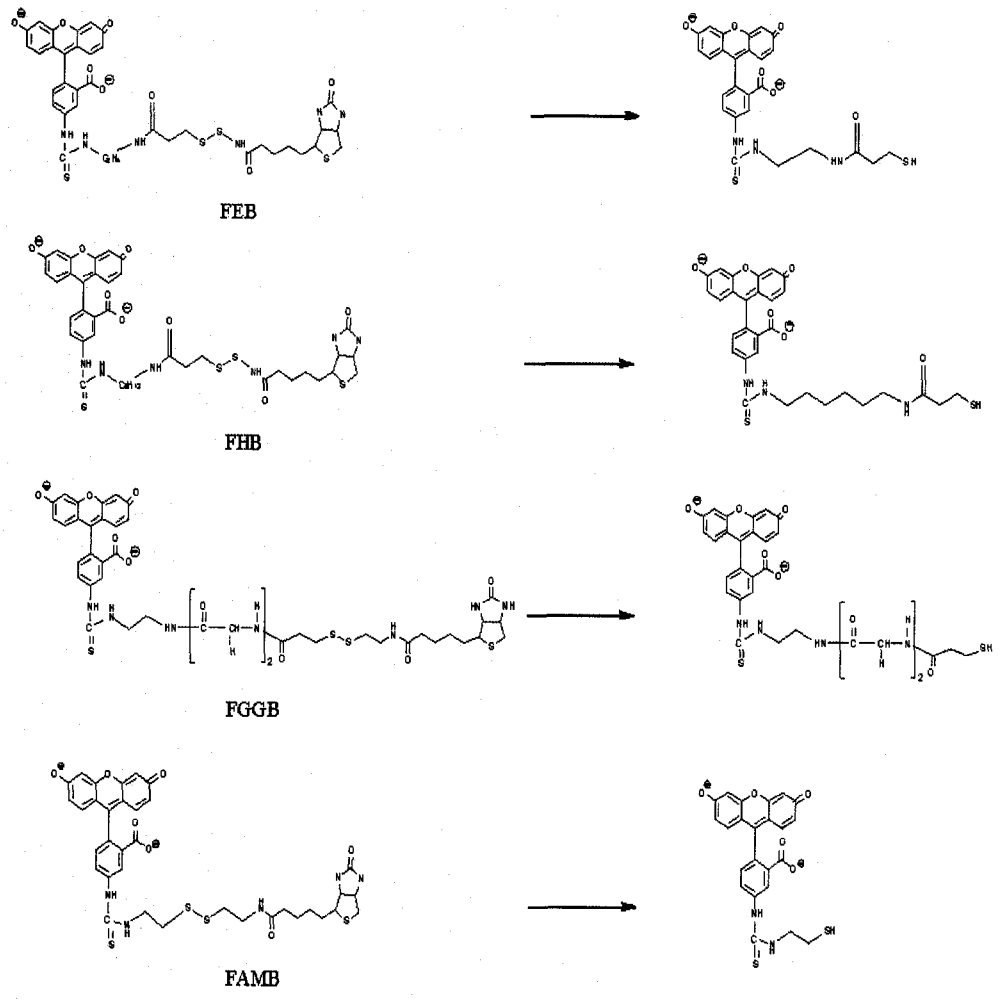

Figure 3.1. CTI tags and resulting fragments. FEB and FHB produced using FRB synthesis. FEGGB produced using gylcine spacer synthesis. FAMB synthesized using cystamine pathway.

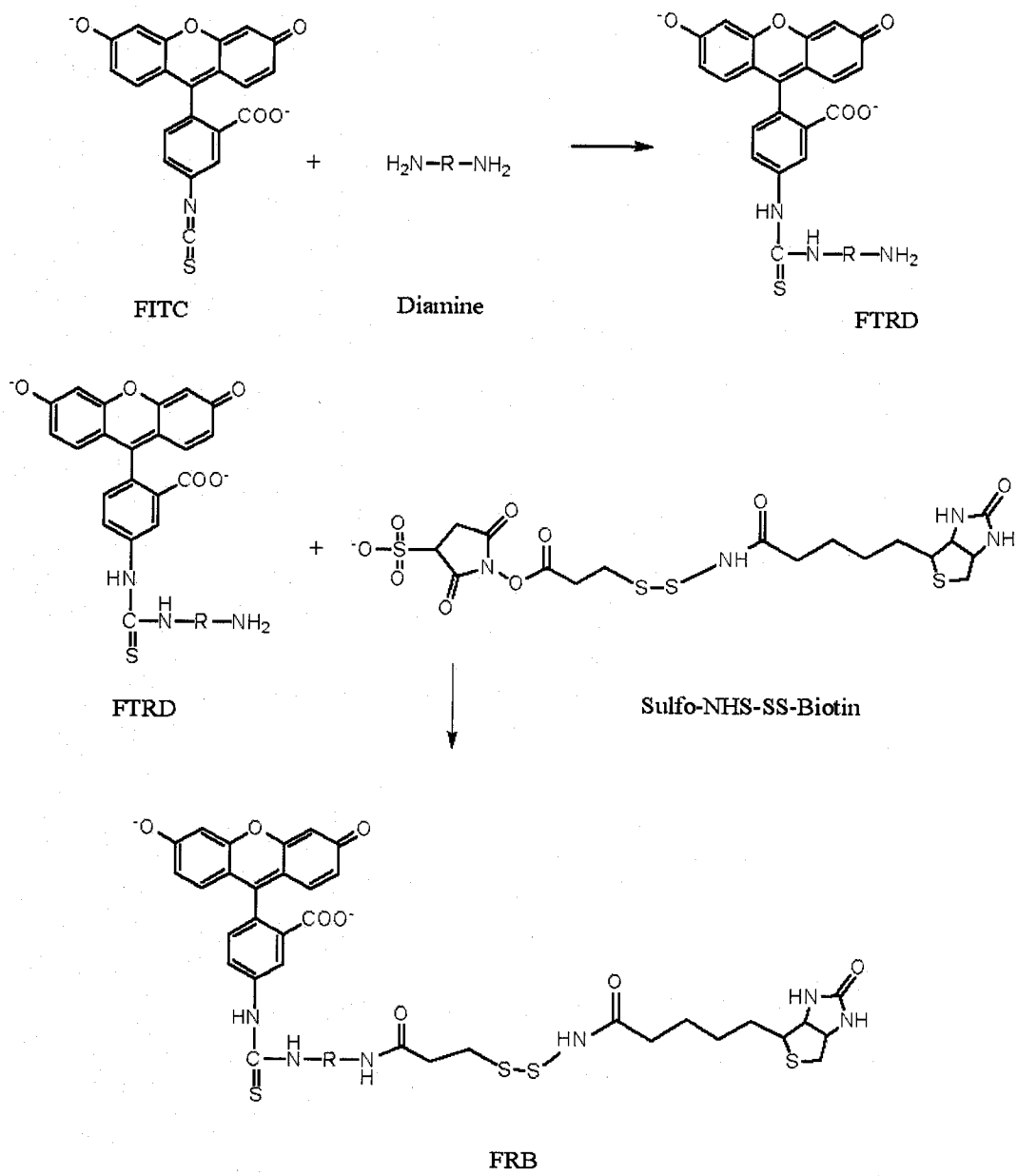

Figure 3.2. FRB synthesis.

water. Once dry, the ethylenediamine was placed in a vial with molecular sieves for storage at 4 °C.

In addition to the FTED synthesis, the first synthesis step has been adapted to produce 2 other unique tags. These tags were produced by replacing the ethylenediamine (C2) with tetramethylenediamine (C4), or hexamethylenediamine (C6) to form tags with 4- and 6-carbon spacer groups respectively. Electropherograms of all three of these tags are shown in Figure 3.3 to demonstrate difference in mobilities of the tags. The intermediate step (FTED, FTPD, and FTHD) are also included in the figure for reference.

3.1.2 Carbodiimide chemistry using glycine peptides as spacer groups

In this synthetic protocol, dimer and trimer peptides of glycine (Gly) were used as spacer groups to form FEGGB and FEGGGB respectively. The spacer (Gly_n) (2 mM) was first reacted with Sulfo-NHS-SS-biotin (2 mM) for 2 hr at room temperature (22 ± 2 °C) in sodium phosphate buffer (20 mM, pH 7.4) followed by the addition of 1-ethyl-3-(3-dimethylaminopropyl) carbodiimide hydrochloride (EDC) (5 mM) and FTED (500 μM) prepared according to the synthesis described previously. The second synthesis step was carried out overnight at 4 °C. In addition to the use of FTED, FTHD was also used for the second step to produce FHGGB and FHGGGB. The carbodiimide tag synthesis is shown in Figure 3.4.

3.1.3 Cystamine containing tag

The first cystamine containing tag, known as FAMB, is synthesized in two steps. In the first step, cystamine dihydrochloride (180 mg) was dissolved in a mixture of

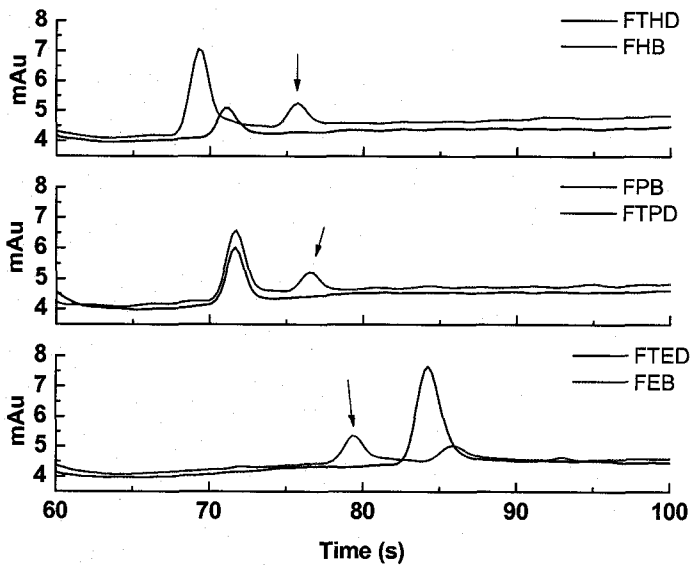

Figure 3.3. Demonstration of differing electrophoretic mobilities for three FRB tags. A. FHB, B. FPB, and C. FEB. The green traces correspond to the final products. FTHD, FTPB, and FTED are included for reference. These three intermediate products are reacted in excess in the second synthesis step and are therefore still present in the final product solution.

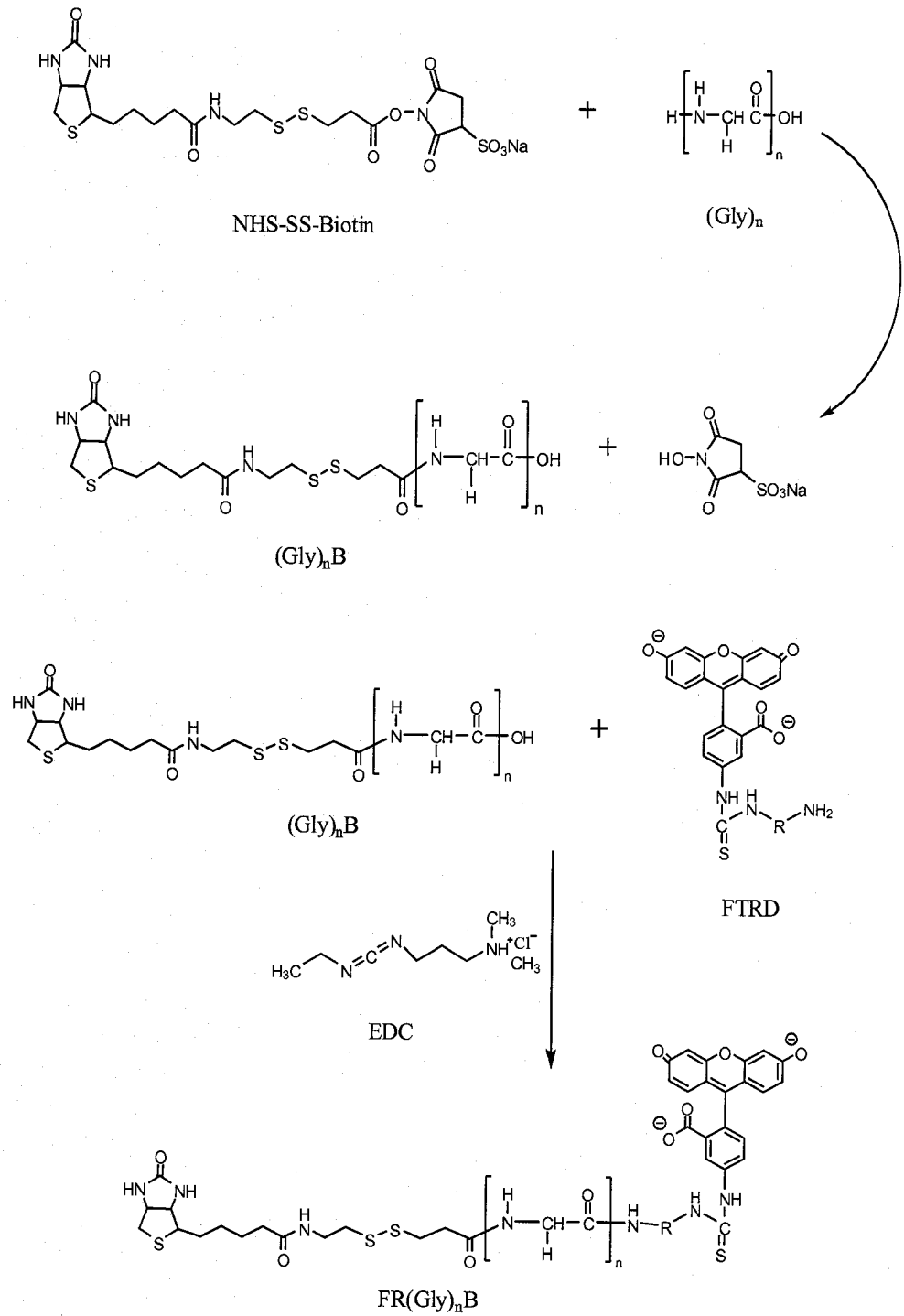

Figure 3.4. FRGGB and FRGGGB synthesis.

methanol (5 mL), water (2 mL) and triethylamine (TEA) (40 μL). FITC (51 mg) was dissolved in methanol (5 mL) and TEA (50 μL) and added dropwise over 30 min to the cystamine dihydrochloride solution. The reaction was allowed to proceed overnight at room temperature (22 ± 2 °C) with stirring. The product was evaporated the following day to a volume of roughly 5 mL by flowing a constant air stream over the solution and precipitated with a 10:1 mixture of acetonitrile:methanol. The solid precipitate was washed with the same acetonitrile:methanol mixture three times and dried under a constant air stream. This process yields approximately 30 mg FAM and the presence of the product was confirmed by CE with the only impurity is small amount of double labeled cystamine (FITC-cystamine-FITC). In the final step, the purified product (1.8 mM) was reacted with Sulfo-NHS-biotin (1.8 mM) in phosphate buffer (20 mM, pH 7.4) overnight at 4°C. The presence of the product was again confirmed using conventional CE. This synthesis is shown in Figure 3.5 and was developed with the help of my colleague Brian M. Murphy.

3.1.4 Other amino acids as spacer groups

The same steps and reaction conditions as described in section 3.1.1 were used to produce tags containing arginine (Arg) and lysine (Lys) as the spacer groups with one exception, 1 mL of DI water was used to dissolve the two amino acids prior to performing the synthesis in the triethylamine and methanol mixture. Isopropanol was used to precipitate FITC-Arg and FITC-Lys. The intermediate products were rinsed three times with isopropanol (10 mL) and allowed to dry under a constant air flow. FITC-Arg

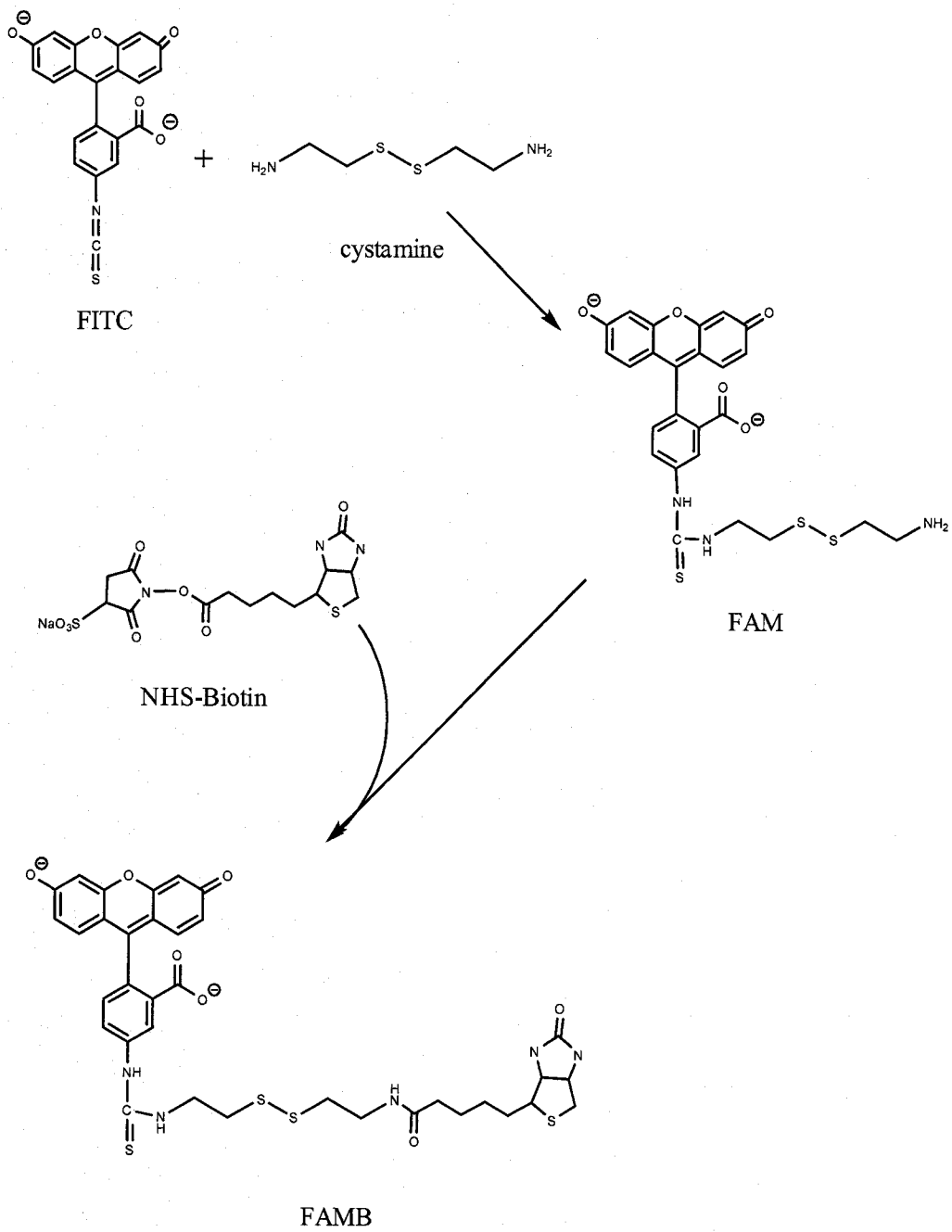

Figure 3.5. FAMB synthesis.

and FITC-Lys were reacted with Sulfo-NHS-SS-biotin as described in section 3.1.1 to obtain the final product.

3.1.5 Variation of the cleavable group: sulfones

The synthesis of this tag was adapted from methods provided by Pierce Biotechnology, Inc.[2] *Bis*[2-succinimidyloxycarbonyloxy)ethyl]sulfone (BSOCOES) (3 mg) was dissolved in DMSO to achieve a final concentration of 25 mM. The dissolved BSOCOES was added to the sample containing FITC-ethylenediamine (300 μM) and biotin-ethylenediamine (300 μM) to achieve a 20-fold excess of BSOCOES. This solution was agitated on low (using a Vortex Gene2) for 30 min at room temperature (22 ± 2 °C). After 30 min, a stop solution (1mM Tris HCl, pH 7.5) was added to a final concentration of 30 mM and allowed to react for 15 min at room temperature (22 ± 2 °C). Figure 3.6 shows the BSOCOES synthesis pathway. After conjugation with avidin, the sulfone group can be cleaved by raising the pH of the buffer solution to 11.6 using 3-(cyclohexylamino)-1-propanesulfonic acid (CAPS) buffer (20 mM, pH 11.6). CAPS was substituted for phosphate buffer because the useful pH range extends above 11.6. CAPS buffer was incubated in the wells for 2 hr at 37°C.

3.1.6 Tag purification

Purification of the FEGGB and the FEGGGB tags was required prior to use. The purification was performed on a reverse phase C-4 column constructed in-house using a glass column and C-4 modified polymer particles (Toyopearl). The bed volume was approximately 25 mL. Due to pressure limitation of glass columns, the flow rate was set

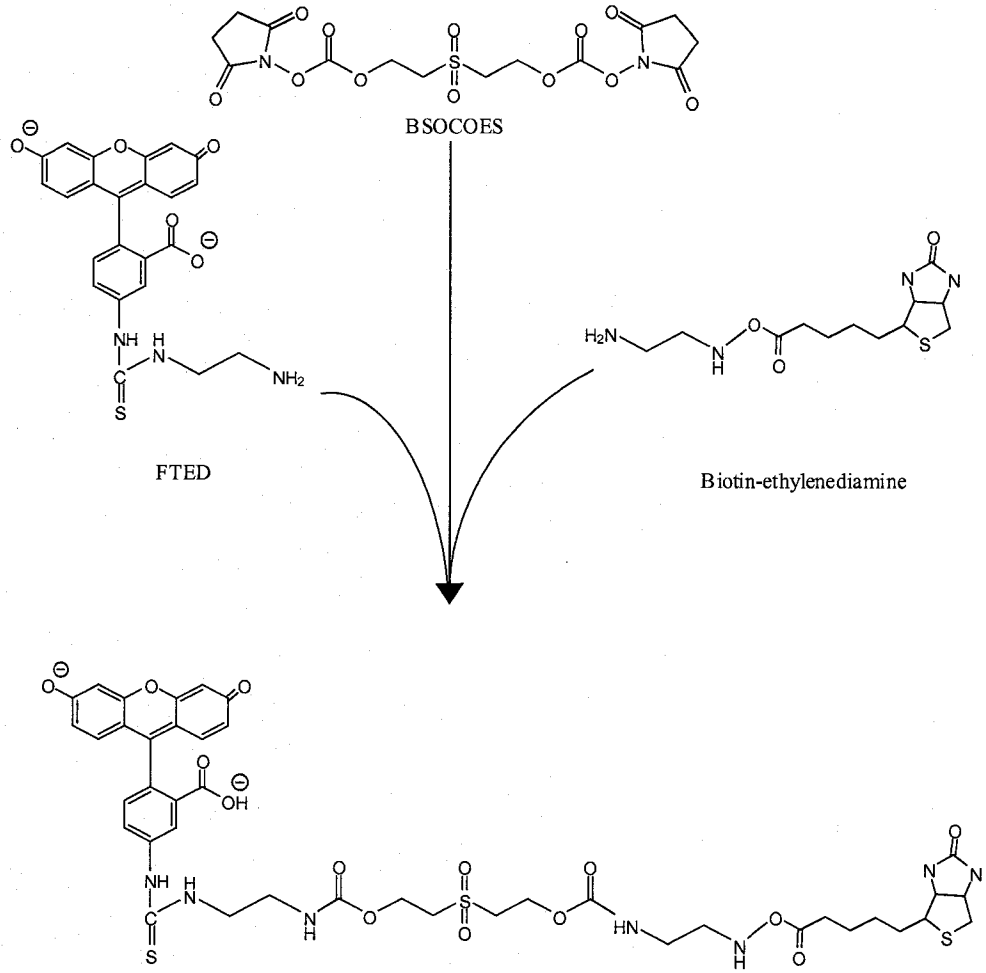

Figure 3.6. BSOCOES cleavable group synthesis.

at 1 mL/min which gave a pressure of approximately 225 psi. A multiple step gradient was used for the separation with the two mobile phase componenets being two different ratios of acetonitrile:water, 90:10 and 10:90. Table 3.1 shows the gradient used. The solution containing the tag was dried under a constant airflow and stored at -4 °C for later use. Purity was confirmed using conventional CE.

3.1.7 Cleavage kinetics

For disulfide cleavage there are two commonly used reducing agents dithiothreitol (DTT) and tris(2-carboxyethyl)phosphine hydrochloride (TCEP). The reaction of these two reducing agents with disulfide containing molecules is shown in Figure 3.7. Both are effective at reducing disulfides in the CTI tags. TCEP was primarily used in this case to prevent the formation of mixed disulfides. TCEP cleavage kinetics were studied by looking at complete cleavage time in solution with respect to TCEP concentration. This study was monitored by conventional CE with E_{sep}=0.83 V/cm and tetra borate (20 mM, pH 9.4) run buffer.

3.2 Results and discussion

3.2.1 FRB synthesis

Characterization of the FRB synthesis was done using CE and NMR. Figure 3.8 shows the ^{1}H NMR of FTED run in D6-DMSO. The portion shown corresponds to the portion of the molecule which differs from FITC. The common portion of the spectra corresponding to the aromatic region is not shown. In the initial FTED NMR there were two extra peaks which could not be explained, however, the ethylenediamine used for

Run time	% 90:10 (water:acetonitrile)	% 10:90 (water:acetonitrile)
0-5 min	100	0
5-13	95	5
13-20	93	7
20-27	90	10
27-30	85	15

Table 3.1. Multiple step gradient used for FEGGB and FEGGGB purification.

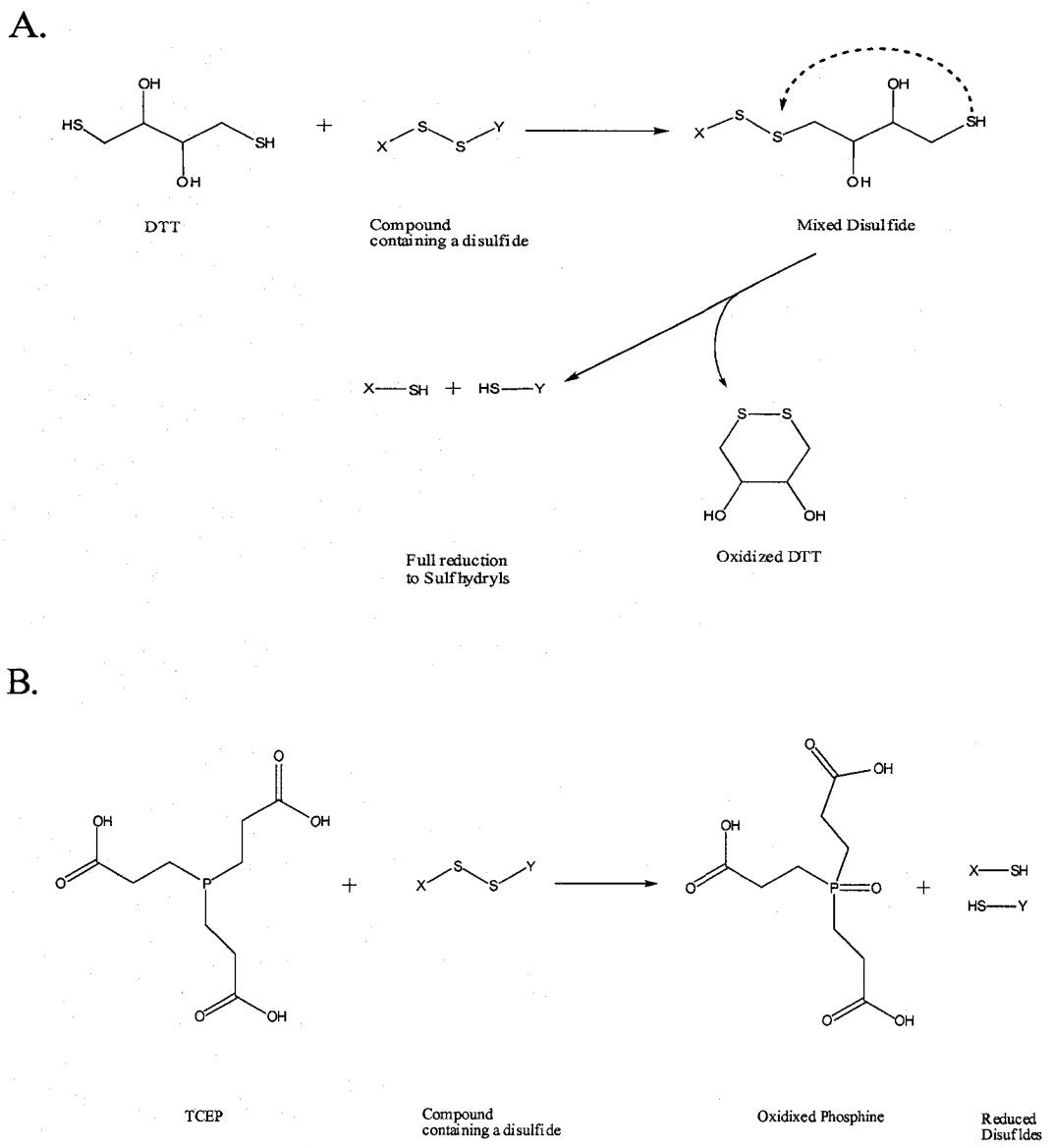

Figure 3.7. Reaction of DTT and TCEP with disulfides. A) DTT cleavage. B) TCEP cleavage.

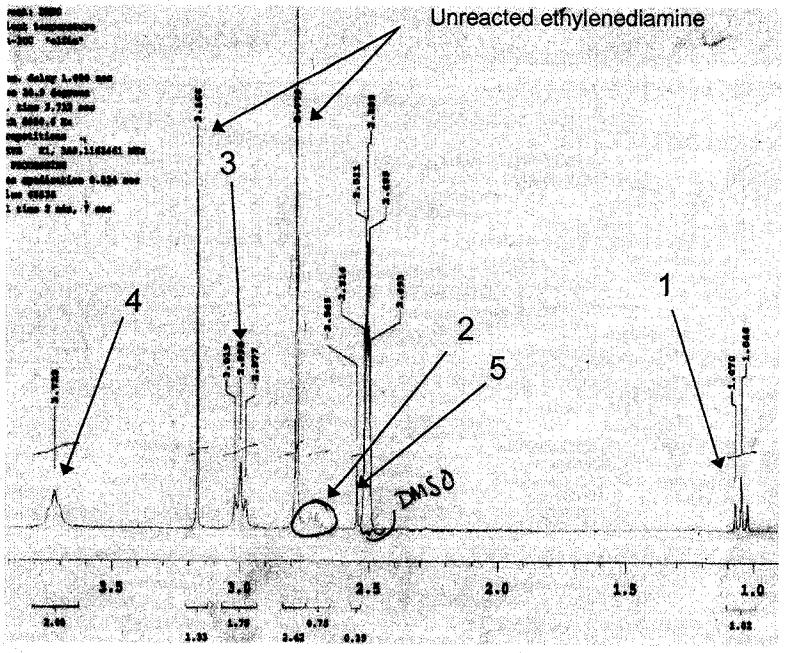

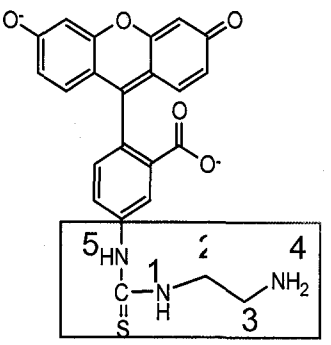

Figure 3.8. ^{1}H NMR of FTED. Solvent: D6-DMSO.

synthesis was not dry and these two peaks were attributed to ethylenediamine. The efficiency of the FTED synthesis is dependent on the reactivity of the ethylenediamine towards FITC. If the ethylenediamine is not dry it begins to react with the water in the original solution instead of with the FITC. Because of this potential problem, ethylenediamine was distilled over KOH to remove the unwanted water prior to use. CE was also run to check the reaction progress. Figure 3.9 shows a pure FTED product which was used in the final step of the FRB synthesis. The top electropherogram of FITC is shown for reference.

Optimization of the ratio for the reaction of FTED with NHS-SS-biotin was also performed to improve the product yield. It was found that a 1:1 or a 1.5:1 (FTED:NHS-SS-biotin) was the best ratio. This result is based on the peak area of the product as well as the amount of FTED and NHS-SS-biotin remaining following the reaction. A theoretical yield was never calculated because the final solution was never dried or purified and was used immediately following the reaction.

The stability of the tag was also monitored for 24 hrs by collecting electropherograms every hour. The results in Figure 3.10 show the product is stable in air at room temperature over 24 hrs. The peak corresponding to the product at 280 s is present at time 0 as well as at 24 hrs. The peak at 160 s is caffeine, included as a neutral flow to allow for run-to-run comparisons. The peak at 180 s is an impurity and does not adversely effect the reaction of FEB with avidin during later assay steps. The study was only carried out for 24 hrs because the tags are always used immediately or frozen within 24 hrs of production. The tag is stable for one month at -20 °C.

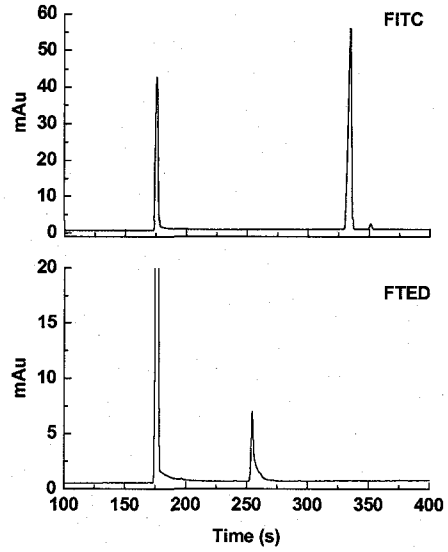

Figure 3.9. Electropherogram of FTED. FITC electropherogram included for reference. Peak at 175s is caffeine which is included as a neutral marker allowing for comparison of different CE runs. The small peak at 180 s is an impurity. Data collected on conventional CE system using UV detection (λ=214 nm).

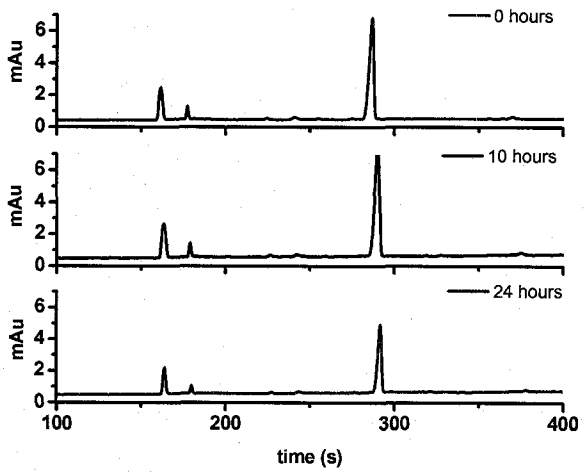

Figure 3.10. FEB product stability. Sample electrpherograms collected for FEB at 0, 10, and 24 hr post-synthesis. The peak at 160 s is caffeine added as a neutral marker. The desired product corresponds to the peak at 280 s. The small peak at 180 s is an impurity. Data collected on conventional CE system using UV detection (λ=214 nm).

There was an issue with the presence of multiple cleavage products following cleavage of FEB, FPB and FHB from both the model avidin particles and the complete CTI. It was first believed that the second peak corresponded to the reformation of the disulfide following cleavage. However, in reexamining the data, only two of the three cleaved products showed multiple peaks on the electropherogram. The cleavage of FAMB never showed more than a single peak. If it was disulfide reformation all three products in the test mixture (FAMB, FHB, and FEB) would show two peaks. This experiment eliminates the possibility that the second product seen was the disulfide. The results of this study can be found in Figure 3.11. The first electropherogram shows only FAMB, the second shows FAMB and FEB and the third shows FAMB, FEB, and FHB. All of the tags were immobilized on avidin coated particles and cleaved using TCEP (2 mM, pH 7). Another possibility for the multiple peaks was the reducing conditions of the TCEP solution. There have been publications on the lifetime of reactivity for TCEP at different pH values and buffer compositions.[3] The buffer most typically used in our lab to cleave disulfide bonds is tetraborate (pH 9.4, 20 mM) with 250 μM TCEP. These conditions worked in the past on the conventional CE, however, when switching to the microchip, run-to-run reproducibility was a problem and several peaks were visible for one product. In the microchip setup used in the lab we are constantly applying a potential to the sample reservoir which could have been reoxidizing the sulfhydryl groups and causing the reformation of disulfides. Other colleagues in my lab have been using TCEP in the run buffer in order to stabilize the sulfhydryl groups with great success and because of this, TCEP was added to the run buffer for the separation of CTI products. A more

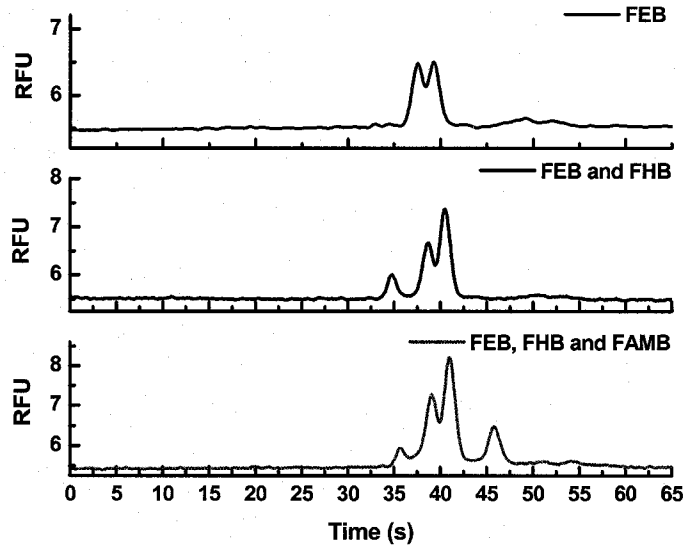

Figure 3.11. Multiple cleavage products. Top electropherogram shows multiple peaks for cleaved FEB. Middle electropherogram shows cleaved FEB and FHB. Bottom electropherogram shows cleaved FEB, FHB and FAMB. Experimental conditions: Field strength: 200 V/cm; Pinched injection time: 30 s; BGE: 10 mM tetraborate, 50 mM SDS, 20% acetonitrile. Detection performed using LIF system with a PMT for detection and a solid state laser for excitation (λ= 475 nm).

consistent electropherogram was seen over several runs, but, there were still multiple peaks (multiple products) for what should have been one cleaved species.

The synthesis had always been performed in the aqueous phase which could have caused problems due to hydrolysis of the NHS group on the Sulfo-NHS-SS-biotin. To combat this problem, a non-water soluble NHS-SS-biotin was used and the reaction performed in organic solvents. The reaction was carried out in THF (5 mL) and triethylamine (added until the solution was basic to ensure the integrity of the disulfide). As shown in Figure 3.12, when the synthesis was performed in organic solvents there was just one peak indicating the presence of only one cleavage product whereas in the electropherogram corresponding to the aqueous phase reaction two cleavage products are seen.

3.2.2 Glycine tags

Carbodiimide chemistry was used to generate several more tags. This chemistry is a useful technique for amide bond formation between a primary amine on one molecule and a carboxyilic acid on the other. N,N'-dicyclohexylcarbodiimide (DCC), N,N'-diisopropylcarbodiimide (DIC), or 1-ethyl-3-(3-dimethylaminopropyl) carbodiimide hydrochloride (EDC) are the most commonly used zero-length cross-linkers. DCC was the first developed zero-length cross-linker for carbodiimide chemistry. DCC is a potent allergen and purification following its use is difficult; therefore, DIC and EDC were produced as alternatives.[4] For this group of tags, EDC was chosen because, unlike DCC and DIC, it is water soluble. While this synthesis pathway requires three steps instead of two, the steps are well known in the bioconjugation chemistry community and

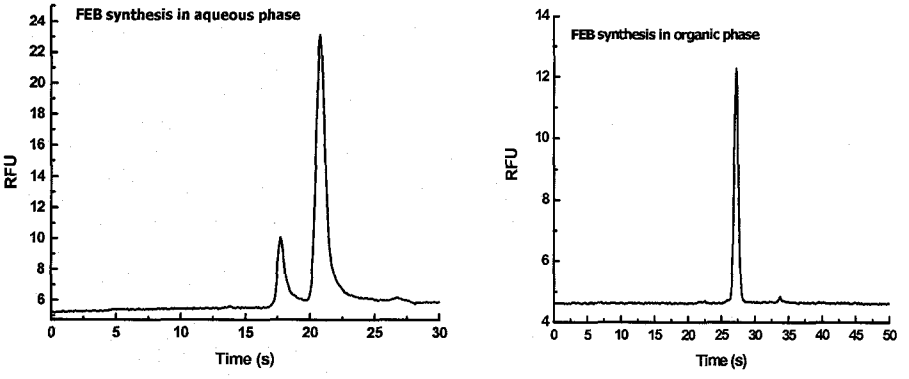

Figure 3.12. Synthesis of FEB performed in aqueous and organic phase. Left) electropherogram shows products obtained for synthesis performed in aqueous phase. Right) FEB product from organic phase synthesis. Data collected using conventional CE system with UV (λ=214 nm).

should therefore be as straightforward as the FRB synthesis. The most important factor for using this synthesis pathway for the production of tags is that by using the FTRD generated in the first step of the FRB synthesis in conjunction with the carbodiimide coupling, the tag library size can be doubled by incorporating one additional synthesis step.

3.2.3 Cystamine tags

The use of cystamine as the cleavable group and spacer in the tag gives the fluorescent portion of the tag a very different electrophoretic mobility than any of the other tags that have been produced thus far. The tag is much smaller with a more negative charge-to-hydrodynamic radius ratio causing it to migrate slower in CZE. Figure 3.13 shows electropherograms of the final two synthesis steps as well as an electropherogram of the cleaved product. The peak at 200 s in the second electropherogram is the desired product, FAMB. In the third electropherogram the peak at approximately 325 s corresponds to the cleaved fluorescent tag. The migration time of this tag is considerably slower than those of the cleaved FRB tags.

3.2.4 FEGGB and FEGGGB purification

In the carbodiimide synthesis pathway, the FTRD can react with either the Gly_n-SS-biotin or any remaining unreacted NHS-SS-Biotin and therefore, purification of the final products was necessary to remove any FRB formed. If purification was not carried out, the FRB produced in this synthesis would cause falsely elevated quantitative results

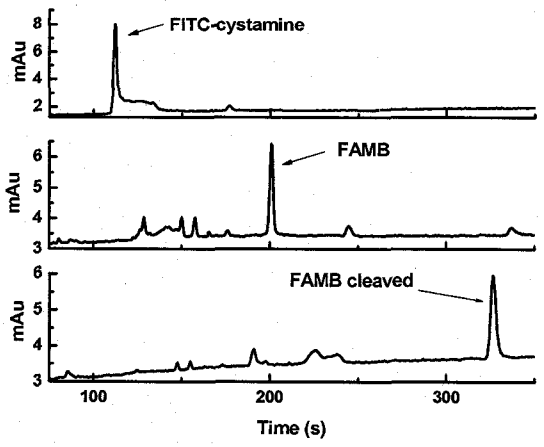

Figure 3.13. FAMB synthesis products. Top) Electropherogram of product for FITC reaction with cystamine. Middle) Final FAMB product. Bottom) Electropherogram of cleaved FAMB to demonstrate mobility.

for the antibody tagged with FRB when using the carbodiimide tags and the FRB tags together in a single CTI.

HPLC was used to purifiy FEGGB and FEGGGB. Initially a C-18 column was used with an isocratic mobile phase of 50:50 methanol:water. The resolution of the two fluorescent products was not amenable to fraction collection of only the desired product. The FEB appeared as a shoulder on the FEGGB or FEGGGB peak in the chromatogram (data not shown). To improve the separation a multiple step gradient was employed and a baseline separation of FEGGGB and FEB with a resolution of 8.3 and nearly baseline separation of FEGGB and FEB with a resolution of 1.0 were obtained making it possible to collect only the desired final tag. Figure 3.14A and B show example chromatograms of FEGGB and FEGGGB purification respectively. Purity of the products and integrity of the disulfides within the tags were checked using CE (Figure 3.15). The peak at 140s in 3.15B is an impurity.

3.2.5 Other amino acids

As stated in the introduction to this chapter, an easy way to quickly increase the number of tags in the tag library is to look at using other hydrophilic amino acids up to 4mer lengths for the spacer group. Two amino acids, lysine (lys) and arginine (arg), were used to test this theory. Both of these amino acids are hydrophilic diamines due to an amine containing side chain and thus can be used in the FRB synthesis.

Concerns arose when FITC-Arg-Biotin and FITC-Lys-Biotin were run on CE. As shown in Figure 3.16, the lysine synthesis produces two distinctly different products in

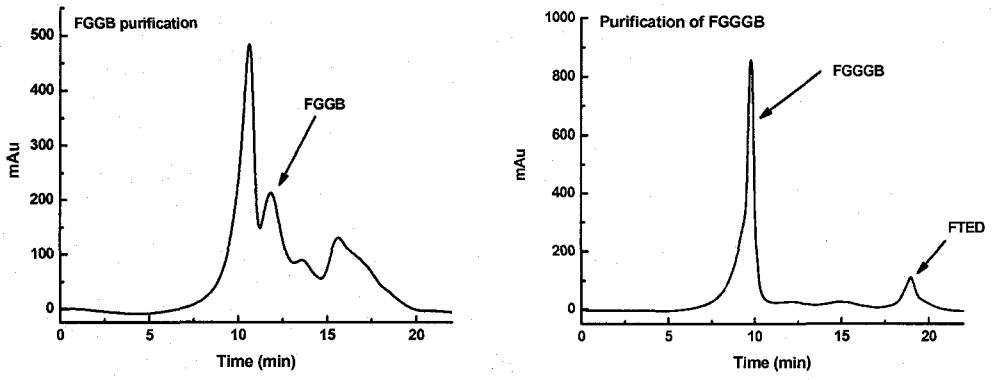

Figure 3.14. Tag purification. A. FEGGB purification. B. FEGGGB purification.

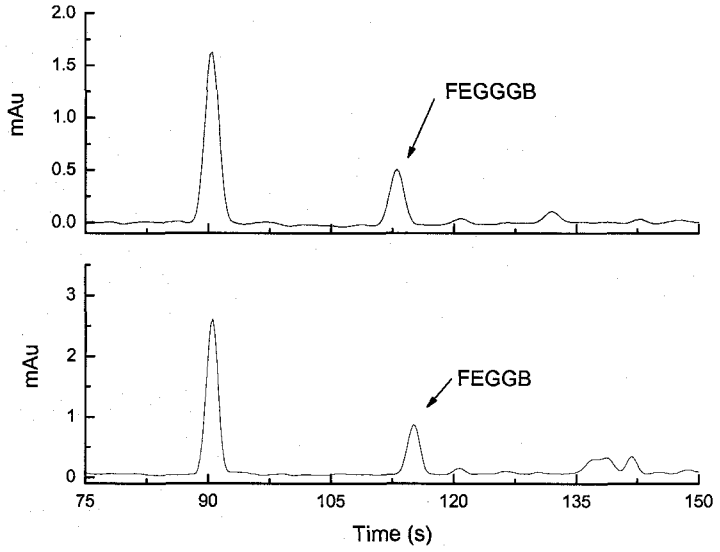

Figure 3.15. Electropherograms of purified products. A. FEGGGB. B. FEGGB. Peak at 90s in both electropherograms is caffeine included as a neutral flow marker. Data collected using conventional CE system with UV detection (λ=214 nm).

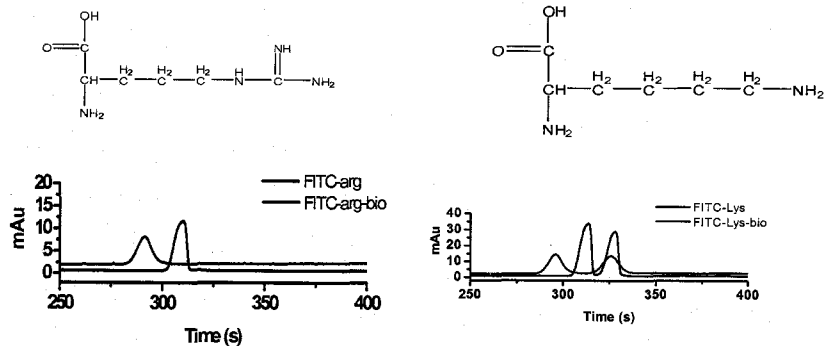

Figure 3.16. Amino acids as spacer groups in FRB synthesis. A. Arginine as spacer group. B. Lysine as spacer group. Data collected using conventional CE system with UV detection (λ=214 nm).

the first step and only one of these reacts with NHS-SS-biotin to form the final product. In contrast, when performing the same synthesis with arginine only one product was formed.

3.2.6 Disulfide cleavage

The drawback when using DTT as a reducing agent is the possibility of incomplete reduction and the formation of mixed disulfides. This was seen in the initial proof-of-principle experiments conducted with IgG and anti-IgG. Figure 3.17 shows electropherograms demonstrating proof-of-principle of the complete model antibody/antigen system. Electropherogram A is the product from first synthesis step (FTED). Electropherogram B is the uncleaved final product (FEB). FTED was in excess during the final synthesis step and is therefore visible in the electropherogram of in the unpurified sample before immobilization and cleavage. Electropherogram C is the immobilized FEB product cleaved from a streptavidin-coated plate (no antibody/antigen system). Electropherogram D shows the cleaved tag from anti-IgG/IgG/tagged anti-IgG complex. All data was collected using microchip CE with fluorescent detection using an inverted fluorescent microscope with a Hg arc lamp excitation source and low-sensitivity imaging CCD detector. Based on calculations of charge/mass ratios and consulting Hermanson's Bioconjugate Techniques book,[5] the peak which appears at 47 seconds in electropherograms C and D is the mixed disulfide formed during reduction when using DTT. Because of this reoccurring problem, TCEP was used in place of DTT for the reduction of the disulfides in the tags. The ability of trialkyl phosphines to reduce protein

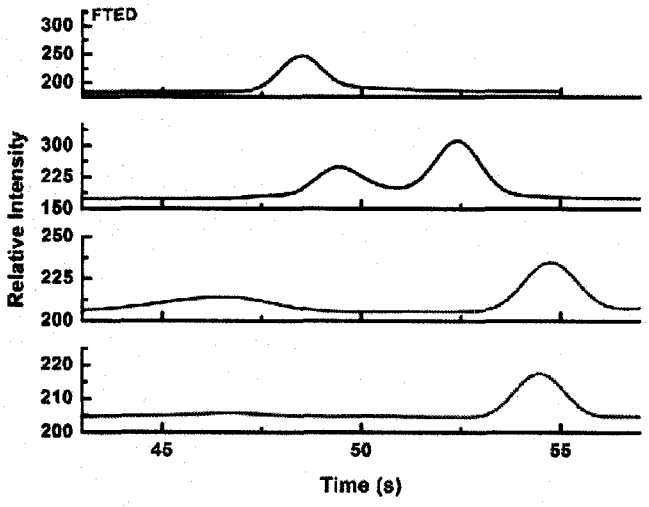

Figure 3.17. Proof-of-concept demonstrating mixed disulfide. A. FTED electropherogram included for reference. B. FEB uncleaved. Peak at 50 s is excess FTED. C. FEB immobilized on a streptavidin-coated microtiter plate and cleaved using DTT. D. FEB cleaved from model system. Peak at 47 s in C and D is mixed disulfide formed with use of DTT.

disulfides has been known for many years. Phosphines are stable in aqueous solutions, selectively reduce disulfide bonds, and are essentially nonreactive toward other functional groups.[6] TCEP is an odorless reducing agent with which there is no possibility of mixed disulfide formation and, because of the mechanism for the disulfide reduction using TCEP, the likelihood of reversal of the reaction back to the disulfide is nearly zero. TCEP works in a wide pH range and a variety of buffer compositions.[3]

One major concern when using TCEP is the period of reactivity. The lifetime of TCEP at alkaline pH is less than 3 days and in buffers which contain phosphate it is no more than 36 hours.[3] Phosphate containing buffers have been used for the cleavage solution with success in our lab as long as the cleaved solutions were run on the microchip system immediately following the cleavage and the TCEP solution was made fresh each day. More importantly, the phosphate buffer gives a more stable baseline over the course of a set of sample runs when compared to running the same sample that has been cleaved in borate buffer.

Ideally, the cleavage portion of the assay would be completed in less than 30 min with a minimum concentration of TCEP to ensure the difference in ionic strength between the sample and the buffer does not cause destacking and excess diffusion during separation. The concentrations studied were 125 μM-5 mM and the FEB concentration was kept constant at 250 μM. TCEP concentration was decreased until an appreciable increase in cleavage time was seen. The results are shown in Figure 3.18. Based on these results, 250 μM TCEP was used because it cleaved the product in 15 minutes. At a TECP

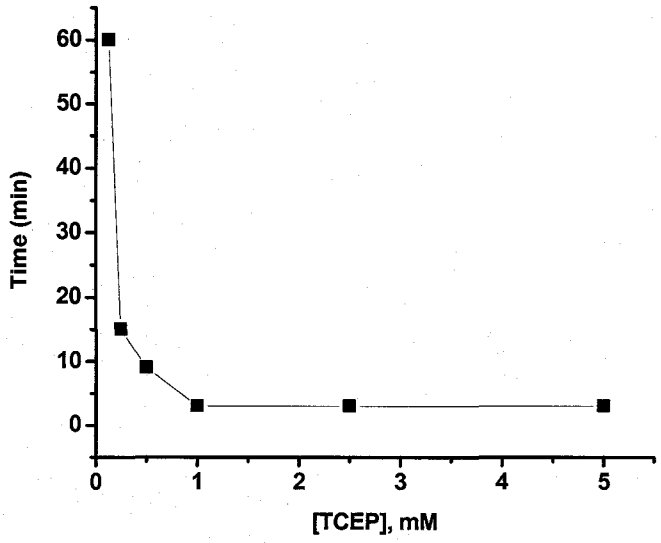

Figure 3.18. Reaction kinetics. Cleavage time of FEB in solution monitored as a function of TCEP concentration. Data collected using conventional CE system with UV detection (λ=214 nm).

concentration of 125 μM it took 60 min to cleave FEB and at concentrations less than 125 μM incomplete cleavage occurred. Since this study was conducted, the concentration of TCEP used for tag cleavage was increased from 250 μM to 2 mM to decrease the cleavage time and the buffer was also changed from tetra borate (20 mM, pH 9.4) to phosphate buffer (20 mM, pH 7.4) containing 2 mM TCEP to improve stability of the product.

3.2.7 BSOCOES

Another viable option for synthesizing cleavable tags is the use of sulfones. Sulfones offer an alternate cleavable group because they are cleavable under alkaline (pH 11.6) conditions. BSOCOES was the initial sulfone selected for study. BSOCOES is a water-insoluble, homobifunctional NHS ester cross-linking molecule. The presence of an NHS ester makes the molecule amine reactive. This tag synthesis was discontinued because BSOCOES does not cleave symmetrically. There is the possibility of two fluorescent products which give two peaks in the electropherogram of the product when cleaved from particles making quantification difficult. Figure 3.19 shows a sample electropherogram of the two fluorescent products. Each peak has been labeled with the corresponding cleavage product.

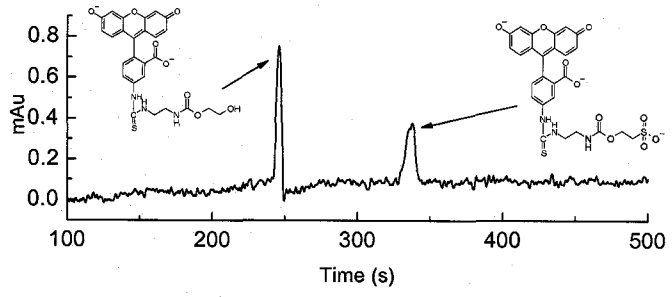

Figure 3.19. BSOCOES cleavage products. Data collected using conventional CE system with UV detection (λ=214nm).

3.3 Summary

In this chapter several synthesis pathways were outlined in detail. This chapter described method development of the synthesis pathways as well as method development for tag purification using HPLC. Organic synthesis was largely new to our group at the start of this project and therefore a great portion of the research for this project involved mastering synthesis and purification techniques. As shown above, a reasonably sized tag library has already been produced and if the proposed idea of using hydrophilic amino acids as spacer groups comes to fruition a very large library of tags can be produced using the three synthesis methods described above in a relatively short period of time.

3.4 Acknowledgements

I would like to thank Brian M. Murphy for his role in the development of the cystamine containing tag synthesis protocol and Lauren M. Ramsay for her assistance in the carbodiimide synthesis. I would also like to extend a thank you to Dr. Tomislav Rovis for his advice on synthesis protocols.

3.5 References

(1) Bertram, V. M.; Bailey, M. P.; Rocks, B. F. *Ann Clin Biochem* **1991**, *28*, 487-491.
(2) Pierce Biotechnology, Inc.: Rockford, 2003, pp 1-3.
(3) Burns, J. A.; Butler, J. C.; Moran, J.; Whitesides, G. M. *J. Org. Chem.* **1991**, *56*, 2648-2650.
(4) Kurzer, F.; Douraghi.K *Chemical Reviews* **1967**, *67*, 107-&.
(5) Hermanson, G. T. In *Bioconjugate Techniques*; Academic Press: Rockford, 1996, pp 292-296.
(6) Kirley, T. L. *Anal. Biochem.* **1989**, *180*, 231-236.

CHAPTER 4

CLEAVABLE TAG IMMUNOASSAY

The cleavable tag immunoassay (CTI) is a low- to medium-density heterogeneous immunoassay designed to detect 1-20 analytes simultaneously. While analyte capture is similar to traditional sandwich immunoassay chemistry, our approach is unique because the signal is not imaged directly on a surface; instead, a fluorescent tag is cleaved from the antibody and analyzed by microchip MEKC. A schematic of the general CTI procedure is shown in Figure 4.1. Briefly, unlabeled capture antibodies for all proteins of interest are immobilized on a particle surface. The sample is then added, allowing proteins to bind to the capture antibodies before a tagged detection antibody is added. After conjugation of the detection antibodies to the corresponding biomarkers, the tags are cleaved and the solution containing the fluorescent fragments analyzed using microchip MEKC. In the CTI, each detection antibody is tagged with a unique fluorescent tag that gives a different charge-to-hydrodynamic radius fragment after cleavage and therefore a unique migration time in CE. Tag synthesis was described in Chapter 3. The use of microchip MEKC eliminates the need for expensive, cumbersome optical scanners and can reduce sample consumption. Furthermore, the ability to detect tags in solution allows for decoupling analyte capture from detection thus removing the need for expensive spotters and ultimately allowing for the development of a simple,

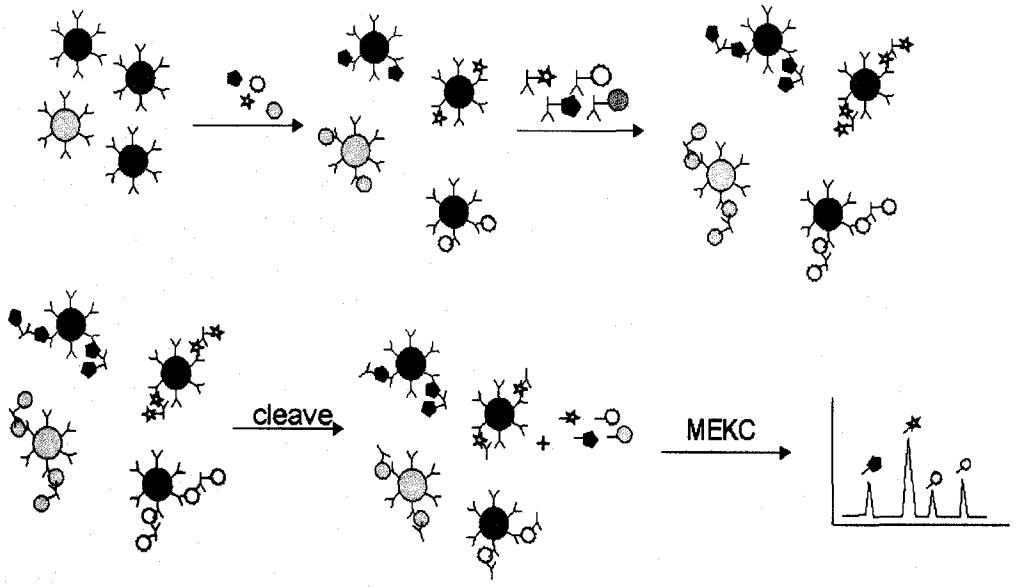

Figure 4.1. CTI Chemistry. Step 1: Sample is added and biomarkers bind to capture antibodies immobilized on the particle surface. Step 2: Detection antibodies added. Step 3: Tags cleaved from immobilized immunocomplex. Step 4: Separation and detection using MEKC with fluorescence detection.

inexpensive point-of-care measurement device using either diode-based lasers or electrochemistry.

There have been two other reports of similar techniques, one from Bertram's group in the UK and the other a commercial effort (Aclara, Inc.). Bertram et al. used cleavable fluorescent tags for detection,[1] cleaving disulfide bonds to release fluorescein from a captured protein analyte. Solution phase detection was performed using a fluorimeter. Bertram's method addressed the problems associated with fluorescence concentration quenching in immunoassays on surfaces; however, this method is limited in the number of analytes because different fluorophores are required to screen for more than one analyte. The use of a fluorimeter not only makes sample preparation and analysis more complicated when compared to the CTI but it also does not lend itself to miniaturization and portability. Aclara, Inc. has developed a similar idea for protein and DNA detection, called eTag.[2, 3] The eTag assay system is useful in quantification of gene and protein expression. Chen-Hui et al. have demonstrated the ability of the eTag assay system to detect small changes in protein expression, protein-protein interactions, protein phosphorylation, and mRNA expression.[3] For monitoring mRNA expression, the tag is enzymatically cleaved from a complementary strand and requires the antibodies be spatially close when bound to the antigen and thus makes antibody production and selection demanding. The CTI chemistry is simpler and allows for pre-concentration of analytes through a solid-phase capture step. This chapter describes the CTI procedure in detail and presents the progress made on the characterization of the system thus far.

4.1 Experimental

4.1.1 Preparation of detection antibody

The interaction of biotin with avidin is among the strongest non-covalent affinities known with a K_d of approximately 1.3×10^{-15} M.[4] It is this affinity that is exploited in the preparation of the detection antibodies. Originally, the possibility of utilizing pre-biotinylated antibodies (Calbiochem) for the detection antibodies was explored in order to simply demonstrate proof-of-concept for the CTI. According to the manufacturer, the degree of biotinylation for these antibodies was approximately 50 mol biotin/mol antibody. Ideally, the degree of biotinylation would be closer to 2-4 mol biotin/mol antibody. There were also other problems with activity for pre-biotinylated antibodies and therefore, a maleimide biotinylation procedure was adopted for biotinylation of all detection antibodies.

Several steps were required to tag the detection antibody. These steps are outlined in Figure 4.2. First, the antibody was biotinylated using a maleimide biotinylation kit according to instructions (Pierce Chemical). Maleimide chemistry was used in order to better control the number of biotins bound to the antibody. The biotinylation kit is a solid phase biotinylation kit which takes advantage of the propensity of antibodies to bind to metal chelate supports. Solid phase biotinylation also gives more control over the derivatization process when compared to solution phase reaction. Binding to the nickel chelate support occurs primarily through the histidine rich Fc region of IgG molecules. Reduction of the disulfides within the Fab regions of the antibody, site-directed biotinylation and removal of excess reagents are easily carried out while the antibody is bound to the support.

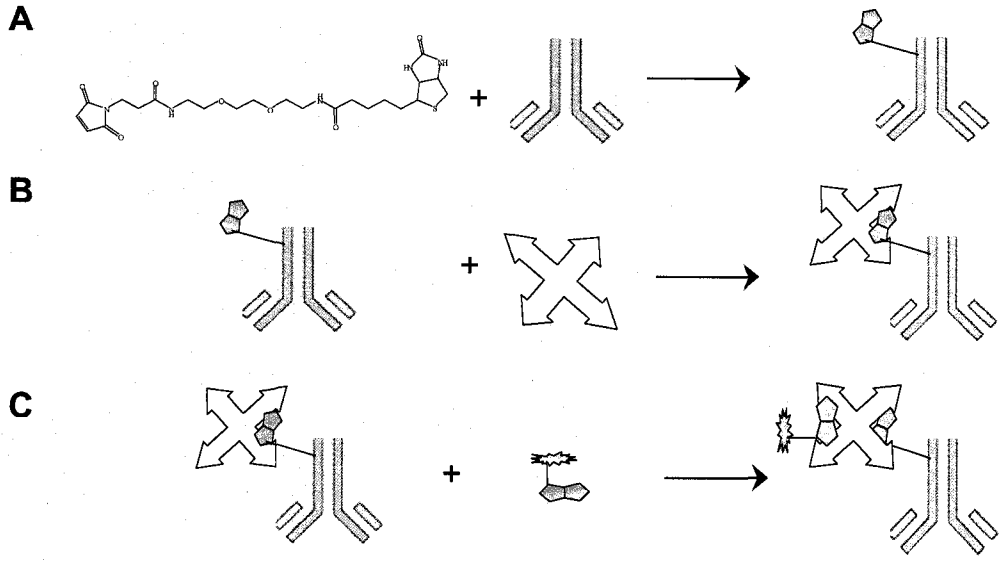

Figure 4.2. Labeling detection antibody. A. Maleimide biotinylation. B. Avidin/biotin coupling. C. Attachment of biotin terminated fluorescent tag to avidin bound to antibody.

For the biotinylation process 100 μg of the detection antibody is added to the hydrated SwellGel nickel chelate disk and allowed to bind for 10 minutes with gentle mixing. The gel is washed with tris buffered saline (TBS) buffer and TCEP (200 μM) is added to reduce the disulfide bonds in the Fab regions of the bound antibodies. The TCEP reduction occurs over 30 min. At this point maleimide-PEO_2-biotin (1 mg) is added to the slurry and mixed for 30 min. Each step of the biotinylation process is followed by a TBS rinse in triplicate. The final biotinylated antibody is removed from the support using an imidazole (200 mM) elution buffer. The biotinylated antibody is stable for 1 month at 4 °C.

Following biotinylation, avidin was added (1:1 biotin bound:avidin) and allowed to bind over a period of 2 hr at room temperature. Finally, the biotin terminated tag was added (3:1 tag:avidin) to the solution and bound to the remaining sites on the avidin. Excess tag was removed using a Nanosep centrifugal concentrator (Pall Corporation) with a 3kD molecular weight cutoff according to instructions from Pall. This process gives 2-8 fluorescent tags per detection antibody.

4.1.2 HABA assay

The traditional way to determine the degree of biotinylation is through the use of the HABA [(2-(4'-Hydroxyazobenzene) Benzoic Acid] assay. The assay is designed to measure the decrease in absorbance of the [$(HABA)_4$:Avidin] complex when HABA is displaced by biotin. Biotin has a higher affinity for avidin and therefore displaces HABA causing a decrease in absorbance at λ=500nm. The absorbance of the HABA-avidin solution is measured before and after the addition of the biotin solution. The change in

absorbance is related to the biotin concentration in the sample through the extinction coefficient of the HABA-avidin complex. Calculations showed that, on average, the ratio was 2.65 mol biotin/mol antibody.

4.1.3 Capture antibody immobilization

Capture antibodies were immobilized on Toyopearl affinity resin functionalized with aldehyde groups (Formyl-650M, Tosoh Biosep). AF-Formyl 650-M particles (800 μL per protein) were washed three times with 1 mL K_2HPO_4 (100 mM, pH 7.5) to remove azide used to preserve the particles. Following this, the particles were separated into 5 separate tubes, centrifuged and the liquid removed. The 5 dilute antibody solutions (2 mL) were each mixed with one of the separate 800 μL of particles and allowed to react with gentle mixing at room temperature (22±2°C) for 2 hr. Sodium cyanoborohydride (10 mg) was added to each of the five tubes to facilitate reductive ammination during the antibody attachment. This reaction forms stable secondary amine linkages between the amine groups on the antibody and aldehyde on the particles. The capture antibodies were diluted prior to immobilization in K_2HPO_4 (1M, pH 7.0) to concentrations in 10-fold excess of the upper reference level for each biomarker. After the coupling reaction was complete, the resin was washed three times with K_2HPO_4 (100mM, pH 7.5) and 2 mL of ethanolamine (1M, pH 8) was added to each vial of particles and allowed to react for 2 hr at room temperature (22±2°C) to block all remaining aldehyde groups. Again, sodium cyanoborohydride (10 mg) was added to aid the coupling reaction. After the reaction with ethanolamine, the particles were again washed three times with K_2HPO_4 (100 mM, pH 7.5). To reduce the amount of non-specific binding in the remaining steps of the CTI, the

beads were rinsed 3 times with SuperBlock blocking buffer (Pierce), phosphate buffered saline containing a proprietary protein mixture, after the final phosphate rinse. Particles are stored in K_2HPO_4 (100 mM, pH 7.5) at 4 °C until use (up to 1 month).

To limit the use of costly antigens and antibodies, particles with immobilized avidin were used for optimization of the cleaved tag separations. Avidin was immobilized according to the procedure described for capture antibody immobilization. A concentration of 5 mg/mL avidin was used to perform the immobilization. Since all synthesized tags are biotin-terminated, the use of avidin was an inexpensive alternative for these experiments. The biotin end of the synthesized cleavable tag was bound to the immobilized avidin on the surface of the particles due to the strong affinity of biotin towards avidin which allows for the ability to cleave and study only the fluorescently labeled portion of the tag.

4.1.4 BCA assay

The bicinchoninic acid assay (BCA assay) is a biochemical assay used for determining the exact protein concentration in a given solution and can also be used to determine the amount of immobilized antibody on a solid surface. It was performed according to the instructions from the manufacturer (Pierce Chemical) for each set of particles. The bovine serum albumin (BSA) standards were each measured once while the particle samples were run in triplicate. Absorbance measurements were performed using a UV/Vis spectrometer (ThermoSpectronic) at λ=562 nm. For the particle samples, three 10 μL aliquots were removed from each vial and allowed to settle. The final particle volume was noted before dilution to 100 μL for the assay. A calibration curve was

generated for the assay using the values from the BSA standards and a linear fit applied. The diluted protein concentrations were calculated and using the initial particle volume an average mg/mL concentration for the total particle volume was calculated. The BCA assay was also run on the avidin particles to determine the coupling density.

4.1.5 Assay procedure

Capture beads (150μL), prepared as described above, were placed into a 1.5mL microcentrifuge tube and rinsed 3 times with phosphate buffer (20 mM, pH 7.4). Following each rinse the beads were centrifuged (45s, 1450rpm) and the rinse discarded. The antigen solution (250μL) was added to the beads and allowed to react for 2 hr at room temperature. The beads were again centrifuged and the liquid discarded. At this point the beads were rinsed 3 times with NaCl (1M) containing 0.05% Tween 20, followed by 3 rinses with phosphate buffer (20mM, pH 7.4). To reduce the amount of non-specific binding, the beads were rinsed 3 times with SuperBlock blocking buffer (Pierce), phosphate buffered saline containing a proprietary protein mixture, after the final phosphate rinse. Finally, the detection antibody (500μL, 500μg/mL) was added to the beads and allowed to react for 2hr at room temperature. Following conjugation of the detection antibody to the corresponding biomarker, the beads were rinsed 5 times with NaCl (1M) followed by 3 times with phosphate buffer (20 mM, pH 7.4) and a cleavage solution was added (2 mM TCEP, 75 μL). Cleavage takes place over 30 min at room temperature (22±2°C). Finally, the solution containing the fluorescent fragment was removed from the beads and analyzed using microchip CE.

4.2 Results and Discussion

4.2.1 Pre-biotinylated antibodies

It was found that the model IgG/anti-IgG system using pre-biotinylated anti-IgG did not work correctly because, following cleavage, nothing was detected using the LIF system. To investigate this problem, size exclusion chromatography (SEC) was performed on the pre-biotinylated anti-IgG as well as IgG and unlabeled anti-IgG. SEC was also run on lysozyme as a known molecular weight control. Figure 4.3 shows the pre-biotinylated anti-IgG compared to IgG and avidin. IgG and pre-biotinylated anti-IgG should have relatively the same molecular weight and should therefore have roughly the same retention time on a size exclusion column. There is a small shoulder on the peak in the pre-biotinylated anti-IgG chromatograph which is probably the true product but the major peak for pre-biotinylated anti-IgG has a retention time closer to that of avidin not IgG. Indicating the molecular weight is probably closer to that of avidin. After looking at the chromatograms generated from SEC, it was determined that the pre-biotinylated anti-IgG should no longer be used and the antibodies were biotinylated in-house. This process was described in detail above.

4.2.2 Four tag separation

The separation of four unique tags, FEB, FHB, FAMB, and FEGGB immobilized at the same concentrations and cleaved from particles is shown in Figure 4.4. Figure 4.4A shows the four tags separated in tetraborate (10 mM), SDS (50 mM), 20% acetonitrile [5] and 4.4B shows the same separation using the same run buffer with a zwitterionic surfactant, N-dodecyl-N,N-dimethyl-3-ammonio-1-propane sulfonate (10 mM)

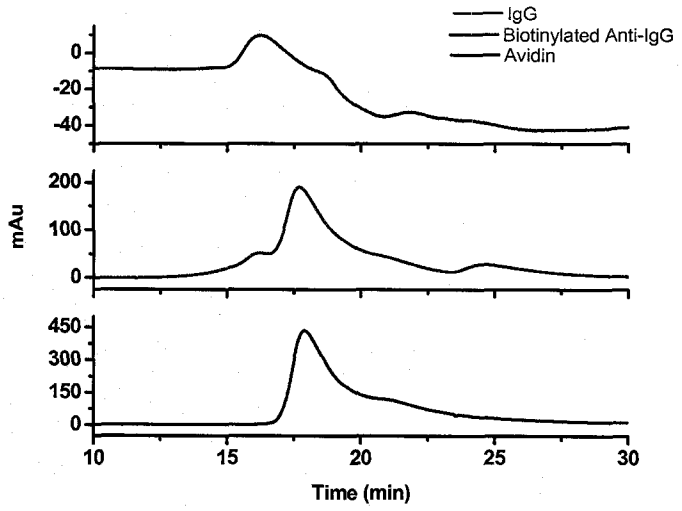

Figure 4.3. Size Exclusion Chromatography (SEC). Mobile phase: K_2HPO_4 (0.1 M, pH 7.4). Flow rate: 0.1 mL/min. Detection wavelength 214nm. Top) IgG. Middle) Pre-biotinylated anti-IgG. Bottom) Avidin, included as molecular weight reference.

A.

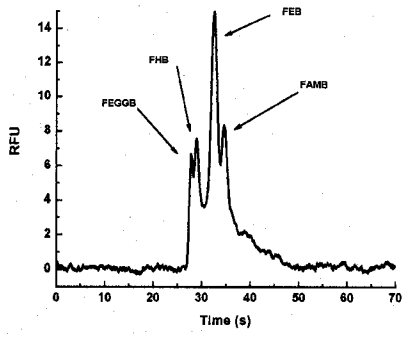

B.

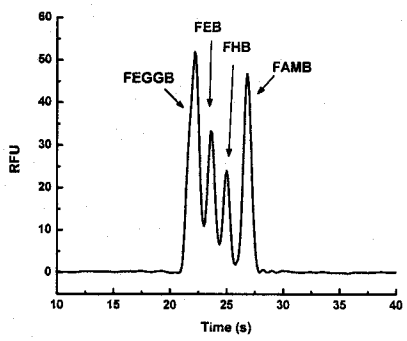

C.

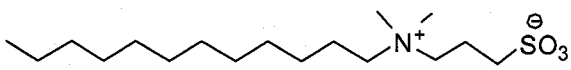

Figure 4.4. Optimization of tag resolution. Each peak is labeled with the corresponding tag. Tags diluted to 1 μM with PBS. These tags were used in the other CTI experiments discussed in this work. Experimental conditions: Field strength: 200 V/cm; Pinched injection time: 30 s; BGE: 10 mM tetraborate, 50 mM SDS, 10 mM N-dodecyl-N,N-dimethyl-3-ammonio-1-propane sulfonate, 20% acetonitrile. Detection performed using LIF system with a PMT for detection and a solid state laser for excitation (λ= 475 nm).

(DDAPS), added. The structure of DDAPS is shown in 4.4C. The identity of the peaks was verified by running each tag individually (data not shown). This allows for the easy identification of the peaks and migration times for the tags used in the complete CTI when all of the analytes (tags) may or may not be present in the sample. The selection of tags is somewhat limited by the separation efficiency of PDMS microchips. It was determined that cleaved tags must differ in mass by at least four carbons. When tetraborate (10 mM), SDS (50 mM) and 20% acetonitrile was the background electrolyte (4.4A), the resolution between FGGB and FHB was calculated to be 0.3, between FHB and FEB was calculated to be 0.76 and between FEB and FAMB was calculated to be 0.7. None of these is sufficient for peak quantification. An alternative buffer needed to be used in order to resolve all four peaks. The needed improvement in resolution came with the use of DDAPS. When SDS and DDAPS were used together above their respective CMC values as part of the run buffer the resolution improved to 1.1. Total analysis time was also shortened by nearly 15 s (32 % reduction). Both of these changes can be attributed to the formation of mixed micelles and the differences in partitioning of analytes with the mixed micelles formed from SDS and DDAPS. The lowest resolution in Figure 4.4B is between the FGGB and FHB and is calculated to be 0.94. The resolution between FHB and FEB and between FEB and FAMB are 1.1 and 1.4 respectively. Although a resolution of 0.94 is not quantifiable, the concentrations of the four tags (1 μM) in this study were much higher than the concentration of tags expected in the assay (low nM). As the concentration of the tags in solution is decreased, it can be expected that further improvement in the resolution will occur. Also of note is that the migration order of FEB and FHB has reversed which can also be attributed to the interaction with

the mixed micelles. The tag migration order was confirmed by running cleaved FEB alone and adding the other tags one by one until all four were in solution.

There is an obvious difference in peak heights of the four tags despite the fact that all of the concentrations were 1 μM prior to immobilization and cleavage. The peak height variability can be attributed to differences in cleavage rate of the disulfides because of variation in sterics between tags. Also, even though the tags were reacted at equimolar concentrations and in excess when compared to bound avidin on the particles, there could be a competitive reaction between the tags for avidin binding sites. The most favorable tag-avidin interactions for this set of tags were FGGB and FAMB followed by FEB and finally FHB.

4.2.3 Calibration curves

Bead-based immunoassay calibration curves are dependent on both the bead (solid-phase) volume and volume of cleaving agent added. By adjusting these parameters, the sensitive portion of the curve can be shifted to a different concentration range for each analyte.[6] In this case, assay parameters were adjusted to ensure the sensitive portion of the curve for each analyte bracketed the upper reference limit. The upper reference limit is usually defined as the level below which 95% of the normal population falls.[7] Calibration curves generated for CK-MB, Myo, cTnI, cTnT, and CRP in phosphate buffered saline (PBS) are shown in Figure 4.5A-E. The data is shown in semi-log format, typical of immunoassay plots. The upper reference limit is marked on each curve in order

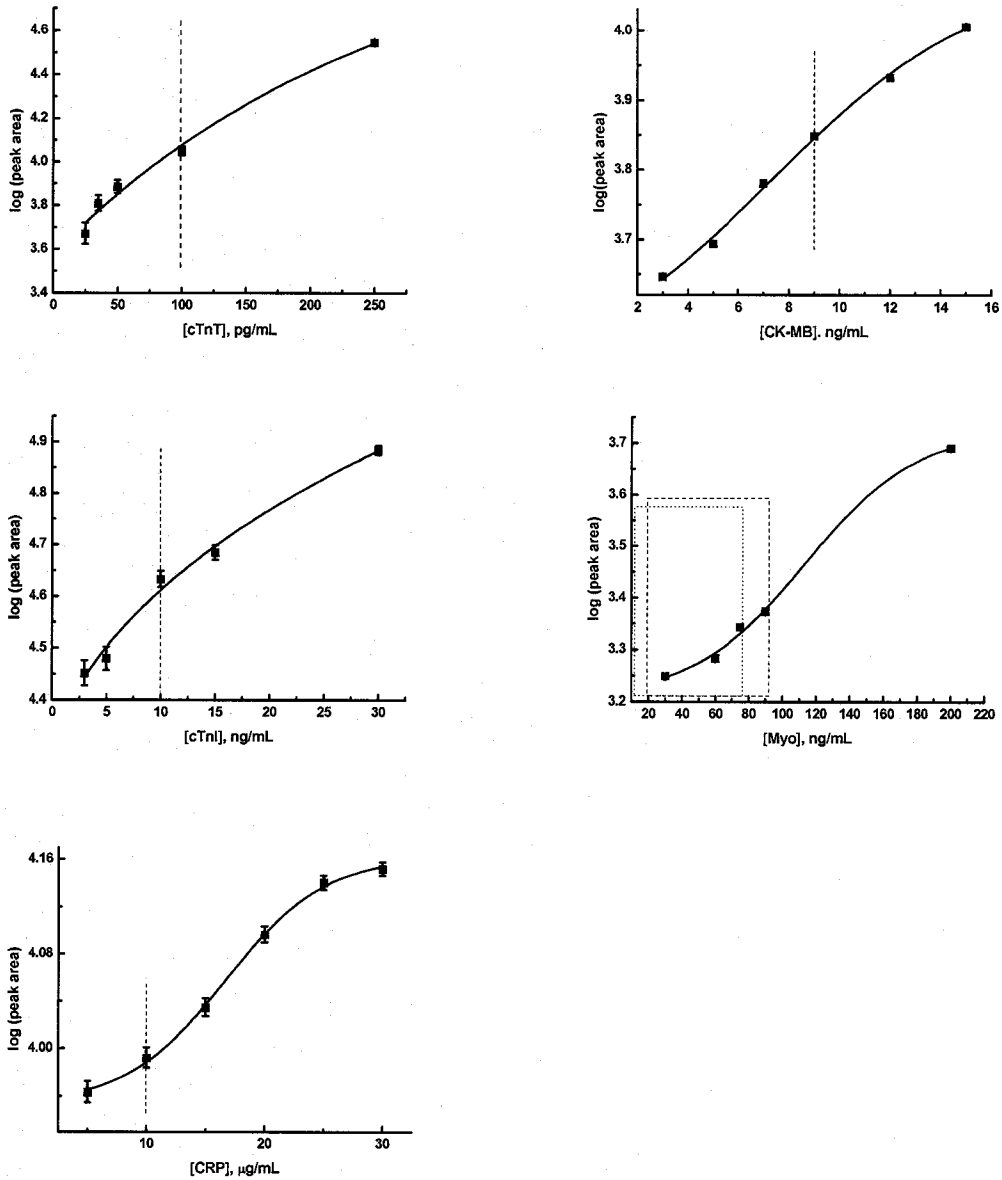

Figure 4.5. Calibration curves: A. cTnI, B. CK-MB, C. cTnT, D. Myo, E. CRP. Concentrations encompass both normal and elevated levels of each of the four biomarkers. Upper reference limit is marked on each curve. The upper reference limit for Myo is a range which is different for male (--) and female (···) patients and is therefore depicted as two boxes on the curve.. Biomarkers diluted in PBS. Experimental conditions: Field strength: 200 V/cm; Pinched injection time: 30 s; BGE: 10 mM tetraborate, 50 mM SDS, 20% acetonitrile. Detection performed using LIF system with a PMT for detection and a solid state laser for excitation (λ= 475 nm) at 2.5 cm.

to illustrate the ability of the CTI to detect biomarker levels considered normal and elevated. It is also important to note that the upper reference limit falls in the steepest portion of the curve meaning a small change in concentration gives a large change in signal (log (peak area)) making it easy to distinguish normal from abnormal results. Limit of detection (LOD) and linear range were determined for each protein. These results are shown in Table 4.1 along with the upper reference limits of each biomarker. Both the linear range and LOD are sufficient for clinically relevant levels of the four proteins known to be elevated during an AMI. The limit of detection here is defined as a signal greater than three times the baseline noise. The small volume of TCEP (75 μL) used in the cleavage step causes a pre-concentration effect thus magnifying the signal seen for a small amount of analyte. It is well known that the use of beads-based immunoassays can effectively act to amplify the assay signal due to the increase in surface area when compared to traditional approaches[8] which makes the low ng/mL and pg/mL LODs of the CTI attainable. Glycine has been known to quench intermolecular fluorescence [9] which could be the reason for the low signal and therefore, the highest LOD for Myo (FEGGB tag). The 25 pg/mL LOD for TnT (FHB tag) can be attributed to the very small dissociation constant between TnT and its detection antibody.

Figure 4.6 shows example electropherograms for each biomarker calibration curve. The concentrations were 5 ng/mL, 100 pg/mL, 60 ng/mL, 3 ng/mL, and 30 μg/mL for CK-MB, TnT, Myo, TnI and CRP respectively. The migration times are similar from analyte to analyte, however, the run buffer used for these samples contained only SDS added as the surfactant not the combination of SDS and DDAPS. Without the DDAPS

Biomarker	Upper Reference Limit	LOD	Linear Range
Myoglobin	Male: 19-92 ng/mL Female: 12-76 ng/mL	5 ng/mL	60-200 ng/mL
cTnT	0-0.1 ng/mL	25 pg/mL	0.035-0.25 ng/mL
cTnI	< 10 ng/mL	2 ng/mL	10-30 ng/mL
CK-MB	0-9 ng/mL	3 ng/mL	7-15 ng/mL

Table 4.1. Experimentally determined LOD and linear range of four AMI proteins. Upper reference limits included for reference.
Buffer conditions: 10 mM tetraborate, 50 mM SDS, 10 mM N-dodecyl-N,N-dimethyl-3-ammonio-1-propane sulfonate, 20% acetonitrile

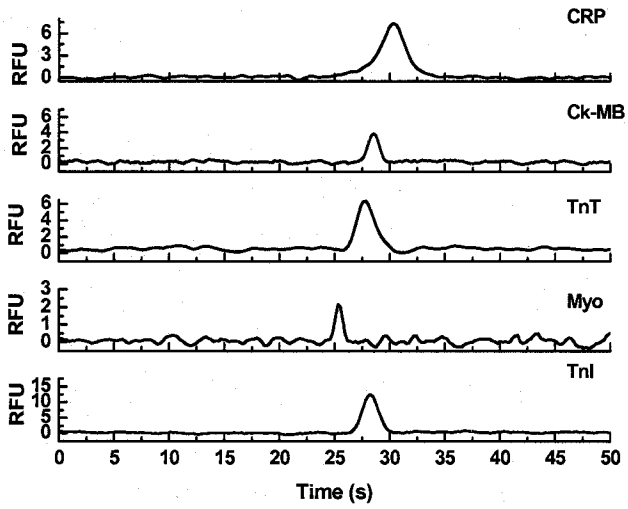

Figure 4.6. Example electropherograms of individual biomarkers for calibration curves of CTI: CRP (FEGGGB) (–), Myo (FEGGB) (–), TnI (FEB) (–), TnT (FHB) (–), CK-MB (FAMB) (–). Experimental conditions: Field strength: 200 V/cm; Pinched injection time: 30 s; BGE: 10 mM tetraborate, 50 mM SDS, 20% acetonitrile. Detection performed using LIF system with a PMT for detection and a solid state laser for excitation (λ= 475 nm) at 2.5 cm.

added, the four products are not resolvable using microchip MEKC. To determine if any of the signal in the assay was attributable to non-specific binding, the CTI was run on a blank buffer sample (no biomarker) of equal volume to that of the biomarker samples. The blanks of each protein did not show any signal indicating no detectable amount of non-specific binding of the detection antibody was occurring (data not shown).

4.2.5 Two protein CTI

Initially, single-protein CTI was performed for C-reactive protein (CRP) and myoglobin (Myo) individually to determine the limit of detection (LOD), linearity, reproducibility and sensitivity of the assay chemistry system.[10] After showing viability of tthe method with a single protein, a multi-analyte assay was performed. In this case the two initial proteins used for proof-of-concept were used in a two protein CTI. In the two protein assay, the CRP detection antibody was labeled with the tag containing a 6-carbon spacer group (FHB) and the myoglobin detection antibody was labeled with the tag containing a 2-carbon spacer group (FEB). The data presented in Figure 4.7 demonstrates the detection of these two proteins from a single sample. The migration time of the peak reflects the difference in electrophoretic mobility of the cleaved tags and the peak area corresponds to the concentration of the protein in the sample prior to performing the CTI. Figure 4.7A shows the electropherogram of sample containing only CRP and Myo. Figure 4.7B is an electropherogram from a sample containing Myo, CRP, and HSA (45mg/mL). HSA, the most abundant protein in the blood, was added at concentrations of over 100-fold higher than the analytes to simulate a clinical sample and to ensure CTI

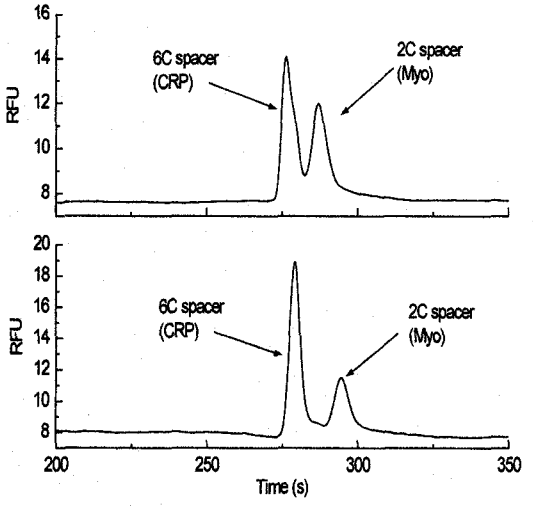

Figure 4.7. Electropherograms of two protein CTI. Detection using microchip CE-LIF at 3cm. Esep=220V/cm. A) Two protein CTI with proteins of interest only in solution. B) Two protein CTI with HSA (45mg/mL) in sample. HSA was added at a concentration equal to the average concentration found in blood to simulate a clinical sample. Figure 2B shows that other proteins present in the sample do not cause interference with the CTI. RFU is relative fluorescence units.

results would not be adversely effected by other high concentration proteins. As shown in Figure 4.7B, no new peaks are present when compared to the sample containing only CRP and Myo. This suggests that it should not be a problem to use the CTI on more complex samples. It also demonstrates the selectivity of the CTI because only those biomarkers with capture and detection antibodies are detected. The addition of HSA did not effect the ability to quantify the two proteins.

4.2.4 Spiked serum samples

The ability to distinguish between normal serum and serum with elevated levels of multiple AMI biomarkers was studied. As reported previously, single-protein CTI was performed for C-reactive protein (CRP) and myoglobin (Myo) to demonstrate the assay chemistry.[10] Figure 4.8 shows a serum sample spiked with elevated concentrations of TnT (FHB), TnI (FEB), Myo (FEGGB) and CK-MB (FAMB). The migration times of the four cleaved tags agree with the migration times of the tags cleaved in buffer allowing for the positive identification of each peak. All four biomarkers are present and quantifiable from the electropherogram using calibration curves. The concentrations in the elevated sample were determined to be 16 ng/mL, 17 ng/mL, 50 pg/mL, and 250 ng/mL for CK-MB, cTnI, cTnT, and Myo respectively.

Human serum contains several classes of proteins including, albumins which are the most abundant (60%), globulins (35%) including α, β, and γ globulins and regulatory proteins including enzymes and hormones. Each of these could potentially cause falsely elevated levels of the AMI markers listed above through non-specific binding and non-specific adsorption. The results reported here demonstrate the high degree of selectivity

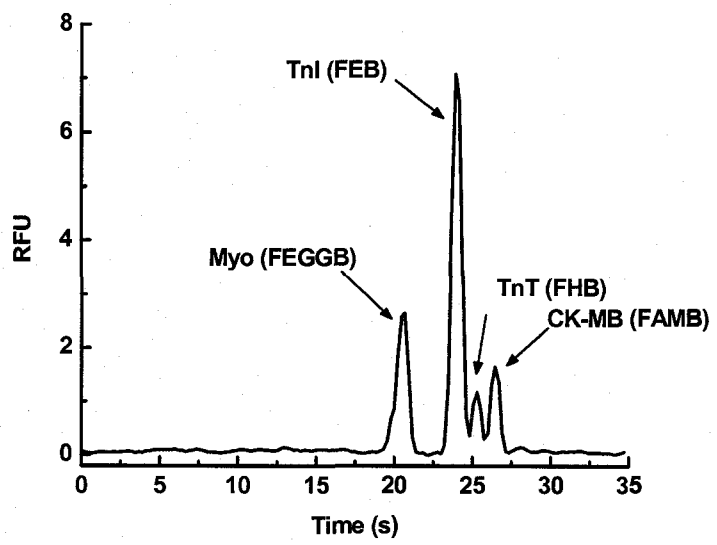

Figure 4.8. Serum sample of four proteins. Each peak is labeled with the corresponding biomarker and tag. Experimental conditions: Field strength: 200 V/cm; Pinched injection time: 30 s; BGE: 10 mM tetraborate, 50 mM SDS, 10 mM N-dodecyl-N,N-dimethyl-3-ammonio-1-propane sulfonate, 20% acetonitrile. Detection performed at 2.5 cm using LIF system with a PMT for detection and a solid state laser for excitation (λ= 475 nm).

of the CTI. Only the desired proteins are detected confirming that potentially interfering proteins do not adversely affect CTI results.

4.3 Summary

This chapter details the steps involved in the CTI. It was shown that the CTI is capable of distinguishing between normal and slightly elevated levels of five clinically relevant proteins for cardiovascular disease, more specifically acute myocardial infarction. The results in this chapter also show that non-specific binding and false positives from other proteins present in solution are not an issue for this chemistry. Improvements in absolute detection limit can be expected by miniaturization and integration of the total assay into a single microfluidic device. In addition the use of an avalanche photodiode instead of a photomultiplier tube (PMT) for detection will improve the LOD significantly.

4.4 References

(1) Bertram, V. M.; Bailey, M. P.; Rocks, B. F. *Ann Clin Biochem* **1991**, *28*, 487-491.
(2) Xue, Q.; Wainright, A.; Gangakhedkar, S.; Gibbons, I. *Electrophoresis* **2001**, *22*, 4000-4007.
(3) Chan-Hui, P. Y.; Stephens, K.; Warnock, R. A.; Singh, S. *Clin Immunol* **2004**, *111*, 162-174.
(4) Hermanson, G. T. In *Bioconjugate Techniques*; Academic Press: Rockford, 1996, pp 570-592.
(5) Roman, G. T.; McDaniel, K.; Culbertson, C. T. *Analyst* **2006**, *131*, 194-201.
(6) Eleftherios P. Diamandis, T. K. C., Ed. *Immunoassay*; Academic Press: San Diego, 1996.
(7) Solberg, H. E. *J Clin Chem Clin Biochem* **1987**, *25*, 337-342.
(8) Verpoorte, E. *Lab Chip* **2003**, *3*, 60N-68N.
(9) Yu, H. T.; Colucci, W. J.; Mclaughlin, M. L.; Barkley, M. D. *J. Am. Chem. Soc.* **1992**, *114*, 8449-8454.
(10) Caulum, M. M.; Henry, C. S. *Analyst* **2006**, *131*, 1091-1093.

CHAPTER 5

IMPROVING SEPARATION EFFICIENCY

Polymers have distinct benefits for microchip production such as cost and ease of fabrication which have caused several groups to focus efforts on producing microchips from polymer substrates.[1-3] Polymers are not without disadvantages, particularly for separation-based applications. Polymer-based devices generally have separation efficiencies that are lower than glass, with PDMS having the lowest separation efficiency.[4] Poor separation performance with PDMS has been attributed to the hydrophobicity of the bulk material and the ability of low molecular weight oligomers to rapidly diffuse to the surface.[5, 6] The result is an unstable hydrophobic material with a heterogeneous surface charge. Control over the surface charge of the capillary wall is very important in both conventional and microchip CE and helps dictate Electroosmotic Flow (EOF).[7, 8] Inconsistent surface charge and analyte absorption as well as peak tailing are all dictated by the surface chemistry of the polymer with hydrophobic surfaces causing more tailing than hydrophilic surfaces. Finally, control of surface chemistry is important for other, non-separation based applications of PDMS microchips including valving,[9] pumping,[10] and surface patterning.[11, 12]

Very few methods have the ability to control the surface chemistry and EOF of PDMS substrates resulting in the low separation efficiency for microchips made from this material.[13-17] A number of groups have sought to overcome the problems with PDMS

through careful control of the surface and bulk chemistry. Whitesides' group was the first to address the problem in microchip CE by oxidizing the material in a simple oxygen plasma.[2] The treatment, however, was unstable due to hydrophobic recovery.[5, 6] More sophisticated methods for surface modification of PDMS have followed with impressive results. Wirth's group used atom-transfer radical polymerization to coat the microchip surface with polyacrylamide.[18] The method generated high efficiency separations for protein mixtures. Allbritton's group demonstrated an alternative surface grafting approach.[19, 20] Surfaces were functionalized with acrylic acid, acrylamide, and poly(ethylene glycol) chemistries and showed a significant improvement in separation efficiency and contact angle relative to native PDMS. Most recently, the Culbertson group published two methods for improving the separation efficiency of PDMS microchips. One method made use of a micellar electrokinetic chromatography (MEKC) buffer containing acetonitrile that resulted in separations with theoretical plates over $1x10^6$ plates/m with the use of laser induced fluorescence detection.[21] In this work, the surfactant (sodium dodecyl sulfate) played an important role in reducing absorption of hydrophobic compounds while also increasing electroosmotic flow. In a second report, the same group reported the development of a novel sol-gel coating inside PDMS microchannels.[21] The coatings improved separation efficiency while also providing the ability to control the surface chemistry by varying the sol composition. While all of these methods improve the performance of PDMS, none of them have been widely adopted because of either a limited set of surface chemistries or the apparent complexity of the treatment process.

Layer-by-layer polyelectrolyte coatings have recently been introduced as semi-permanent coatings for conventional [7, 22, 23] and microchip[24] capillary zone electrophoresis. Polyelectrolyte multilayers (PEMs) are uniformly thin films formed by layer-by-layer deposition of charged polymers, or polyelectrolytes, on a surface. This method was first developed by Decher et al.[25, 26] The mechanisms of formation and charge distribution of PEMs, have been probed by electrokinetics[7, 24, 26] and radiochemical techniques.[27, 28] Alternate adsorption of cationic and anionic polyelectrolytes leads to a very stable coating and the formation of layer-by-layer (LBL) coatings that are simple to deposit, have many potential chemistries, and are robust and reproducible.[27-29]

There have been several reports on the use of polyelectrolytes to stabilize EOF and/or control surface adsorption in CE applications. Maichel et al. and Potocek et al both reported the use of poly(diallyldimethylammonium) (PDADMA) as a replaceable pseudostationary phase in electrokinetic chromatography.[30, 31] Wang and Dubin also worked with PDADMA to minimize protein adsorption.[32] Chiu et al. used polyarginine (PA) as a capillary coating for conventional electrophoretic separations. They showed separation efficiencies of more than 2 million theoretical plates per meter using this coating.[33] Katayama et al. reported the use of polybrene (PB) and dextran sulfate (DS) in multiple ionic-layer coatings to control electroosmotic flow as a function of pH.[22] Cordova et al. investigated the properties of four polycationic polymers as noncovalent coatings to address the problem of protein adsorption in conventional CE.[34] Graul and Schlenoff characterized formation of adsorbed PEMs composed of PDADMA and poly(styrenesulfonate) (PSS) for capillary zone electrophoresis.[7] All of these reports,

however, focused on conventional CE. Only a limited number of examples of PEM coatings have been published for microchips. Barker et al. has published on the use of PEM coatings to alter surfaces in order to control EOF of microchips devices made from polystyrene (PS) and poly(ethylene terephthalate) glycol (PETG).[16, 35] Our group has also previously published on the use of PEMs for control of EOF as a function of pH in PDMS microchips.[24] In none of the above examples, however, was the impact of PEM coatings on separation efficiency measured.

This chapter discusses progress in improving separation efficiency made in our lab, more specifically, my contributions to two manuscripts written within our group that cover separation efficiency optimization. The first manuscript focused on surface modification of PDMS using PEM coatings (manuscript in preparation) and the second manuscript covered solvent extraction of PDMS to permanently modify the channel surface as well as the bulk properties of PDMS.[36] The PEM work included the characterization of several different cationic and anionic multilayer coatings on PDMS microchips for control of flow and improvement of separation efficiency. The coating method was adapted from the successive multiple ionic-layer approach described by Katayama et al.[22] and our previous work.[37] The method utilizes a cationic polymer coating followed by an anionic polymer coating to control surface charge and EOF. The goal of this study was to determine what effect, if any, the chemistry of the polyelectrolyte and the deposition conditions has on coating performance. In these experiments, one of three cationic polymers, polybrene (PB), poly(ethyleneimine) (PEI), or poly(allylamine) hydrochloride (PAH), was used in conjunction with one of two anionic polymers, dextran sulfate (DS) or poly(acrylicacid) (PAA). These polymers,

shown in Figure 5.1 were chosen for their range of chemical functionalities in an effort to determine the impact of polymer functional groups on device performance. EOF measurements were made to determine the impact of coatings on the surface charge as well as the reproducibility and stability of the coatings. Electrophoresis was performed on coated microchips to determine separation efficiency versus native PDMS. In all combinations, a significant increase in the number of theoretical plates (N) was shown as well as improved EOF stability.

A simple method for removal of low-molecular weight oligomers and subsequent generation of a stable SiO_2 surface on PDMS was also developed and characterized. The solvent compatibility of PDMS was recently established by Lee et al.[38] They noted a significant swelling of PDMS in the presence of certain organic solvents indicating the permeation of the solvent into the bulk material. The solvent removes the low molecular weight oligomers, as marked by the reduction in weight by ~5% of the final PDMS microchip. In our approach SiO_2 is generated on the resulting surface of the microchip by treatment with a plasma oxidation step. X-ray photoelectron spectroscopy shows a high percentage of SiO_2 on the surface of treated PDMS that lasts for at least 7 days when stored in air. The resulting microchips exhibit electroosmotic flow velocities similar to those of glass (6.8×10^{-4} cm^2/Vs). Finally, using extracted-oxidized microchips, separation efficiencies of 600,000 N/m were achieved using a 250 μm double-T injector and fluorescence detection. These are among the highest separation efficiencies reported to date for PDMS with an injector of this size.

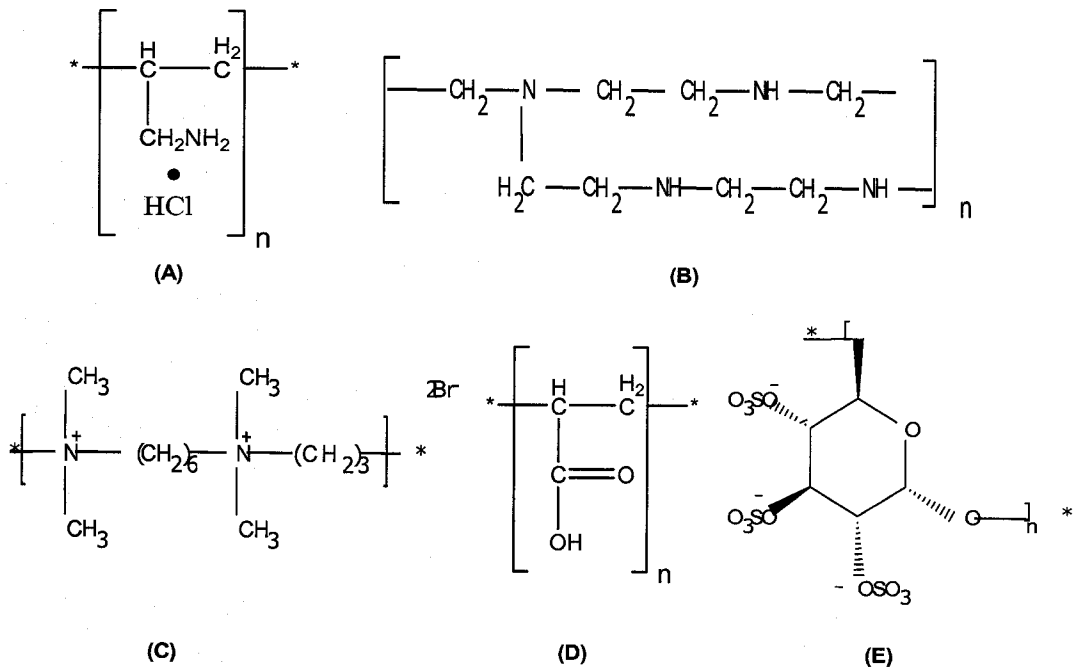

Figure 5.1. Polyelectrolyte coatings: (A) poly(allylamine)hydrochloride, PAH (B) poly(ethyleneimine), PEI (C) polybrene, PB (D) poly(acrylic acid), PAA (E), dextran sulfate, DS.

5.1 Experimental Methods

5.1.1 Layer-by-layer coating procedure

Microchip capillaries were coated with one of the following cationic polyelectrolytes: polybrene (PB), poly(ethyleneimine) (PEI), or poly(allylamine) hydrochloride (PAH) followed by an anionic polyelectrolyte: poly(acrylic acid) (PAA) or dextran sulfate (DS) according to procedures in our previous work.[37] Briefly, the channel was rinsed with 1.0 M NaOH for 30 min followed by coating with a positively charged polyelectrolyte for 5 min. After rinsing with water for 1 min, the channel was coated with the negatively charged polymer for 5 min followed by a rinse with water for 1 min. Alternating between cationic and anionic layers was repeated until the desired number of layers was reached. All polyelectrolyte concentrations were 0.5% (w/v).

5.1.2 PDMS Extraction

For extraction, a molded PDMS piece and a blank piece of PDMS were immersed in 200 mL of a triethylamine solution at 25° C and allowed to stir for 2 hrs. The triethylamine was replaced with fresh solution after 1 hr. The PDMS was removed from the triethylamine and placed in 200 mL of an ethyl acetate at 25° C for 2 hrs with stirring, replacing with fresh solvent after 1 hr. The PDMS pieces were then placed in 200 mL of acetone for 2 hrs. Finally the pieces were allowed to dry completely in a 65° C oven for 2 – 6 hrs. The percent extracted PDMS (w/w) was calculated by determining the difference in the mass between the native and extracted PDMS and dividing by the mass of the native PDMS.

5.1.3 Fluorescence detection

For the PEM studies, fluorescence detection was performed using an epi-fluorescence system with a solid state laser (λ=475nm) for excitation and a photomultiplier tube (PMT) based on similar designs reported by Johnson and Landers.[39] Detection of 1,4-diaminobutane derivatized with FITC (FTPD, 1.5 μM) was performed 2.5 cm down the separation channel using TES (20mM, pH 7.4) as the background electrolyte. Electropherograms were analyzed using peak fitting algorithms in OriginPro 7.

Detection for the extracted-oxidized PDMS of FTPD was performed on an inverted microscope (Nikon, TE-2000U) using epi-fluorescence with a Hg arc lamp for excitation and a CCD camera (Cool Snap cf) for detection at 3 cm from the double-T injector. Data was collected and analyzed using Metamorph Imaging System software (Molecular Devices). The background electrolyte was 10mM boric acid (pH 9.4). FTPD was synthesized in our lab. [40]

Microchips used with fluorescence detection had an identical configuration to the microchips used with electrochemical detection with the exception that the fluorescence microchips did not contain any decoupler or detection electrodes. Furthermore, during injection on the fluorescence chip a push back voltage of 300V was also applied to the buffer waste reservoir to help confine the sample to the double-T for an injection volume of 625 pL.

5.2 Results and Discussion

5.2.1 Polyelectrolyte multilayers

Surface modification using PEMs is attractive because of the wide variety of chemistries available for controlling surface properties. In this study, five different polymers that represent primary (PAH), secondary (PEI), tertiary (PEI), and quaternary (PB) amines as well as a strong (DS) and weak (PAA) anions were studied in an effort to determine how differences in polymer chemistry impacted overall separation performance. The structures of the polyelectrolytes are shown in Figure 5.1. The difference in functional groups may affect surface chemistry. The pI of the amine dictates the degree of protonation of the cationic polyelectrolyte depending on the pH of the run buffer. In addition, the quaternary amine is always protonated and is not affected by the pH of the buffer. The anionic polyelectrolytes will act to increase the EOF due to an increase in anionic surface charge until the pI is reached.

Improvements in separation efficiency using PEM coated microchips with LIF detection are shown in Figure 5.2. Separation efficiency for three different coating combinations (PB/DS, PEI/PAA, PAH/PAA) as a function of the layer number is shown. In each case there is a layer number where N reaches a maximum: for PB/DS after 6 layers (N=12,883 ± 1046), for PEI/PAA after 6 layers (N=11,402 ± 426) and for PAH/PAA after 4 layers (N=11,912 ± 248). These values are roughly a 5-fold improvement in separation efficiency when compared to native PDMS of the three combinations tested. PB/DS generated the highest separation efficiency while PAH/PAA reaches maximum separation efficiency after only four layers. The improvement in

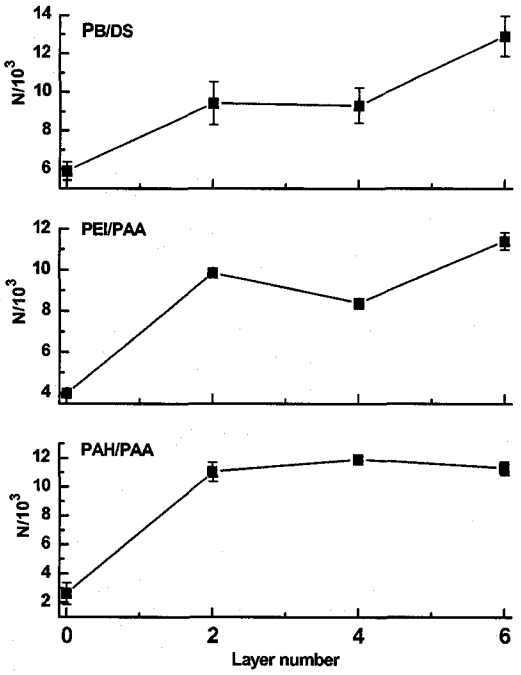

Figure 5.2. Number of theoretical plates (N) as a function of layer number. A) PB/DS alternating layers. B) PEI/PAA alternating layers. C) PAH/PAA alternating layers.

separation efficiency is most likely due to an increase in hydrophilicity of the channel walls causing a decrease in the interaction of the analyte with the channel wall. The remaining characterization of PEM coatings including EOF measurements and separations using EC detection was performed by Kanokporn Boonsong.

5.2.2 Extracted-oxidized PDMS

Extracted PDMS microchips were constructed for both microchip CE-EC and microchip CE-Fluorescence. A significant improvement in peak shape, peak height and peak skew can be seen for both forms of the extracted microchips.

A strong irreversible seal was seen in the chips that were treated between 30 and 180 s. After 180 s the seal was weak or non-existent. After assembly, microchip CE was performed and separation efficiency and peak skew were measured to determine reproducibility and functionality of the chips. Peak skews of 1.1 – 1.3 were seen for all the microchips and did not change with the changing oxidation times. A 40% increase in separation efficiency was seen from 30 to 60 s oxidation times, above 60 s there was no statistical increase in separation efficiency. From this the optimized protocol was determined to be an oxidation of PDMS pieces for 60-120s before sealing them together.

Decreased migration times were observed for all separations and are attributed to an increase in EOF from 4.1×10^{-4} $cm^2/V \cdot s \pm 0.6$ for native PDMS to 6.8×10^{-4} $cm^2/V \cdot s \pm 0.3$ for extracted-oxidized PDMS. The increased EOF can be attributed to the presence of a glass-like SiO_2 surface and a resulting increase in surface charge.

Migration times, peak shape and separation efficiencies for 1.3 μM FTPD were compared on native and extracted PDMS microchips (Figure 5.3) using fluorescence

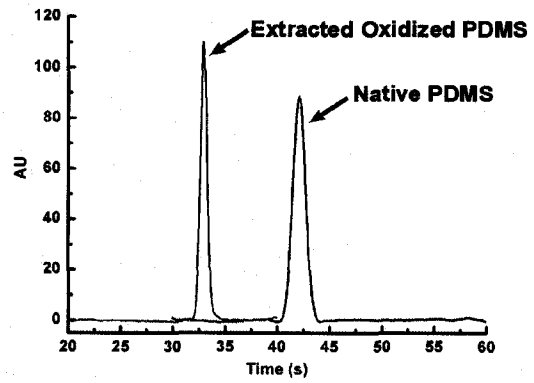

Figure 5.3. Example electropherograms of fluorescent detection of FTPD on native (black) and extracted-oxidized microchips (red). Experimental conditions: Field strength: 220 V/cm; Pinched injection: 20 s; BGE: 20 mM boric acid (pH 10.0).

detection. FTPD is a small hydrophilic organic molecule with a -1 charge that exhibits significant broadening with native PDMS. The peak shape improved with a peak skew of 1.15 for the extracted-oxidized PDMS compared to 1.3 for the native PDMS. Overall the separation efficiency for the extracted-oxidized microchip a separation efficiency of 580,000 ± 36,000 N/m was measured in comparison to only 130,000 ± 18,000 N/m for native PDMS using FTPD. Calculations using the diffusion coefficient of FITC (similar size and charge to FTPD) show peaks to be diffusion limited. Higher separation efficiencies have been measured with PDMS,[20, 21] however, in those examples, either true pinched injection or very fast gated injection was used to significantly reduce the sample volume relative to 0.6-1.1 nL used here.

The % SiO_2 on the surface of native and extracted PDMS for non-oxidized and oxidized pieces was determined through XPS. From XPS peak fits, the percentage of total silicon in SiO_2 form on the surface was determined. In the native PDMS, a rapid decline in SiO_2 on the surface is seen in 3 hrs. Extracted PDMS on the other hand shows only a 7% decrease in SiO_2 (from 91% to 84%) over a 7 day period while stored in air. Contact angle measurements were also made in an effort to further characterize the surface of the PDMS. Contact angle measurements for native and extracted non-oxidized PDMS were 110.2° ± 2.3 and 105.6° ± 4.3 respectively. Once oxidized, the contact angles decreased to 57.9° ± 3.2 for native PDMS and 30.1° ± 1.9 for extracted PDMS. After seven days both PDMS pieces were tested again. The native oxidized PDMS was 110° ± 3.6 but the extracted oxidized PDMS was 40.3° ± 2.3. The contact angles measured provide additional proof that the oxidized surface is stable over significantly extended times while stored in air relative to native PDMS. The changes in contact

angle and SiO_2 content with extracted oxidized PDMS can be attributed to the extraction of the unreacted oligomers that are present in native PDMS. XPS and contact angle measurements were all collected and analyzed by Jonathan A. Vickers.

5.3 Summary

In summary, layer-by-layer polyelectrolyte multilayer coatings can stabilize the EOF of PDMS and also enhance the separation performance. The best results were found with poly(ethyleneimine) (PEI) and poly(acrylic acid) (PAA) in terms of stability and separation efficiency. It was also found that PEM coated chips showed enhanced pH stability when compared to native PDMS. A simple and effective way to generate a stable hydrophilic glass-like surface on PDMS for use with microchip CE-EC and CE-fluorescence was also presented. The ability to oxidize PDMS to form a SiO_2 surface that is stable for a period of at least 7 days was achieved using a simple extraction oxidation procedure allowing for the use of PDMS microchips where high efficiency separations are required and simplifies chip operations by making the channels self wetting. A large improvement in separation efficiency for microchip CE-LIF was shown for both PEM coatings and solvent extracted/oxidized chips with the maximum separation efficiency being 480000 N/m and 580053 N/m respectively as compared to native PDMS with a separation efficiency of just 174241 N/m. In addition, it was also determined that the oxidation time for the sealing process is crucial with a 30s oxidation time giving 444127 N/m as compared to a 60 s oxidation time which gave a separation efficiency of 580053 N/m.

5.4 Acknowledgements

Special thanks goes to Jonathan A. Vickers for his all of his work on the extracted-oxidized PDMS project and Kanokporn Boonsong for her work on the PEM coatings project. I would also like to thank Christopher Easley, Daniel Leslie, and James Landers for their useful discussions regarding extraction protocols.

5.5 References

(1) Soper, S. A.; Ford, S. M.; Qi, S.; McCarley, R. L.; Kelly, K.; Murphy, M. C. *Analytical Chemistry* **2000**, *72*, 642A-651A.
(2) Duffy, D. C.; McDonald, J. C.; Schueller, O. J. A.; Whitesides, G. M. *Anal Chem* **1998**, *70*, 4974-4984.
(3) Fiorini, G. S.; Lorenz, R. M.; Kuo, J. S.; Chiu, D. T. *Analytical Chemistry* **2004**, *76*, 4697-4704.
(4) Lacher, N. A.; Garrison, K. E.; Martin, R. S.; Lunte, S. M. *Electrophoresis* **2001**, *22*, 2526-2536.
(5) Fritz, J. L.; Owen, M. J. *Journal of Adhesion* **1995**, *54*, 33-45.
(6) Thomas, J. H.; Kim, S. K.; Hesketh, P. J.; Halsall, H. B.; Heineman, W. R. *Analytical Chemistry* **2004**, *76*, 2700-2707.
(7) Graul, T. W.; Schlenoff, J. B. *Analytical Chemistry* **1999**, *71*, 4007-4013.
(8) Jorgenson, J. W.; Lukacs, K. D. *Analytical Chemistry* **1981**, *53*, 1298-1302.
(9) Eddington, D. T.; Beebe, D. J. *Journal of Microelectromechanical Systems* **2004**, *13*, 586-593.
(10) Karlinsey, J. M.; Monahan, J.; Marchiarullo, D. J.; Ferrance, J. P.; Landers, J. P. *Analytical Chemistry* **2005**, *77*, 3637-3643.
(11) Khademhosseini, A.; Langer, R.; Borenstein, J.; Vacanti, J. P. *Proceedings of the National Academy of Sciences of the United States of America* **2006**, *103*, 2480-2487.
(12) Dahlin, A. P.; Wetterhall, M.; Liljegren, G.; Bergstroem, S. K.; Andren, P.; Nyholm, L.; Markides, K. E.; Bergquist, J. *Analyst (Cambridge, United Kingdom)* **2005**, *130*, 193-199.
(13) Hu, S.; Ren, X.; Bachman, M.; Sims, C. E.; Li, G. P.; Allbritton, N. *Anal Chem* **2002**, *74*, 4117-4123.
(14) Linder, V.; Verpoorte, E.; Thormann, W.; de Rooij, N. F.; Sigrist, H. *Anal Chem* **2001**, *73*, 4181-4189.
(15) Barker, S. L.; Tarlov, M. J.; Canavan, H.; Hickman, J. J.; Locascio, L. E. *Anal Chem* **2000**, *72*, 4899-4903.
(16) Barker, S. L.; Ross, D.; Tarlov, M. J.; Gaitan, M.; Locascio, L. E. *Anal Chem* **2000**, *72*, 5925-5929.

(17) Henry, A. C.; Tutt, T. J.; Galloway, M.; Davidson, Y. Y.; McWhorter, C. S.; Soper, S. A.; McCarley, R. L. *Analytical Chemistry* **2000**, *72*, 5331-5337.
(18) Koomen, J. M.; Shih, L. N.; Coombes, K. R.; Li, D.; Xiao, L. C.; Fidler, I. J.; Abbruzzese, J. L.; Kobayashi, R. *Clin Cancer Res* **2005**, *11*, 1110-1118.
(19) Hu, S. W.; Ren, X. Q.; Bachman, M.; Sims, C. E.; Li, G. P.; Allbritton, N. L. *Anal Chem* **2004**, *76*, 1865-1870.
(20) Hu, S. W.; Ren, X. Q.; Bachman, M.; Sims, C. E.; Li, G. P.; Allbritton, N. L. *Langmuir* **2004**, *20*, 5569-5574.
(21) Roman, G. T.; McDaniel, K.; Culbertson, C. T. *Analyst* **2006**, *131*, 194-201.
(22) Katayama, H.; Ishihama, Y.; Asakawa, N. *Analytical Chemistry* **1998**, *70*, 2254-2260.
(23) Katayama, H.; Ishihama, Y.; Asakawa, N. *Analytical Chemistry* **1998**, *70*, 5272-5277.
(24) Liu, Y.; Fanguy, J. C.; Bledsoe, J. M.; Henry, C. S. *Analytical Chemistry* **2000**, *72*, 5939-5944.
(25) Decher, G.; Hong, J. D.; Schmitt, J. *Thin Solid Films* **1992**, *210*, 831-835.
(26) Decher, G. *Photonic and Optoelectronic Polymers* **1997**, *672*, 445-459.
(27) Schlenoff, J. B.; Dubas, S. T. *Macromolecules* **2001**, *34*, 592-598.
(28) Schlenoff, J. B.; Ly, H.; Li, M. *Journal of the American Chemical Society* **1998**, *120*, 7626-7634.
(29) Gao, H.; Jiang, T.; Heineman, W. R.; Halsall, H. B.; Caruso, J. L. *Fresenius' Journal of Analytical Chemistry* **1999**, *364*, 170-174.
(30) Maichel, B.; Gas, B.; Kenndler, E. *Electrophoresis* **2000**, *21*, 1505-1512.
(31) Potocek, B.; Chmela, E.; Maichel, B.; Tesarova, E.; Kenndler, E.; Gas, B. *Analytical Chemistry* **2000**, *72*, 74-80.
(32) Wang, Y.; Dubin, P. L. *Analytical Chemistry* **1999**, *71*, 3463-3468.
(33) Chiu, R. W.; Jimenez, J. C.; Monnig, C. A. *Analytica Chimica Acta* **1995**, *307*, 193-201.
(34) Cordova, E.; Gao, J. M.; Whitesides, G. M. *Analytical Chemistry* **1997**, *69*, 1370-1379.
(35) Barker, S. L. R.; Tarlov, M. J.; Canavan, H.; Hickman, J. J.; Locascio, L. E. *Analytical Chemistry* **2000**, *72*, 4899-4903.
(36) Vickers, J. A.; Caulum, M. M.; Henry, C. S. *Anal Chem* **2006**, *78*, 7446-7452.
(37) Liu, Y.; Fanguy, J. C.; Bledsoe, J. M.; Henry, C. S. *Anal Chem* **2000**, *72*, 5939-5944.
(38) Lee, J. N.; Park, C.; Whitesides, G. M. *Anal Chem* **2003**, *75*, 6544-6554.
(39) Johnson, M. E.; Landers, J. P. *Electrophoresis* **2004**, *25*, 3513-3527.
(40) Caulum, M. M.; Henry, C. S. *Analyst* **2006**, *131*, 1091-1093.

CHAPTER 6

SINGLE PARTICLE REACTION KINETICS IN MICROFLUIDIC DEVICES

Recently there has been an increase in the use of microfluidic devices for surface-based biochemical assays.[1] Microfluidic devices give the advantages of reduced sample volume and waste generation. There is the added advantage of an increase in surface-to-volume ratio which leads to shorter assay times due to reduced diffusional distances when compared to traditional immunoassay approaches.[2] The use of beads within a microchannel for solid-phase immunoassays can further increase the binding area per unit volume which acts as a pre-concentration step to amplify the assay signal.[3, 4]

On-chip, bead-based chemistry generally involves a form of bead immobilization within the device which include physical barriers or surface immobilization. Physical structures must serve a dual purpose to trap beads and still allow reagents to be delivered to all parts of the chip. One design which accomplishes the physical requirements was reported by Oleschuk et al. in which leaky walls were fabricated surrounding a microchamber. The device was demonstrated to be useful for selective preconcentration of theophylline using Protein A immunoaffinity chromatography.[5] The immobilization of beads in a microfluidic device has also been demonstrated through the use of temperature-sensitive polymers. The microfluidic channel is filled with beads functionalized with the temperature-sensitive polymer at room temperature and upon temperature elevation, the beads aggregate and adhere to the channel walls.[6] Particles can

also be actively trapped and transported in microfluidic devices. Recently, Verpoorte's group has developed fluid focusing techniques for particle manipulation.[7]

Magnetic beads offer still another advantage in that they can be manipulated with great control using permanent magnets or electromagnets.[8] The ability to effectively manipulate magnetic beads eliminates the need for physical barriers to trap beads which in turn simplifies microfluidic chip designs. There have been several reports published on the use of magnetic beads in fluidic systems.[2, 9, 10] In work published by Rashkovetsky et al., magnetic beads were used in conjunction with commercial CE systems to perform enzymatic and inhibition assays.[11] The unique properties of magnetic beads have lead to their wide incorporation as a solid support in immuonassays,[12] cell sorting, mRNA isolation,[13] and flow injection immunoassays.[14]

The long-term goal of the CTI project is to develop a point-of-care analyzer to quantitatively screen for multiple biomarkers simultaneously. Initially, magnetic beads will be incorporated as the stationary phase for capture antibody immobilization. One of the most important aspects to address with the use of magnetic particles in a microfluidic device is the optimization of reaction kinetics. Reaction kinetics for each step of the CTI need to be studied and optimized in order to develop an integrated CTI analyzer for rapid point-of-care screening. This chapter presents preliminary studies in single particle kinetics for use in solid-phase microchip immuoassays. Solution-phase kinetics were studied for tags used in the CTI, however, solid-phase kinetics were never studied prior to performing the assay. Excess time was simply given for the cleavage process when using the particles to ensure all of the tag was cleaved from the detection antibodies. Therefore, the next logical step was to study the reaction kinetics on particles. To study the particle

based cleavage kinetics magnetic particles labeled with the tags used in the CTI were trapped in PDMS microchips and change in fluorescence intensity was measured over time. Magnetic beads (1-4 μm diameter) were used because of the ability to trap them at specific locations within the microchip channel using small stationary magnets. It is our intent to use the magnetic particles as part of an integrated CTI analyzer. Cleavage kinetics were studied for tris(2-carboxyethyl) phosphine (TCEP), dithiothreitol (DTT) and 2-mercaptoethanol (β-ME). The ability to use an extracted-oxidized chip (Chapter 5) to trap magnetic particles, perform kinetics studies on the trapped particles, and release the particles in order to re-use the chip was demonstrated. This work also compares pH dependence of the various reducing agents. Based on the results of this study, stopped-flow kinetics with TCEP will be required for cleavage step of the CTI assay.

6.1 Experimental Methods

6.1.1 Labeling magnetic beads

The initial magnetic bead studies were conducted using streptavidin coated magnetic particles in an effort once again to reduce antibody consumption. This also allows for the ability to study each tag individually and characterize the system including kinetics of tag cleavage without the antibodies and antigens present. Streptavidin coated magnetic particles (Magnabeads) were tagged with FEB. The synthesis of FEB was described in Chapter 3 of this work and has been previously published.[15] The tag was immobilized on the magnetic particles through biotin-avidin interactions according to instructions from Pierce. The magnetic particles (1 mL) were rinsed three times with phosphate buffer (20 mM, pH 7) by magnetically separating the particles from the

solution using Neodymium-Iron-Boron (NdFeB) magnets, removing the liquid, and adding fresh buffer. Following this phosphate buffer (1 mL) was added to the particles along with FEB (1 mL, 1 mM) and allowed to react with the particles for 30 min at room temperature (22 ± 2 °C) with gentle mixing. To ensure minimal aggregation of the particles occurred, particles were never centrifuged or vortexed and only the magnets were used to separate the particles from solution. The FEB was reacted in excess compared to the streptavidin on the particles to ensure all of the particles were labeled. Following the reaction, the particles were again rinsed three times with phosphate buffer (20 mM, pH 7). At this point the particles were stored in fresh phosphate buffer at 4 °C and protected from light.

6.1.2 Manipulation of magnetic beads

NdFeB permanent magnets (3.175 mm diameter) were used to capture the magnetic particles as they traveled down the separation channel. Initially the magnets were placed on top of the chip, however, the magnetic force generated in the channel was not strong enough to hold the particles in place so holes were punched to house the magnets as close as possible to the channel prior to extraction and chip assembly. The assembled chip is shown in Figure 6.1. The magnets could be easily removed to release the particles and placed back in the chip to capture new particles.

A.

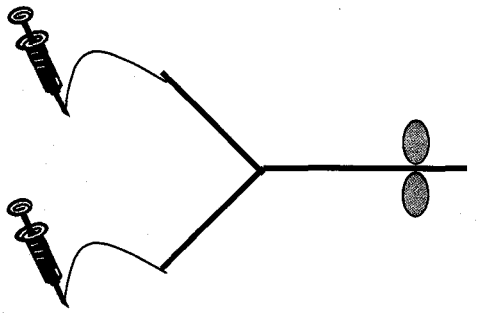

B.

Figure 6.1. Microchip design. A. Schematic of chip used to study reaction kinetics where each of the solid lines represents a channel and the orange circles are magnets. B. Photograph of magnets placed in microchip. Black line in center of drawing is the channel.

6.1.3 Cleavage kinetics using magnetic beads

Previous studies had been done on the cleavage kinetics in solution for the tags used in the CTI. The next step in moving towards an integrated microchip CTI was to determine the kinetics of the tags when bound to a surface. To study this, labeled beads (50 μL) were injected into the chip using a syringe pump (New Era Pump Systems, Inc.) at a flow rate of 0.6 μL/min and captured in the channel using stationary NdFeB magnets. The remaining solution was washed away and the reducing agent was flowed over the beads using a second syringe pump with a flow rate of 1.5 μL/min. Fluorescence intensity was measured and plotted as a function of cleavage time. Different TCEP concentrations were tested from 0.125-5 mM. Cleavage time for TCEP (2 mM) was compared to DTT (2 mM) and β-ME (2 mM). Dependence of cleavage time on pH was also studied for each of the reducing agents.

6.1.4 PDMS device fabrication

All experiments detailed here were performed using extracted-oxidized poly(dimethylsiloxane) (PDMS) microchips fabricated using established protocols detailed in Chapter 2[16-19] and extracted according to methods described in Chapter 5.[20] The reservoirs for the syringe pump tubing were punched using a 1.6 mm hole punch and the reservoirs for the magnets were punched using a standard 6 mm hole punch.

6.2 Results and Discussion

6.2.1 Effect of TCEP concentration on cleavage rate

Cleavage time of FEB with respect to TCEP concentration was studied. The fluorescence intensity of the labeled beads was measured as a function of time. Cleavage was considered complete when no change in fluorescence intensity was seen. Time-lapse data was collected for all captured particles and individual particles (n=6) were selected using MetaMorph software for fluorescence measurements and cleavage times were averaged for each condition studied. The TCEP concentrations studied were 0.125-5 mM. Looking at cleavage time as a function of TCEP concentration as shown in Figure 6.2A, TCEP concentrations greater than 2 mM showed little decrease in cleavage time; therefore, it is not necessary to use a concentration of TCEP higher than 2 mM in the CTI. Complete disulfide cleavage at a TCEP concentration of 2 mM took 15.7 min. In comparison, 2 mM TCEP completely cleaved FEB in solution under 20 min. The graph of 1/[TCEP] versus time is a linear plot which indicates reduction of the disulfide bonds in FEB by TCEP is a second order reaction with respect to TCEP. Figure 6.2B shows the results of the bead-based cleavage kinetics study plotted as 1/[TCEP] versus time. Stopped flow kinetics will be required to obtain an accurate concentration of cleaved tag because the time required for solution to reach the detection point following injection is significantly less than the time required for cleavage (45 s versus 30 min).

6.2.2 TCEP versus other reducing agents

A second study conducted compared three different reducing agents, TCEP, DTT, and β-ME. All three of these agents are used to reduce disulfide bonds. TCEP, DTT, and

A.

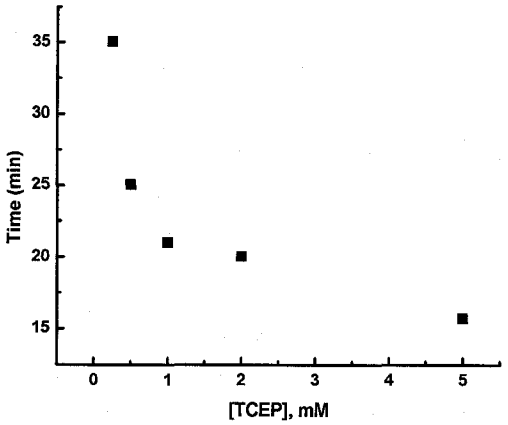

B.

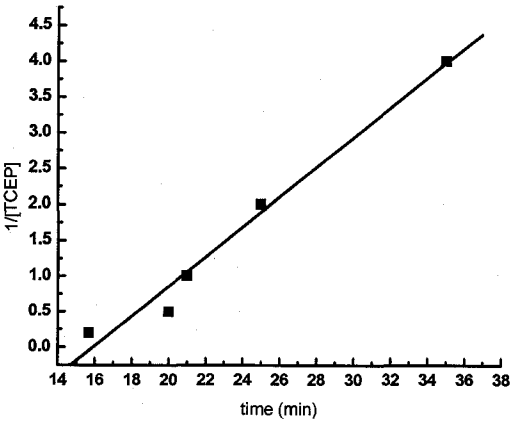

Figure 6.2. Effect of TCEP on cleavage time. A. Cleavage time versus TCEP concentration (mM). B. 1/[TCEP] versus time showing reduction using TCEP is second order.

β-ME, all at 2 mM concentration, were compared over a broad pH range (4.5-10.4) to test the pH dependence of disulfide reduction. Figure 6.3 shows the results of the pH study. Due to chip malfunction, no fluorescence data was collected for TCEP at pH 9, however, the remaining data points show TCEP exhibited essentially no pH dependence compared to the pH dependence seen with DTT and β-ME. The shortest cleavage time was at a pH of 4.5 for DTT (32 min) and 6.4 for β-ME (35 min). Each of these cleavage rates was still much slower than TCEP at any pH. Figure 6.3 shows cleavage time for TCEP is less than the cleavage time for DTT and β-ME at all pH values tested proving TCEP is more effective at reducing the disulfide of FEB. There are reasons for the pH dependence of DTT and β-ME including overall stability of the reducing agents and the reaction mechanisms.

TCEP has been reported to be stable at $1.5 < pH < 9.0$ and more effective than DTT at $pH < 8.0$.[21] The lack of stability for DTT and β-ME could account for some of the variation in pH dependence. The useful pH range for both DTT and β-ME is much more narrow and slightly skewed towards acidic pH values with pH range for DTT being 6.5-9.0 and pH 6-9 for β-ME. DTT and β-ME were shown to be more effective at disulfide reduction at acidic pH compared to alkaline pH. The reaction mechanisms of DTT and β-ME also explain the pH dependence of the disulfide reduction. Reductions using DTT or β-ME are thermodynamically controlled whereas reduction with TCEP is kinetically controlled.[22] The mechanism of disulfide reduction using β-ME is a two step process where the first step is the formation of a mixed disulfide and the second requires a second β-ME molecule to complete the reduction of the disulfide to thiolated compounds causing the formation of a dimer of the reducing agent. The equilibrium of

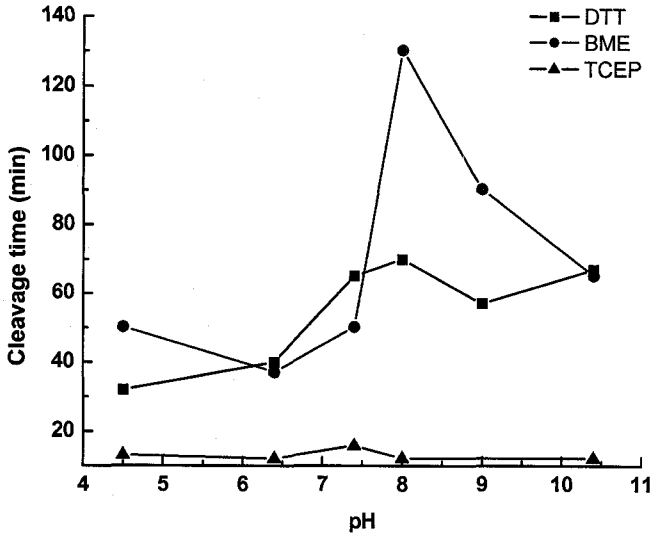

Figure 6.3. pH dependence of disulfide cleavage. This graph compares three different reducing agents, TCEP (--▲--), DTT (--■--), and β-ME (--●--)for pH values 4.5-10.4.

disulfide exchange in reactions involving β-ME is nearly equal between the target analyte and the reductant requiring an excess of monothiol reducing compounds such as β-ME for the reaction to go to completion. DTT oxidation forms a sterically favored intermolecular ring structure.[23] This unique molecular property may effect the pH dependence of disulfide bond reduction. The equilibrium of this reaction is driven towards the reduction of the target disulfides due to the formation of the favored cyclic disulfide of oxidized DTT.

As stated previously, cleavage was considered complete when no change in fluorescence intensity was seen. In all cases, there was still residual fluorescence on the particles following completed cleavage. An example of this can be seen in Figure 6.4 where a graph of fluorescence intensity versus time for β-ME (2 mM, pH 9) is shown. Representative particle pictures are shown in 6.4B-D. Figure 6.4B was taken immediately following the switch from the syringe containing buffer to the syringe containing cleavage solution, 6.4C was taken at 30 min and 6.4D was taken when cleavage was considered complete (90 min). The particles are still slightly visible at the end of the experiment. In these experiments, FEB was synthesized as described in Chapter 3 with excess FTED present which could have become attached to the particles through non-specific binding and was not washed away during the rinse steps. FTED is not cleavable and therefore would still be present after all FEB was cleaved from the particles. The apparent residual fluorescence could also be caused by diffraction. If the fluorescence is due to diffraction of light by the particles captured in the channel, particles that have not been labeled would appear fluorescent in the channel.

A.

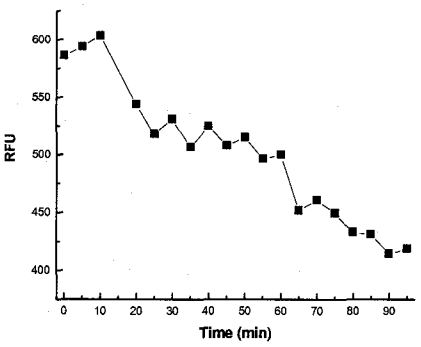

B.

C.

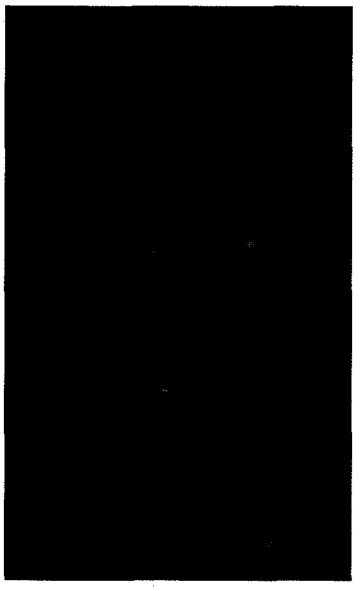

D.

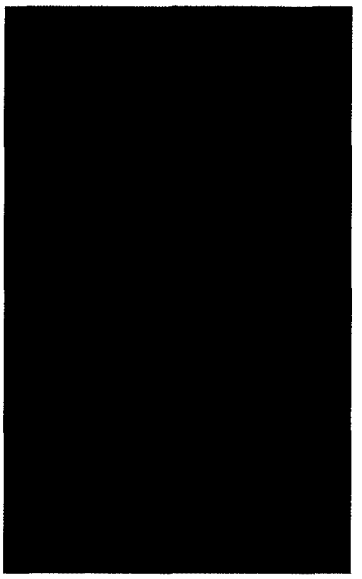

Figure 6.4. Example data for cleavage study. A. Fluorescence intensity versus time for FEB cleavage using β-ME (2 mM, pH 8). B. Photograph of microchip channel containing beads taken at 0 min. C. Photograph of channel containing beads at 30 min. D. Photograph of channel containing beads at 80 min.

6.2.3 Extracted-oxidized chips

As previously published by our group, extracted-oxidized PDMS has been shown to exhibit similar surface properties to an SiO_2 surface.[20] Here the glass-like PDMS channel surface has been shown to virtually eliminate particle adsorption to the channel walls of the PDMS microchip which is a known problem with PDMS. In contrast to previously published work which used a sodium hydroxide rinse prior to re-using the PDMS chip[24], no pre-treatment was needed before running an additional assay with an extracted-oxidized PDMS chip. Figure 6.5 shows the capture and release of FEB labeled magnetic particles in an extracted-oxidized PDMS microchip. Particles shown in this figure have aggregated and therefore appear quite large. Of important note here is that in this case no particles remain after the magnets are removed from the chip. Additional experiments need to be conducted to quantitatively determine the decrease in particle adhesion using different buffers as well as nanoparticles with different functional groups.

6.3 Summary

This chapter details studies conducted in single particle reaction kinetics focused on the cleavage step of the CTI. The effect of TCEP concentration on cleavage time was studied and showed concentrations of 2 mM or greater did not further increase the disulfide cleavage rate. The pH dependence of three different reducing agents, TCEP, DTT, and β-ME was compared. Results included in this chapter indicate stopped flow kinetics will need to be used with the CTI when converting to an on-chip assay. In addition, the use of extracted-oxidized PDMS eliminates particle adhesion problems normally present when working with native PDMS.

A.

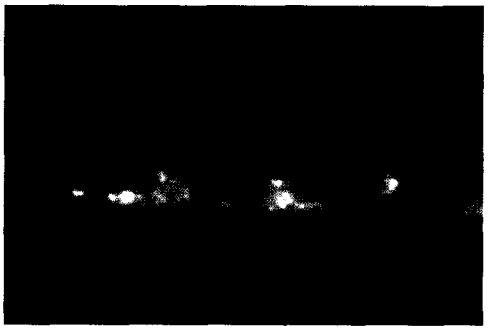

B.

C.

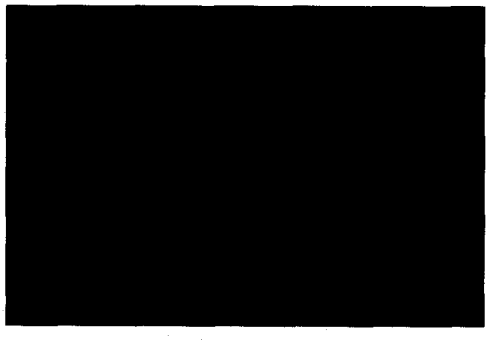

Figure 6.5. Capture and release of magnetic particles in an extracted-oxidized chip. A. Fluorescently labeled particles captured using external rare earth magnets. B. Particles at moment magnets were removed. C. 30 s following magnet removal with hydrodynamic flow applied to channel.

6.4 References

(1) Gijs, M. A. M. *Microfluidics and Nanofluidics* **2004**, *1*, 22-40.
(2) Rida, A.; Gijs, M. A. *Anal Chem* **2004**, *76*, 6239-6246.
(3) Verpoorte, E. *Lab Chip* **2003**, *3*, 60N-68N.
(4) Krogh, T. N.; Berg, T.; Hojrup, P. *Anal Biochem* **1999**, *274*, 153-162.
(5) Wang, C.; Oleschuk, R.; Ouchen, F.; Li, J.; Thibault, P.; Harrison, D. J. *Rapid Commun Mass Spectrom* **2000**, *14*, 1377-1383.
(6) Malmstadt, N.; Yager, P.; Hoffman, A. S.; Stayton, P. S. *Anal Chem* **2003**, *75*, 2943-2949.
(7) Lettieri, G. L.; Dodge, A.; Boer, G.; de Rooij, N. F.; Verpoorte, E. *Lab Chip* **2003**, *3*, 34-39.
(8) Ostergaard, S.; Blankenstein, G.; Dirac, H.; Leistiko, O. *Journal of Magnetism and Magnetic Materials* **1999**, *194*, 156-162.
(9) Hayes, M. A.; Polson, T. N.; Phayre, A. N.; Garcia, A. A. *Anal Chem* **2001**, *73*, 5896-5902.
(10) Zhao, X. Y.; Shippy, S. A. *Analytical Chemistry* **2004**, *76*, 1871-1876.
(11) Rashkovetsky, L. G.; Lyubarskaya, Y. V.; Foret, F.; Hughes, D. E.; Karger, B. L. *Journal of Chromatography A* **1997**, *781*, 197-204.
(12) Haukanes, B. I.; Kvam, C. *Biotechnology (N Y)* **1993**, *11*, 60-63.
(13) Jiang, G.; Harrison, D. J. *Analyst* **2000**, *125*, 2176-2179.
(14) Pollema, C. H.; Ruzicka, J.; Christian, G. D.; Lernmark, A. *Anal Chem* **1992**, *64*, 1356-1361.
(15) Caulum, M. M.; Henry, C. S. *Analyst* **2006**, *131*, 1091-1093.
(16) Liu, Y.; Vickers, J. A.; Henry, C. S. *Analytical Chemistry* **2004**, *76*, 1513-1517.
(17) Liu, Y.; Wipf, D. O.; Henry, C. S. *Analyst* **2001**, *126*, 1248-1251.
(18) McDonald, J. C.; Whitesides, G. M. *Accounts of Chemical Research* **2002**, *35*, 491-499.
(19) Liu, Y.; Fanguy, J. C.; Bledsoe, J. M.; Henry, C. S. *Anal Chem* **2000**, *72*, 5939-5944.
(20) Vickers, J. A.; Caulum, M. M.; Henry, C. S. *Anal Chem* **2006**, *78*, 7446-7452.
(21) Han, J. C.; Han, G. Y. *Anal Biochem* **1994**, *220*, 5-10.
(22) Burns, J. A.; Butler, J. C.; Moran, J.; Whitesides, G. M. *Journal of Organic Chemistry* **1991**, *56*, 2648-2650.
(23) Cleland, W. W. *Biochemistry* **1964**, *3*, 480-&.
(24) Slovakova, M.; Minc, N.; Bilkova, Z.; Smadja, C.; Faigle, W.; Futterer, C.; Taverna, M.; Viovy, J. L. *Lab on a Chip* **2005**, *5*, 935-942.

CHAPTER 7

CONCLUSIONS AND FUTURE DIRECTIONS

7.1 Conclusion and summary

The work of this doctoral dissertation focused on development of a novel immunoassay that combines cleavable tags with microchip micellar electrokinetic chromatography (MEKC) to perform multi-analyte protein profiling in such a way that fills the gap between low- and high-throughput screening methods. The Cleavable Tag Immunoassay (CTI), is a medium-density heterogeneous immunoassay designed to detect 1-20 analytes simultaneously. While similar to traditional sandwich immunoassay chemistry in terms of analyte capture, this approach is unique because the signal is not imaged directly on a surface; instead, a fluorescent tag is cleaved from the antibody and analyzed by microchip MEKC.

A large portion of my dissertation work concentrated on the development of synthesis protocols for CTI tags. The methods used for tag synthesis produced fluorescent, cleavable tags with an affinity for avidin. To date, three different synthesis protocols have been developed and optimized to produce tags for the CTI.

Optimization of background electrolyte was performed to obtain resolution required for quantification of the tags (biomarkers). The CTI was performed on serum samples spiked with elevated concentrations of four cardiac biomarkers: TnT, TnI, CK-MB, and Myo. Initially, the biomarkers were run separately to obtain the calibration

curves, limits of detection (LOD), and linear ranges for all four proteins. The bead volume and volume of cleaving agent were optimized so that the sensitive portion of the curve bracketed the upper reference limit for each protein. The experimentally measured LOD and linear range for each protein in the CTI were reported in this work. We have successfully shown that the CTI can quantitatively detect elevated levels of four key heart attack biomarkers and by expanding the tag library should be easily adapted for detection of many more analytes in complex samples. Improvements in absolute detection limit can be expected by miniaturization and integration of the total assay into a single microfluidic device. In addition the use of an avalanche photodiode instead of a photomultiplier tube (PMT) for detection will improve the LOD significantly.

Progress has been made on integrating the CTI on-chip for a micro-total analysis system (μ-TAS). Ultimately, the use of antibodies immobilized inside an integrated microfluidic device will provide the fastest reaction times due to the reduction in diffusional distances. Preliminary studies have been conducted using streptavidin coated magnetic particles labelled in-house with the cleavable tags used in the CTI to monitor solid-phase cleavage kinetics. To monitor the cleavage process, the reducing agent was flowed over the labelled beads using hydrodynamic flow and the fluorescence intensity measured as a function of time for three different reducing agents over a pH range of 4.5-10.4. Based on the results of this study, stopped-flow kinetics will be required to complete the cleavage step of the CTI μ-TAS.

A portion of my dissertation was focused on improving separation efficiency of PDMS microchips through two different approaches. The first technique focused on surface modification of PDMS using PEM coatings (manuscript in preparation) and the

second technique was the use of solvent extraction of PDMS to permanently modify the channel surface as well as the bulk properties of PDMS.[1] The PEM work included the characterization of several different cationic and anionic multilayer coatings on PDMS microchips for control of flow and improvement of separation efficiency. The polymers were chosen for their range of chemical functionalities in an effort to determine the impact of polymer functional groups on device performance. In all combinations, a significant increase in the number of theoretical plates (N) was shown as well as improved EOF stability. A simple method for removal of low-molecular weight oligomers and subsequent generation of a stable SiO_2 surface on PDMS was also developed and characterized. Using extracted-oxidized microchips, separation efficiencies of 600,000 N/m were achieved using a 250 μm double-T injector and fluorescence detection. These are among the highest separation efficiencies reported to date for PDMS with an injector of this size.

7.2 Future directions

The next logical step for this project is to combine non-competitive and competitive forms of CTI in one assay for several different biomarkers. My colleague, Brian Murphy, has been developing the competitive CTI for a different set of biomarkers.

In order to move more towards a point-of-care device, alternative detection formats will need to be explored. A very viable alternative to fluorescence detection is the use of electrochemical detection. The cleaved tags are thiols which are electrochemically active and can be detected using PAD mode II or iPAD.[2] There is also the possibility of using a small diode laser instead of a solid-state laser as the excitation

source while still employing fluorescence detection. Both of these alternative detection methods would allow for further miniaturization when compared to the current methods employed for the excitation source and the detection methods leading to the definite possibility of a portable device no bigger than a typical briefcase.

The overall final goal of this project is to create a lab-on-a-chip CTI device. This involves the integration of all of the CTI components including the assay assembly, whole blood sample introduction, separation and detection on one microchip through the use of valving, on-chip mixers, and stationary magnets. Initally, the detection antibody will be labelled and the capture antibodies immobilized on magnetic particles prior to introduction into the device. There are currently several other lab members working on the various components of this micro-total analysis system.

7.3 References

(1) Vickers, J. A.; Caulum, M. M.; Henry, C. S. *Anal Chem* **2006**, *78*, 7446-7452.
(2) Modi, S. J.; LaCourse, W. R.; Shansky, R. E. *Journal of Pharmaceutical and Biomedical Analysis* **2005**, *37*, 19-25.

APPENDIX 1: RESEARCH PROPOSAL

MINIATURIZED COMET ASSAY TO MONITOR OXIDATIVE DNA DAMAGE IN HUMAN CELLS

A. Specific Aims

Reactive oxidative species (ROS) lead to the occurrence of at least 50 different human diseases including type II diabetes, Alzheimer's disease, and cancer through oxidative DNA damage.[1-3] These ROS cause DNA mutations which in turn cause lesions, such as 8-hydroxyguanine (8-OH-dG), that are established biomarkers of oxidative stress. Methods for measuring oxidative DNA damage and stress include GC/MS, HPLC, ELISA, and the Comet Assay. The primary molecular marker currently used to measure oxidative stress is 8-OH-dG. Current methods for measuring 8-OH-dG show variation of 20% for 8-OH-dG levels as reported by a multi-laboratory study through ESCODD (European Standards Committee on Oxidative DNA Damage).[4] Recently, the comet assay has gained attention as a method for monitoring global DNA damage. It directly measures the amount of damage in a single cell by detecting DNA strand breaks. The results obtained for the comet assay are, however, very subjective. The discrepancies in current methods show the necessity for a rapid, inexpensive, reliable and quantitative biochemical method for monitoring DNA damage within cells. *Here, we propose to develop a novel miniaturized comet assay for monitoring DNA damage in human cells, more specifically, leukocytes.* The miniaturized comet assay (MCA) will reduce sample consumption, analysis time, and overall analysis cost while increasing the reproducibility and accuracy of the assay. The specific aims of this proposal are:

1. Develop hydrodynamically opposed electrophoresis for the separation and quantification of DNA fragments
2. Use known microfluidic concepts to develop on-chip sample preparation by optimizing sample introduction as well as using functionalized magnetic beads to extract leukocytes from whole blood and perform various chemical processes including cell lyses and fluorescent labeling on these captured cells
3. Merge the components developed in specific aims one and two by developing an all inclusive microchip which contains a series of valves to help combine these two major components of the miniaturized comet assay and test the viability as compared to the conventional comet assay using pure leukocyte samples as well as whole blood

The miniaturized comet assay will have a significant impact on the field of clinical chemistry as well as fundamental free radical biology by providing an efficient, inexpensive way to quickly and quantitatively measure oxidative DNA damage and repair rates in chemotherapy patients. Furthermore, hydrodynamically opposed electrophoresis should have a broader impact on the field of microchip separations by providing a new size-based separation method which offers improvements in speed and resolution.

B. Background

Within the past 20 years, efforts have focused on the development of assays to screen for oxidative DNA damage within cells.[5] Oxidative damage is a normal occurrence in cellular metabolism and is primarily in a steady-state equilibrium with DNA repair. Reactive oxygen species (ROS) are normally produced by the mitochondria during cellular respiration. ROS are thought to influence the development of more than 50 human diseases including cancer.[1, 2] Oxidized DNA bases such as 8-OH-dG are thought to result from attack by ROS during biochemical utilization of O_2. During this process, O_2^- is converted by superoxide dismutase into H_2O_2 which can in turn be transformed to highly reactive hydroxyl radical through Fenton chemistry.[6] Figure B1 shows several products of oxidative damage. Of these products, 8-OH-dG is the most abundant and the most extensively studied oxidation product.[7] 8-OH-dG is potentially mutagenic and is a

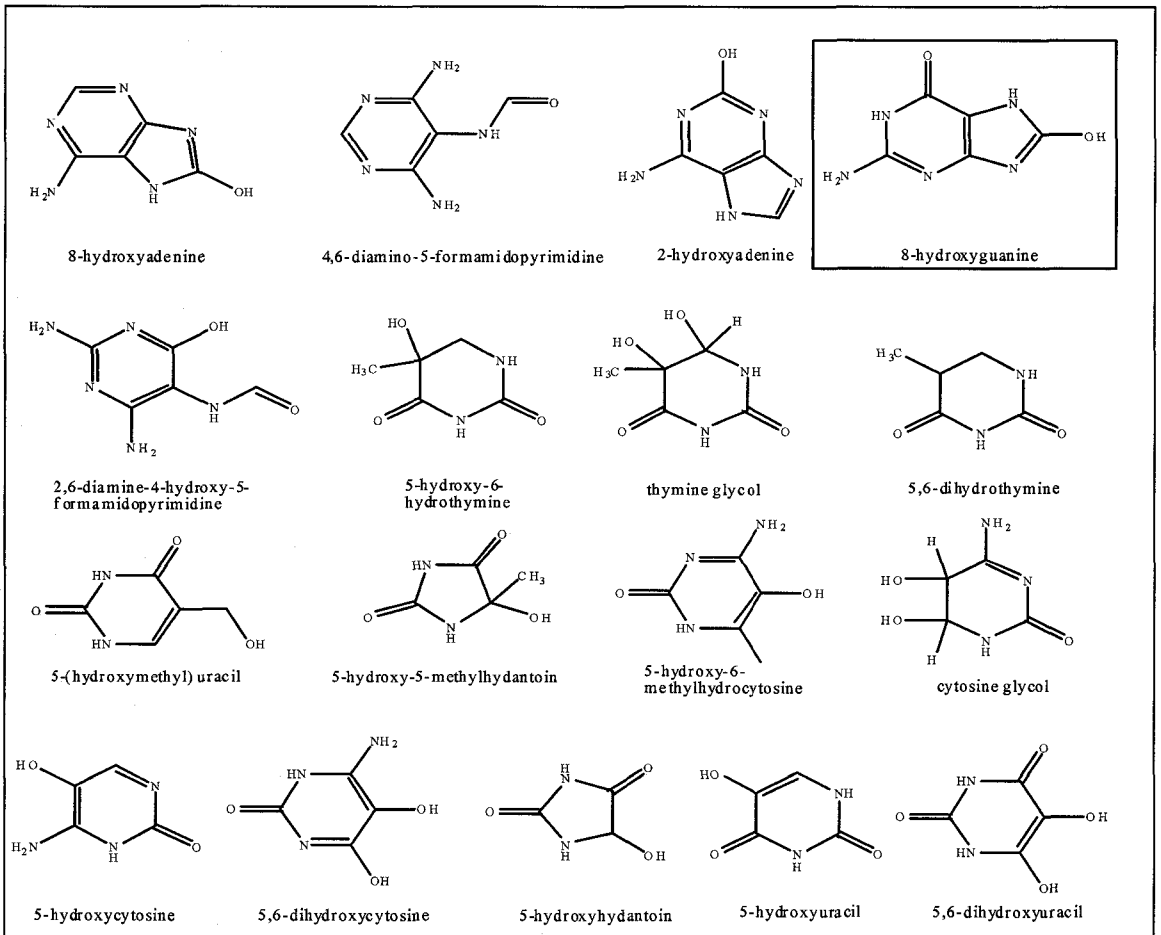

Figure B1. Products of oxidative DNA damage.

widely accepted marker of both oxidative stress and oxidative DNA damage. The identification and quantification of this molecule is essential in order to measure DNA damage accurately and distinguish normal levels from abnormal levels of DNA damage.

Many assays have been developed to monitor 8-OH-dG levels including gas chromatography coupled to mass spectrometry (GC/MS), Liquid chromatography with electrochemical detection or mass spectrometry (LCEC or LCMS), capillary

electrophoresis with electrochemical detection (CEEC), postlabelling with ^{32}P, and enzyme linked immunosorbent assay (ELISA).[1] These methods are described in the sections that follow.

B.1. GC/MS. GC/MS is used to measure several modified bases and is the only technique currently available for detection and quantification of all four bases (A, G, C, and T) simultaneously with limits of detection at low femtomolar concentrations.[8, 9] GC/MS, however, suffers from several limitations and disadvantages for DNA damage measurements including complex, expensive instrumentation, difficult derivitization processes, sample preparation requirements and extraction procedures which can produce artifactual oxidation products and contribute to increased levels of certain oxidized bases and nucleosides.[1] Artifactual oxidation is a huge problem with current methods because it causes elevated levels of oxidative damage and also causes the large margin of error and lack of reproducibility associated with these techniques which can essentially invalidate the assay for most researchers.

B.2. LC methods. LC separation techniques have been coupled with both MS and EC for detection. LCEC is the most widely used method for detection of 7,8-dihydro-8-oxo-guanine (8-OH-dG).[10] This method can be used to measure 8-OH-dG concentrations in a variety of samples including urine,[11] blood[12] and tissue [13] with detection limits in the sub-picomolar range. Most LC methods utilize a reverse-phase (C18) column.

B.3. Postlabeling methods. There are several advantages to postlabelling methods when compared to GC/MS and LC/MS including the lack of increased temperature or harsh chemical reaction when preparing the sample for analysis which cuts down on artifacts and it uses less sample (50 ng to 5 μg vs 40-100 μg).[14, 15] This method, however, involves extended incubation times and deals with radioactive labels.

B.4. ELISA. ELISA has been used to measure oxidative stress in humans undergoing chemotherapy and radiation therapy by Erhola et al.[16] The ELISA procedure for 8-OH-dG is performed using monoclonal antibodies in a competitive format.[17] The problem here is that if the concentration of 8-OH-dG falls outside the calibration curve the sample needs to either be diluted or pre-concentrated before repeating the test or a new calibration curve needs to be created making this assay very time consuming.

B.5. Capillary electrophoresis. CE separations are based on differences in electrophoretic mobility of analytes present in a sample. CE uses very small sample volume (nL) per injection and separations occur in minutes with high separation efficiency. In order to obtain the needed sensitivity, fluorescence detection is widely used.

B.6. Comet Assay. The comet assay, or single-cell gel electrophoresis (SCGE) is a simple, relatively inexpensive, yet sensitive method for monitoring and detecting double- and single-strand breaks in DNA, alkali-labile sites and delayed repair site in single eukaryotic cells.[18] SCGE has become one of the standards for measuring oxidative DNA damage and is widely used in the fields of genetic toxicology and oncology.[19] In this

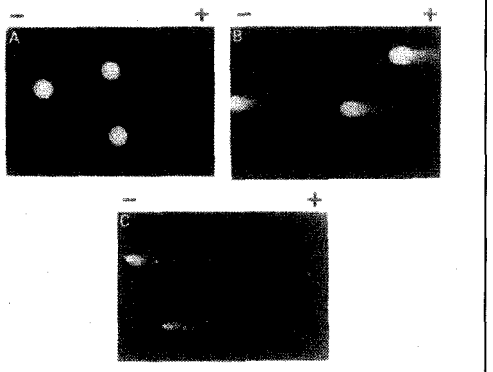

Figure B2. Different degrees of DNA damage as detected using a

assay, there is a nearly linear relationship between DNA break frequency and percent of tail DNA.[1] SCGE does not measure specific molecular species but rather the degree of DNA strand breakage and therefore total oxidative damage It has been reported that SCGE can resolve break frequencies up to a few hundred per cell.[5, 20] The current comet assay protocol was developed in the labs of Singh[21] and Olive.[22] Both methods are nearly identical in principle and practice; however, the method developed by Singh et al. uses alkaline conditions for separation while Olive uses neutral conditions. The Singh et al. method uses a suspension of cells embedded in low-melting-temp agarose gel on a microscope slide. The cells are lysed by detergents and high salt concentrations at pH 10 to remove cell contents leaving only the nuclear material. The DNA remains tightly coiled but unwinds under alkali conditions.[21] Cells with increased DNA damage display an increased "tail moment" or migration of DNA from the nucleus towards the anode during electrophoresis. Figure B2, taken from work done by Singh et al., shows typical DNA patterns following electrophoresis.[21] All three figures exhibit a different amount of damage with A being the control (no damage) and C having the most damage and therefore the largest comet tail moment.[21, 23] The procedure for the comet assay is outlined in Figure B3. Briefly, the cellular suspension is embedded in low-melting temperature agarose and placed on a microscope slide. After the agarose has solidified, the cells are placed in a lysing buffer in order to remove the cell membrane, nuclear envelope and any other unwanted cellular structures leaving only the nuclear material. At this point, enzymes are added to the nuclear material to initiate strand breaks at specific damage cites. The two major enzymes used for detection of pyrimidine oxidation products and purine oxidation products are Endonuclease III and Formamidopyrimidine DNA glycosylase (FPG) respectively. The final step prior to electrophoresis is the unwinding of the nuclear DNA which takes place under alkaline conditions. Unwinding is initiated at the break sites caused by the enzymes in the previous step. At this point, electrophoresis is performed on the immobilized nuclear material followed by fluorescent labeling of the sample. Each cell is analyzed individually using a fluorescent microscope either by eye using a standard scale or using computer software. Primary interest of this

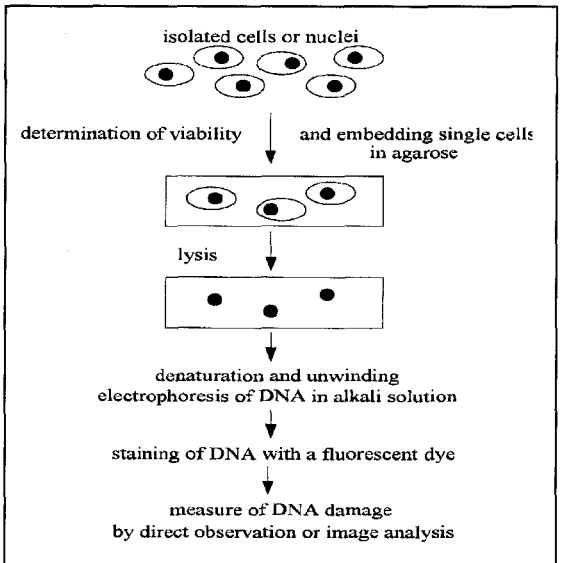

Figure B3. Schematic of conventional comet assay

proposal lies in looking at the major oxidation product of purines, 8-OH-dG. In human lymphocyte DNA, there are 2-8 8-OH-dG molecules for every 10^5 unaltered bases.[23] There are several problems associated with the current comet assay which emphasize the need for a new form of the assay. Problems include the length of time required for the assay (6+ hrs), the subjectivity of measurement of DNA damage using a scale of 0-4 based on the tail moment and the need to immobilize a single layer of cells in the agarose gel. The comet assay also requires screening at least 50 cells to get a broad sampling of damage within a sample which, when screening a sample using the human eye and a microscope can take nearly a full day to complete. The development of the miniaturized comet assay will address many if not all of the problems listed because steps required prior to measuring the damage can all be done on-chip along with the separation step.

C. Research Methods/Experimental Design.

Development of the miniaturized comet assay (MCA) is presented here and will take place in 3 parts:

- Develop hydrodynamically opposed electrophoresis
- Use known microfluidic techniques to perform on-chip sample preparation
- Integrate hydrodynamically opposed electrophoresis with on-chip sample preparation

The basic steps for the microchip comet assay are shown in Figure C1. These steps are similar to the conventional comet assay; however, all steps will be performed on-chip in the microchip comet assay.

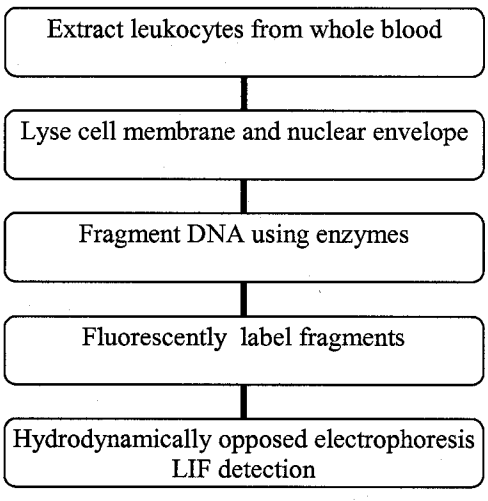

Figure C1. Steps in microchip comet assay.

C.1. Specific Aim 1. The first specific aim is to develop a new separation technique termed hydrodynamically opposed electrophoresis (HOE) to separate DNA fragments in the miniaturized comet assay. HOE is a hybrid separation technique which uses pressure driven flow in a sieving matrix-filled capillary coupled to an opposing electrophoretic mobility within the same separation channel. Theory on this method has been previously published by Ista et al.[24] However, they did not show a separation and only describe how this technique could have potential applications in microfluidic separations. Bulk flow will be driven towards the detection point in the channel by pressure and the separation of comet head and tail will occur because of the voltage applied in the opposing direction. In contrast to the traditional comet assay, we will focus on using a sieving matrix instead of a stationary gel for the DNA separation. Specific Aim 1 will be carried out in two major tasks.

Task 1. Optimization of sieving matrix. Task 1 of Specific Aim 1 will be conducted using a conventional capillary electrophoresis (CE) instrument and either commercially available DNA ladders or pre-lysed cells with a known amount of DNA damage as control samples. The conventional CE instrument is automated and will therefore allow us to cover a large number of sieving matrices and separation conditions in a short amount of time. There are several different matrices to test at this point such as polyethylene glycol (PEG),[25] dextran,[25] hydroxyethyl cellulose (HEC),[26-29] and methyl cellulose (MC).[27] Our primary focus will be on the use of HEC and MC both of which are used extensively in DNA separations. HEC was selected for its low fluorescent background and longevity of performance.[30, 31] Initially, HEC will be used at concentrations of 0.5 to 2% to separate dsDNA fragments using conventional CE to determine the optimal concentration of HEC. These concentrations and initial separation conditions are based on previously published work by Landers' group.[30] All separations will need to be done under alkaline conditions to minimize compression of ssDNA and allow for separation based primarily on length of the linear DNA strand. If the DNA is allowed to compress, strands of the same length may form different secondary structures which will cause the DNA to have different migration times.[32] If HEC does not give a good separation, we will switch to MC or another sieving matrix. Optimization will involve separations using pressure in conjunction and opposition of the negative separation voltage to determine the ideal pressure and voltage for the best resolution of compounds in the samples. Capillaries with relatively short effective lengths (20 cm) will be used to more closely match the channel length on a microchip.

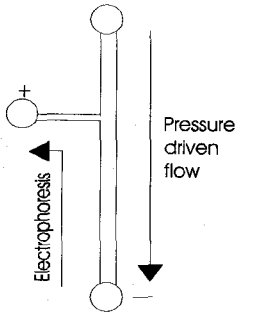

Figure C2. Schematic of microchip for HOE optimization.

Task 2. Design microchip to test hydrodynamically opposed electrophoresis conditions. Task 2 of specific aim 1 will focus on the production of a simple microchip to test the viability of performing hydrodynamically opposed electrophoresis developed in task 1 on a PDMS microchip. A sample design of this microchip is shown in Figure C2. In order to prevent the matrix from flowing down the side channel, the width of the side channel will be much narrower than the main separation channel. In this way, the path of least resistance for bulk flow will be down the main separation channel to the detection point. Major problems with this task are not anticipated except for the possibility of further optimization of separation conditions for the microchip. Care will have to be taken to verify only a single cell is being detected at a time. For this step, lysed cells will be used not the DNA ladder. The detection of several cells at a time will cause inaccuracy in the data generated because the signal will be artificially enhanced leading to the possibility of overestimating the amount of damage. At this stage, fluorescent microscopy will be used to visually monitor the separation and make necessary adjustments to flow rates such that only one cell is detected at a time.

C.2. Specific Aim 2. In order for the miniaturized comet assay to be performed from start to finish within a single microchip, on-chip sample preparation is required. The second aim, therefore, is to design a sample delivery system for the microchip. Optimization of flow rates by altering pressures and channel dimensions to allow for proper sample mixing will need to be performed. In addition, this aim will employ the use of magnetic beads for leukocyte immobilization and isolation from whole blood. There are two tasks for Specific Aim 2.

Task 1. Initial chip design and flow profiling. The first task of Specific Aim 2 will be to perform computational fluid dynamics simulations to model flow patterns and mixing patterns. This will allow us to optimize channel geometry and ensure proper mixing of reagents given that each assay component will have a different viscosity. The optimal channel dimensions will be applied in the production of the MCA mask. There are two possibilities for the microchip design, one which utilizes solution kinetics and on-chip mixing of reagents and the other which uses magnetic beads as a solid-phase reaction surface. These designs are detailed below in Figure C3. In the magnetic bead chip, a system of valves will need to be used to keep the two regions separated in order to remove all unwanted components following sample preparation and prior to analysis. This is described in more detail in Specific Aim 3.

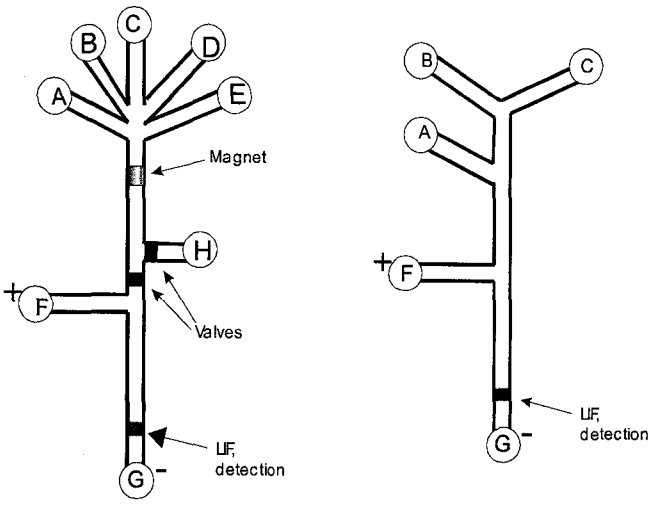

Figure C3. Two different options for MCA chips. Buffer labels in diagrams are as follows: A) Fluorescent label. B) Lysing buffer. C) Sample. D) Magnetic beads labeled with leukocyte common antigen (LCA). E) Buffer. F) HEC containing buffer. G) HEC containing buffer. H) Buffer. A voltage is applied between reservoirs F and G during separation.

Task 2. Incorporation of magnetic beads for analyte capture and processing. As stated above, one possibility for sample manipulation is the use of magnetic beads. The beads would allow for the capture of leukocytes from whole blood and the leukocytes would remain in place for the duration of sample preparation. All reagents would be passed over the captured beads in a flow-through system. Studies have been done on the manipulation of magnetic beads in microchips and we will base our initial conditions on this work.[33] The leukocytes would be captured using beads coated with leukocyte common antigen (LCA) (USBiological) which correspond to epitopes found only on the cell membrane of

leukocytes. The only additional requirement here is an external magnet to hold the beads at one location in the channel. These magnets are fairly inexpensive and easily miniaturized.

One possible issue to consider during this task is whether or not the lysing would be complete. There is the possibility that only the cell membrane will be lysed and not the nuclear membrane. Attention needs to be focused on the efficiency of cell lysis. There have been several reports published regarding on-chip cell lysis[34, 35] and we therefore do not foresee any major problems performing cell lysis within the microchip comet assay. Another method to collect DNA for analysis is hybridization. In this case, however, hybridization is not the appropriate method of DNA collection due to the possibility of unraveling of DNA too early in the assay and possibly causing artifacts.

If specific aim 2 is not successful, the results of specific aim 1 can still be utilized for the analysis of damaged DNA. Sample preparation will need to be performed off-chip in a similar fashion to the conventional comet assay but separation and detection will be performed on a microchip using HOE.

C.3. Specific Aim 3. Upon the success of both specific aim 1 and specific aim 2, a prototype microchip which incorporates all of the components from the hydrodynamically opposed electrophoresis as well as the optimized channel dimensions and geometries for the sample introduction system on a single PDMS microchip will be developed. We expect there will be a need to add valves to separate the two stages of the comet assay in order to control the flow of cells to the detection point. The valves incorporated in the MCA will be based on work by the Mathies group.[36] These valves operate in normally closed mode and are actuated using pressure when flow to a specific channel is desired.[36] A design of the initial prototype for the total microchip comet assay is shown in Figure C3. The schematic on the left is significantly more complex than the one on the right; however, both are viable options for the MCA. Design A incorporates a stationary magnet below the PMDS chip and has two very distinct regions of the chip. The top portion is where the sample preparation takes place whereas the lower region of the chip is were HOE is performed. The magnet is a small electromagnet that can be actuated in order to capture magnetic beads that have been functionalized with LCA holding the beads in place for the entire assay. The reagents can be loaded in each reservoir and passed over the beads one at a time using individual pressure lines. In addition, there is an extra waste reservoir (H) as well as a series of valves to enable the user to flush out any unwanted, excess reagents prior to sending the cells into the separation channel for analysis. The advantages for utilizing design A include the need for only small amounts of sample and reagents. The other key point to using design A is that all excess reagents will be removed from the sample prior to HOE eliminating all possibility of background and interferences. If design A proves too difficult to fabricate, design B will be used. In design B, the geometry and dimensions of the channels will be critical and stopped flow may be required for ample reaction time. Design B, unlike design A, does not have any valves or magnets and is therefore a much simpler design which relies heavily on solution phase kinetics. In each model, the reservoirs containing the comet assay components are introduced into the system using pressure. The pressure will be controlled using a syringe pump.

Hydrodynamically opposed electrophoresis will allow for the separation of the comet head from the comet tail. Both the tail and head will be analyzed to calculate a relative distribution the ratio of damaged and undamaged DNA. The undamaged DNA will remain in the comet head and the damaged DNA will migrate as the comet tail. A calibration curve will be generated for known amounts of damage in order to compare and quantify unknown patient samples. Electropherograms of the comet tails will be collected using laser induced fluorescence with a cooled CCD camera for detection. Quantification will be accomplished by comparing the unknown sample to a standard calibration curve. Sampling rate and sensitivity of the camera will need to be considered. We are not looking at single molecules, however, the camera will need to have a sufficient sampling rate, on the order of 1000 Hz or greater, to guarantee that one cell is analyzed at a time. If the sampling rate is too slow, more than one cell could be detected or if the sampling rate is too fast, valuable data may be lost as some cells may not be detected at all.. Most commercially available cameras range from 1MHz to 20 MHz sampling rates. Sensitivity of the CCD camera will not be a big issue because each DNA strand has multiple fluorescent labels causing at least a 100-fold signal amplification for each fragment.

Once the prototype miniaturized comet assay is produced, it will be compared to the traditional comet assay. This will be done by running both the traditional and microchip assays using the same samples. In each case a negative control as well as samples with varying amounts of DNA damage will be analyzed. Damaged cells will be created through exposure to methylene blue and light in order to create single strand DNA damage and an increase in 8-OH-dG. Furthermore, we will also induce damage through peroxide exposure to mimic a more in vivo type of oxidative damage and therefore be able to study fundamental aspects of radical and oxidative stress biology. We do not anticipate any problems accomplishing this specific aim.

D. Summary

Oxidative DNA damage is a natural occurrence in human cells; however, it is usually counterbalanced with DNA repair. When this balance is skewed towards damage, diseases such as carcinogenesis may occur. Clinicians need the ability to quickly and reliably monitor the amount of DNA damage and repair rates occurring whether it be in response to chemotherapy or exposure to radiation and known carcinogens. This proposal outlines the development of a new assay for DNA damage, the miniaturized comet assay which allows for rapid determination of DNA damage within single cells. The MCA will allow scientists to more reliably study fundamental aspects of radical biology by giving a clear, quantitative result in a short amount of time when looking at DNA damage caused by oxidative stress. This assay provides a rapid, more reliable comet assay that can be performed completely on-chip from sample processing to analysis. Finally, hydrodynamically opposed electrophoresis will have a much broader impact on the field of separations by providing the bioanalytical community with a new technique that will lend itself to improvements in speed and resolution.

E. References

(1) Guetens, G.; De Boeck, G.; Highley, M.; van Oosterom, A. T.; de Bruijn, E. A. *Crit Rev Clin Lab Sci* **2002**, *39*, 331-457.

(2) Cerutti, P. A. *Lancet* **1994**, *344*, 862-863.

(3) Cooke, M. S.; Evans, M. D.; Dizdaroglu, M.; Lunec, J. *Faseb J* **2003**, *17*, 1195-1214.

(4) *Free Radic Res* **2002**, *36*, 239-245.

(5) Collins, A. R.; Dobson, V. L.; Dusinska, M.; Kennedy, G.; Stetina, R. *Mutat Res* **1997**, *375*, 183-193.

(6) Kurz, T.; Leake, A.; von Zglinicki, T.; Brunk, U. T. *Strategies for Engineered Negligible Senescence: Why Genuine Control of Aging May Be Foreseeable* **2004**, *1019*, 285-288.

(7) Gedik, C. M.; Collins, A.; Escodd; *Faseb Journal* **2004**, *18*, -.

(8) Dizdaroglu, M.; Jaruga, P.; Rodriguez, H. *Nucleic Acids Res* **2001**, *29*, E12.

(9) Jaruga, P.; Rodriguez, H.; Dizdaroglu, M. *Free Radic Biol Med* **2001**, *31*, 336-344.

(10) Weiss, D. J.; Lunte, C. E. *Electrophoresis* **2000**, *21*, 2080-2085.

(11) Loft, S.; Fischernielsen, A.; Jeding, I. B.; Vistisen, K.; Poulsen, H. E. *Journal of Toxicology and Environmental Health* **1993**, *40*, 391-404.

(12) Tarng, D. C.; Huang, T. P.; Liu, T. Y.; Chen, H. W.; Sung, Y. J.; Wei, Y. H. *Kidney International* **2000**, *58*, 790-799.

(13) Matsui, A.; Ikeda, T.; Enomoto, K.; Hosoda, K.; Nakashima, H.; Omae, K.; Watanabe, M.; Hibi, T.; Kitajima, M. *Cancer Letters* **2000**, *151*, 87-95.

(14) Podmore, K.; Farmer, P. B.; Herbert, K. E.; Jones, G. D. D.; Martin, E. A. *Mutation Research-Fundamental and Molecular Mechanisms of Mutagenesis* **1997**, *378*, 139-149.

(15) Devanaboyina, U.; Gupta, R. C. *Carcinogenesis* **1996**, *17*, 917-924.

(16) Erhola, M.; Toyokuni, S.; Okada, K.; Tanaka, T.; Hiai, H.; Ochi, H.; Uchida, K.; Osawa, T.; Nieminen, M. M.; Alho, H.; KellokumpuLehtinen, P. *Febs Letters* **1997**, *409*, 287-291.

(17) Toyokuni, S.; Tanaka, T.; Hatton, Y.; Nishiyama, Y.; Yoshida, A.; Uchida, K.; Hiai, H.; Ochi, H.; Osawa, T. *Laboratory Investigation* **1997**, *76*, 365-374.

(18) Rojas, E.; Lopez, M. C.; Valverde, M. *J Chromatogr B Biomed Sci Appl* **1999**, *722*, 225-254.

(19) Olive, P. L. *Int J Radiat Biol* **1999**, *75*, 395-405.

(20) McKelvey-Martin, V. J.; Green, M. H.; Schmezer, P.; Pool-Zobel, B. L.; De Meo, M. P.; Collins, A. *Mutat Res* **1993**, *288*, 47-63.

(21) Singh, N. P.; McCoy, M. T.; Tice, R. R.; Schneider, E. L. *Exp Cell Res* **1988**, *175*, 184-191.

(22) Olive, P. L.; Banath, J. P.; Durand, R. E. *J Natl Cancer Inst* **1990**, *82*, 779-783.

(23) Gedik, C. M.; Boyle, S. P.; Wood, S. G.; Vaughan, N. J.; Collins, A. R. *Carcinogenesis* **2002**, *23*, 1441-1446.

(24) Ista, L. K.; Lopez, G. P.; Ivory, C. F.; Ortiz, M. J.; Schifani, T. A.; Schwappach, C. D.; Sibbett, S. S. *Lab on a Chip* **2003**, *3*, 266-272.

(25) Bergman, M.; Claessens, H.; Cramers, C. *Journal of Microcolumn Separations* **1998**, *10*, 19-26.

(26) Grossman, P. D.; Soane, D. S. *Biopolymers* **1991**, *31*, 1221-1228.
(27) Thomas, G. A.; Williams, D. L.; Soper, S. A. *Clin Chem* **2001**, *47*, 1195-1203.
(28) Bashkin, J.; Marsh, M.; Barker, D.; Johnston, R. *Applied and Theoretical Electrophoresis* **1996**, *6*, 23-28.
(29) Woolley, A. T.; Mathies, R. A. *Proc Natl Acad Sci U S A* **1994**, *91*, 11348-11352.
(30) Tian, H.; Landers, J. P. *Anal Biochem* **2002**, *309*, 212-223.
(31) Hsieh, M. M.; Chiu, T. C.; Tseng, W. L.; Chang, H. T. *Current Analytical Chemistry* **2006**, *2*, 17-33.
(32) Liu, Y.; Kuhr, W. G. *Analytical Chemistry* **1999**, *71*, 1668-1673.
(33) Rashkovetsky, L. G.; Lyubarskaya, Y. V.; Foret, F.; Hughes, D. E.; Karger, B. L. *Journal of Chromatography A* **1997**, *781*, 197-204.
(34) Waters, L. C.; Jacobson, S. C.; Kroutchinina, N.; Khandurina, J.; Foote, R. S.; Ramsey, J. M. *Anal Chem* **1998**, *70*, 158-162.
(35) Li, P. C. H.; Harrison, D. J. *Analytical Chemistry* **1997**, *69*, 1564-1568.
(36) Grover, W. H.; Skelley, A. M.; Liu, C. N.; Lagally, E. T.; Mathies, R. A. *Sensors and Actuators B-Chemical* **2003**, *89*, 315-323.

APPENDIX 2: LIST OF PUBLICATIONS

1. Caulum, M. M. and Henry, C. S., "Multi-Analyte Immunoassay using Cleavable Tags and Microchip Micellar Electrokinetic Chromatography (MEKC)," *Analyst* 2006 131, 1091-1093.

2 Vickers, J.A., Caulum, M. M., and Henry, C. S., "Generation of Hydrophilic Poly(Dimethylsiloxane) For High Performance Microchip Electrophoresis," *Anal Chem* 2006, 78(21), 7446-7452.

3. Boonsong, K., Caulum M. M., Dressen, B. M., Chailapakul, O., Cropek, D. M., Henry, C. S., "Layer-by-layer Polyelectrolyte Coatings for Microchip Electrophoresis," 2006 manuscript in preparation, *J. Chrom B.*

4. Caulum, M.M., Muphy, B.M., Ramsay, L.R., and Henry, C.H., "Multi-analyte Cleavable Tag Immunoassay" 2006 manuscript in preparation, *Anal Chem.*

5. Caulum, M.M. and Henry C.S., "Single Particle Reaction Kinetics in Microfluidic Devices" 2006 manuscript in preparation, *Lab on a Chip.*